Unitarity pion production and the multi-ladder pomeron

Ali Hayder Shehadeh

UNITARITY, PION PRODUCTION AND THE MULTI-LADDER POMERON

by

Ali Hayder Shehadeh

A thesis presented for the degree of
Doctor of Philosophy
at the University of Durham

December 1977
Mathematics Department,
University of Durham.

ABSTRACT

In general this thesis is concerned with high energy elementary particle physics. In particular it discusses the solution of the unitarity equation when the input multiparticle production amplitude is given by a specific model. The main quantities which are calculated and predicted are; (i) the intercepts of Reggeon and exotic trajectories, (ii) the average multiplicities of the produced particles and charge transfere (ΔQ), (iii) and finally the relative probabilities of Charge exchange $|\Delta Q| = 2/(\Delta Q=0+ |\Delta Q| =2)$ and $|\Delta Q| =3/(|\Delta Q|=1+ |\Delta Q| =3)$.

Chapter one is a general introduction to the field. The physical motivations for using a peripheral description for $2 \to 2$ amplitude and a multiperipheral description for the $2 \to n$ amplitude are discussed.

The physical consequences of dual unitarization (or topological expansion) are discussed in Chapter two. Using quark-duality diagrams we have calculated many interesting physical quantities, e.g. the Residue and intercept of exotic exchange, the IOZ rule and its violation.

In chapter three we introduce our pion production model for the $A_2 \to n$ amplitude, where we do not impose exchange degeneracy between the I = 0 and I =1 trajectories, and we include (in addition to I=0, 1 trajectories) two exotic trajectories (X, Y) of opposite G-parity. The intercept of the output Reggeons and Exotic are calculated and a reasonable spectrum is obtained.

In chapter four we repeat the calculations of chapter three when the I-Spin 0 partner of the pions, i.e. the η is produced (in addition to π's) Since, however, η is heavier than the pions, we associate a suppression factor $\underline{X}$ when η is produced. The main effect of the inclusion of η is to push up (dow the positive (negative) G-parity states. This effect, however, is small compared to the original results, i.e. the results when only pions are produced.

The average multiplicities of the produced particles and charge transfer (ΔQ) are calculated in Chapter five in the context of both models of Chapters 3 and 4. These results are compatible with the moderate energy data but they are too small compared to high energy data.

Finally, in Chapter six we introduce a multi-ladder model for the Pomeron, and we show how the data at high energy can be described by the model. In particular, we compare the relative probabilities of charge exchange predicted by the model with the new data of Lamsa et al.[16]

CONTENTS

CHAPTER I

UNITARITY AND MULTIPERIPHERALISM

1. Introduction

The S-channel unitarity equation gives an expression of the imaginary part of the two-body amplitude as a sum of contributions from two and multiparticle intermediate states:

$$\mathrm{Im}\langle f|T|i\rangle = \sum_x \langle f|T^*|x\rangle\langle x|T|i\rangle \qquad (1)$$

Now if we separate the terms on the right into diffractive and non-diffractive, and if we ignore the diffractive term (it is known experimentaly that up to ISR energies, diffractive processes including elastic scattering constitute only a minor part ($\gtrsim$ 30 per cent of the total cross-section) we can calculate the dominant imaginary part of the two-body amplitude from the shadow of only the non-diffractive component

$$\mathrm{Im}\langle f|T|i\rangle \simeq \sum_n \langle f|T^*|n\rangle\langle n|T|i\rangle \qquad (2)$$

$$\mathrm{Im}\,T(s,t) \simeq \sum_n \int T^*_{f\to n}\, T_{i\to n}\, d\Phi$$

(3), Fig. (1

In fact in the model which we will use in Chapter 3, the input amplitude in the right hand side of the unitarity equation includes somehow diffractive contribution because we do not impose exchange degeneracy between vector and tensor trajectories, and the pomeron

contribution comes through the inclusion of f. Notice that because the unitarity condition relates the dynamics of two particle to multiparticle channels, it turns out that any model for multiparticle production should satisfy two things:

(1) it should give the well known properties of many particle production, which have been established from experiment;

(2) it should re-produce via (1) the distinctive features of elastic scattering, and the symmetry structure established in two body process.

The rest of this chapter is organized as follows: In Section 2 we give a number of outstanding features concerning elastic scattering and two body amplitudes. The general features of many particle production are given in Section 3. In Section 4 we introduce our model for the non-diffractive component, namely the multiperipheral Regge Model, and we show in particular how the consistency between the input and the output Regge poles provides a natural bootstrap mechanism. We discuss in some details the Chew-Pignotti model,[1] where a prerequisite of the model is Dolen-Horn-Schmid duality which justifies a rough multi-Regge description of high energy multiple production that ignores resonances and concentrates on those final particles which are stable with respect to strong interaction.[2] Finally in section 5 we discuss a dual multiperipheral model proposed by Huan Lee,[3] where duality is incorporated into the model by using dual Resonance amplitudes as input amplitudes in the unitarity equation (eq.3).

2. Some of the distinctive features of elastic scattering and two-body amplitudes

2.1. Elastic scattering

The forward diffraction peak for elastic processes is nearly stable in its height and in its dependence in t. This fact is quite consistent with the pomeron exchange being the dominant contribution, with intercept close to 1 and small slope $\alpha_P(0) \sim 1$, $\alpha'_P(0) \sim 0.3$ Gev^{-2}.

2.2. Charge exchange processes

The forward diffraction peak for these processes shows much less stability in its s and t dependence than elastic processes. In Regge terminology this fact is characterised by the exchange of Reggeon with $\alpha_R(0) \sim 0.5$, $\alpha'_R(0) \sim 1$ Gev^{-2}.

2.3. Exotic exchange processes

The amplitudes which correspond to exotic exchange (e.g. double charge exchange) are zero or at least suppressed compared to non-exotic exchange. For example the u-channel of $K^-P \to K^-P$ is $K^+P \to K^+P$ which has exotic quantum numbers, and so there are no Reggeons which can be exchanged (except the exotic one if it exists), and indeed the backward peak of $K^-P \to K^-P$ is strongly suppressed.

2.4. Exchange degeneracy

Exchange degeneracies are relations between the leading Regge trajectories (excluding the pomeron) and result from the absence of exchange forces in t or u channel. We illustrate this by the following example, let us consider $\pi^+\pi^+$ elastic scattering. Since the direct channel is exotic, duality implies cancellation between the leading trajectories in t channel. The I = 1, 0 leading trajectories in t channel are ρ and f respectively, they are exchange degenerate, i.e. their

trajectory functions are equal but they have opposite signature (ρ has odd spin and the signature factor τ is -1, while f has even spin, and $\tau = +1$). However exchange degeneracy is not well-satisifed experimentally, e.g. recently direct measurements at FNAL and Serpukho: give $\alpha_\rho(0) - \alpha_{A_2}(0) \sim 0.1$ and in fact a lot of efforts have been devoted recently to calculate the breaking of exchange degeneracy.[4,7]

3. General features of multi particle production

3.1 The production of pions

A striking fact is that most particles that are produced in the high energy collisions are pions. E.g. in the reaction $\pi^- P$ at 25 Gev[5] only 16 per cent of the produced channels include strange particle production. This implies

$$\frac{\langle n\rangle_{\pi^\mp}}{\langle n\rangle_{\text{tot. charged}}} = \frac{\langle n\rangle_{\pi^\mp}}{\langle n\rangle_{\pi^\mp} + \langle n\rangle_{K^\mp}} =$$

$$\frac{84\langle n\rangle + 16[\langle n\rangle - 2]}{84\langle n\rangle + 16[\langle n\rangle - 2] + (16)(2)} = \frac{100\langle n\rangle - 32}{100\langle n\rangle}$$

If we take the parametrization of the mean multiplicity of charged particles from reference (6), at $S \simeq 50$ Gev^2 we get

$$\frac{\langle n\rangle_{\pi^\mp}}{\langle n\rangle_{\text{tot. cha.}}} = \frac{100(4) - 32}{100(4)} = \frac{370}{400} \simeq 92\%$$

hence

$$\frac{\langle n\rangle_{K^\mp}}{\langle n\rangle_{\text{tot. cha.}}} = 0.08$$

which is in excellent agreement with the data of Reference (6). Since the production of other stable particles (with respect to strong interaction) like η and N are quite small compared to pion production, we will in much of this thesis be considering only pions as stable particles in the intermediate states of the unitarity equation.

3.2. Low transverse momenta

The number of particles produced falls off very rapidly as a function of $p_\perp$, the magnitude of momentum transverse to the incident beam. The average value $\langle p_\perp \rangle \approx 0.3$ to 0.4 Gev/c is approximately independent of the incident energy, and does not depend strongly on the type of particle or multiplicity of particles produced.

3.3. Low multiplicity of particle produced.

The average number of particles produced grows slowly with energy, much more slowly than would be the case if most of the available energy were converted into particles. E.g. the maximum number N of particles (π, say) produced in process where the incident energy "$\sqrt{s}$" is given by;

$$N_{max.} = \sqrt{s} / m_\pi \qquad (4)$$

while the data on the multiplicity of changed particles are well fitted by a logarithmic increase with energy[6)]

$$\langle n \rangle_{ch.} = A + B \ln S \qquad (5)$$

This fact together with the rule of smallness of transverse momenta, implies that most of the available energy remains in the longitudinal motion.

4.3. Poisson-type distribution.

In a multiparticle reaction where one is concerned with the number of particles produced, the data collected are numbers of events as a function of the number of charged prongs (since the neutrals are usually not observed), and as a function of beam energy. The resulting two dimensional distribution $\sigma(n_{ch.}, E)$ is called a topological cross-section. The data on $\pi^- p$ at 16 Gev shows that when σ_n is plotted VS. the number of prongs, the curve has the characteristic shape of a poisson distribution.

The logarithmic increase of multiplicity and the poisson distribution of σ_n, are among the well known predictions of multi-peripheral models as we shall see in the next section.

Before we close this section we would like to mention the following remark; although at energies $E \sim 10 - 30$ Gev the observed distributions are close to poisson distributions. However for $E \gtrsim 10^2$ Gev experiments show an essential deviation from the poisson distribution for large n. In reference (8) it is shown that this effect can be understood as a result of the simultaneous production of several multiperipheral showers. A similar phenomenon, is the charge exchange ratios, whereas at moderate energies a single multiperipheral ladder gives almost the correct charge exchange ratios which are observed experimentally, the situation at high energies is different, and as we shall see in Chapter VI the simultaneous production of several multiperipheral ladders is able to accommodate the new effects.

4. The Multiperipheral Regge Models

4.1 Extension of peripheral to multi-peripheral processes.

Since the early sixties there was experimental evidence[11,12] indicating the importance of a long range interaction $(\sim 1/m_\pi)$ in high energy collision of pions with nucleons and of nucleons with nucleons. This indicates the importance of a peripheral collision, in which the two incident particles collide by exchanging a single pion. The meaning of the word peripheral was extended after that to include any interaction which is transmitted through the exchange of a single virtual particle (not necessarily the lightest one, i.e. π).

Now a two body amplitude (See Fig (2)) can be written as:

$$A(s,t) \simeq G\, e^{at}\, (s/s_0)^{\alpha(t)}$$

which for fixed S and linear trajectory $\alpha(t) = \alpha(0) + \alpha' t$ leads to

$$A(s,t) \propto e^{\alpha' \log s \cdot t}$$

with $\alpha' \log s \approx 2\text{-}6\ \text{Gev}^{-2}$, indicating the dominance of the collisions in which the square of the virtual exchange particle's four momentum (i.e. t) is small. So that the beam can be thought of as interacting strongly with the periphery of the target, and the amplitude is rapidly damped in t . So if we take τ as some peripheral range of momentum transfer ($\tau \approx 0.5\ \text{Gev}^2$) we say that an interaction is peripheral if $|t| \lesssim \tau$ includes the bulk of the events. Similarly the many particle amplitude of Fig. (3), is said to be peripheral if $|t| \lesssim \tau$, and we expect this to be the dominant t - region for $s \gg s_1, s_2$. However in this limit the $|t_{min}|$ is given by , (where $|t_{min}|$ is the minimum possible value of $|t|$)

$$t_{min} \approx - s_1 s_2 / s \qquad (8)$$

Therefore the peripheral description of this process is meaningfull when

$$\tau \gtrsim s_1 s_2 / s \approx |t_{min}| \qquad (9)$$

and the full amplitude can be written as a product of the $1 + \pi \to s_1$ amplitude and the $\bar{\pi} + 2 \to s_2$ amplitude times some propagator for the exchanged virtual particle X. Now once this singly peripheral description becomes acceptable, a further decomposition of the amplitude can be performed as long as the kinematics allow it to be meaningfull. If the total energy s is large, s_2 can be large enough as that also admits a singly peripheral description (see Fig. (4)). The criterion now is

$$s_2' s_3 / s_2 \approx t_{2\,min} \qquad (10)$$

be small. Continuing to N blobs, this gives

$$\frac{s_1 s_2 \cdots s_N}{s\, \tau^{N-1}} \lesssim 1 \qquad (11)$$

This equation provides a simple, rough derivation of the law of logarithmic growth of multiplicities. Taking all s_i equal to some average value blob mass-squared s_0, eq. (11) gives

$$\langle n \rangle \lesssim \ln \frac{\tau}{s_0} \cdot \ln \frac{s}{\tau} \qquad (12)$$

So the average number of blobs increases at most logarithmically with S.

4.2. The basic ingredients of multiperipheralism.

The basic idea behind the multiperipheral model is that at high energy the dominant production mechanism should be like Fig (5). The different versions of the model differ in the choice of what objects being exchanged and what objects being produced. However all these models have the following common features.

(1) The momentum transfer dependence between successive links in the multi-peripheral chain is damped rapidly. This restriction is necessary in order to limit the transverse momenta, $\underline{P}_{\perp i}$ of the produced secondary particles. Thus for $S \gg m^2$ in the Laboratory and Center of mass systems the four vectors q_i and p_i of the virtual and produced particles are almost in the light cone, so that the transverse momenta are all small and the energies are approximately equal to the longitudinal momenta. i.e.

$$P_{iz}^2 \gg m_i^2 + \underline{P}^2, \quad q_{iz}^2 \gg q_{i0}^2 + q_{i\perp}^2 \tag{13}$$

$$|q_{i0}^2| \sim P_{i\perp}^2 \sim q_{i\perp}^2 \sim m^2 \tag{14}$$

where z is the beam direction, and $\underline{P}_{i\perp}, \underline{q}_{i\perp}$ are two dimensional vectors perpendicular to the z direction.

(2) The heart of multiperipheral dynamics lies in the factorization property of the full amplitude into a product of factors describing the dynamics in local regions of the multi-peripheral chain. In Amati, Fubini and Stanghellini[9] (AFS) model each factor

depends only on a single q_i^2 , being the elementary propagator for the line labelled by q_i "There is a minimal interparticle correlation here". A recursion relation between T_N and T_{N-1} is then immediate:

$$T_N(p_A, q_i) = \prod_{i=1}^{N} \lambda(q_{i-1}^2, q_i^2)\, D(q_i^2)$$
$$= \lambda(p_A^2, q_1^2)\, D(q_1^2)\, T_{N-1}(q_1, q_i) \qquad (15)$$

where $D(q_i^2)$ is the propagator of the line labelled by q_i , and $\lambda(q_{i-1}^2, q_i^2)$ is the vertex associated with the ith produced particle in Fig (5), which decrease rapidly as (q_i^2) becomes larger than a quantity m^2 of order of the square of a particle mass. The original AFS model was based on multi-pion exchange due to the proximity of the pion pole to the physical region, and the consequent enhancement for small momentum transfer. As it is shown in reference (9), the substitution of the AFS amplitude, eq. (15) and in general any multiperipheral amplitude which has the above mentioned features , yields a Regge behaviour for the imaginary part of the scattering amplitude.

After the original AFS model, (which gives no dynamical correlation between produced particle momenta), more realistic models have been suggested which allow correlation between neighbouring particles, and in which the exchanged particles are Reggeized. It is convenient to define this concept of "neighbouring" in terms of rapidity:

$$y_i = \frac{1}{2} \ln \frac{E_i + P_{i,z}}{E_i - P_{i,z}} \qquad (16)$$

and we say that two particles are neighbouring if the Lorentz boost parameter that relates their rest frames is less than a prescribed constant value.

4.3. Chew-Pignotti Model

We now examine a particular multiperipheral model to illustrate how the general features of multiperipheral models come about. We have already noted that, since all the transverse momenta are limited, the real degree of freedom in multiparticle production processes lies in the longitudinal motion. Following Detar,[10] we ignore the transverse momenta and formulate the model in one dimension. The process we consider is (Fig. 6)

$$a+b \longrightarrow 0+1+\cdots+n+n+1$$

In the laboratory system, where particle a is at rest and particle b moves along the z direction, we specify the momenta of the out going particles in terms of the rapidity variable:

$$\begin{aligned} p_a &= (m_a, 0, 0, 0) \\ p_b &= (m_b \cosh y_b, 0, 0, m_b \sinh y_b) \\ p_i &= (\omega_i \cosh y_i, p_{ix}, p_{iy}, \omega_i \sinh y_i) \end{aligned} \tag{17}$$

where $\omega_i = (m_i^2 + p_{i\perp}^2)^{1/2}$ is the longitudinal mass. For large S we have

$$S = m_a^2 + m_b^2 + 2 m_a m_b \cosh y_b \simeq m_a m_b e^{y_b} \tag{18}$$

One of the assumptions of the model is that all the sub-energies $s_{i,i+1}$ are large, this gives

$$s_{i,i+1} = (p_i + p_{i+1})^2 \simeq \omega_i \omega_{i+1} e^{y_{i+1} - y_i} \tag{19}$$

Thus if each $s_{i,i+1}$ is large then $y_{i+1} \gg y_i$ for each i. In this region of phase space we have what is called "strong ordering in rapidity" i.e. the ordering of the particles in rapidity (Fig. 7) Correspond to the ordering of their coupling (Fig. 6).

The n particle production cross-section is given by

$$\sigma_n \propto e^{-y_b} \int g^{2n} \prod_{i=0}^{n} (s_{i,i+1})^{2\bar{\alpha}} \, d\Phi_n \tag{20}$$

where e^{-y_b} is the usual flux factor s^{-1}, $\bar{\alpha}$ is an effective Regge trajectory and g is the coupling constant at the Reggeon-Reggeon particle vertex. The differential element of phase-space is

$$d\Phi_n = \prod_{i=0}^{n+1} \frac{d^3 \underline{p}_i}{E_i} \, \delta^4 \left(\sum_{i=0}^{n+1} p_i - p_a - p_b \right) \tag{21}$$

which, by making use of the new variables, $E_i + p_{iz}$ and $E_i - p_{iz}$ becomes

$$d\Phi_n = \frac{1}{2} \prod_{i=0}^{n+1} d^2 \underline{p}_{\perp i} \, dy_i \, \delta^2 \left(\sum_{i=0}^{n+1} \underline{p}_{\perp i} \right)$$
$$\times \delta \left[\sum_{i=0}^{n+1} \omega_i e^{-y_i} - m_a - m_b e^{-y_b} \right] \delta \left[\sum_{i=0}^{n+1} \omega_i e^{y_i} - m_a - m_b e^{y_b} \right] \tag{22}$$

In the strong ordering limit these delta functions may be approximated by

$$\frac{e^{-y_b}}{m_a m_b}\,\delta(y_0 - x_a)\,\delta(y_b - y_{n+1} - x_b) \tag{23}$$

where $x_a = \ln \omega_0/m_a$, $x_b = \ln \omega_{n+1}/m_b$ and the total energy is given by

$$S \simeq \frac{s_{01}\, s_{12} \cdots s_{n,n+1}}{\omega_1^2 \omega_2^2 \cdots \omega_n^2} \tag{24}$$

If we substitute the above relevant equations in equation (20) we get

$$\sigma_n \propto e^{-y_b} g^{2n} e^{y_b(2\bar{\alpha}-1)} \int \prod_{i=1}^{n+1} dy_i\, \delta(y_b - y_{i+1})$$

$$\propto e^{-y_b} g^{2n} e^{y_b(2\bar{\alpha}-1)} \int_{dy_n}^{y_b} \int_{dy_{n-1}}^{y_n} \cdots \int^{y_2} dy_1 \tag{25}$$

$$\propto g^{2n} e^{y_b(2\bar{\alpha}-2)} \frac{y_b^n}{n!}$$

$$\propto s^{2\bar{\alpha}-2} \frac{(g^2 \ln s)^n}{n!}$$

where we have taken $\omega_i = m_i$, $m_a = m_0$, $m_b = m_{n+1}$ and $\underline{p}_{\perp i}$ is ignored in eq. (22).

The total cross-section is simply

$$\sigma_{tot.} = \sum_{n=0}^{\infty} \sigma_n \quad \alpha \quad s^{2\bar{\alpha}-2+g^2} \tag{26}$$

Thus a Regge behaviour emerges in a multiperipheral model. In order to obtain constant cross-section one requires

$$2\bar{\alpha}-2+g^2=0 \tag{27}$$

using this relation in eq. (25) we get

$$\sigma_n \alpha (g^2 \ln s)^n \; e^{-g^2 \ln s} / n! \tag{28}$$

which is a poisson distribution with an average multiplicity which grows Logarithmically with energy

$$\langle n \rangle = g^2 \ln s \tag{29}$$

Finally, from optical theorem and eq. (26) we get

$$\sigma_t \sim s^{\alpha^{out}-1} = s^{2\bar{\alpha}-2+g^2}$$

$$\Rightarrow \alpha^{out} = 2\bar{\alpha}-1+g^2 \tag{30}$$

this equation is illustrated schematically in Fig. (8).

4.4. The multiperipheral bootstrap.

The simple multiperipheral model discussed in the previous section suggest that the multi-Regge model in conjunction with the unitarity relation, can be used to obtain bootstrap-like conditions involving Regge parameters. This is achieved by imposing the condition that the Regge behaviour obtained for a suitably chosen two body amplitude at high energies is controlled by the same trajectory that is exchanged along the multi-Regge line. Notice, however, that we can not apply this self-consistency condition to the previous model, eq. (30) because meson trajectories have been employed only to generate the pomeron and not to generate themselves (in fact the dominant contribution to $\bar{\alpha}_{in}$ is the lower meson trajectories (ρ, ω, f, A_2) because we know that the pomeron is not important in the production processes).

5. The generation of the Pomeron in a dual multiperipheral model

When we write a multi-Regge form for the n particle production amplitude, we assume that all the momentum transfers $|t_i| \leq \tau$ and $s_{i,i+1} > \bar{s}$ where $\bar{s}$ is some cut value above which Regge formula valid. Experimentally, however, many events have low sub-energies, due probably to the production of resonance, and to apply the model for these events, it is necessary to make use of some duality assumptions, that this high sub-energy form of the amplitude applies, at least in the average sense, for low $s_{i,i+1}$ as well.[2] Once this assumption is made, all the particles in the intermediate states become stable and the problem of double counting is over.

In this section we make a full use of two-component duality[3] (the pomeron is generated by the sum of background contributions, and the Reggeon is generated by the sum of resonating contributions), in the framework of multi-Regge model.

To illustrate the model let us take first $a + b \longrightarrow 1 + 2$ (fig. 9) Here there are just two diagrams for Reggen exchange in the t channel, one s - t planar, the other t - u planar.

In the first (second) diagram, the particles a and b are adjacent (not adjacent), so it has (has no) s - channel resonances. Similarly for $a + b \longrightarrow 1 + 2 + 3$, there are four diagrams for Reggeons exchange in t channel, only the first one (see fig. 10) has s-channel resonances since a and b are in adjacent order. The other three have no s-channel resonances since a and b are in a non adjacent order. And so on, there being 2^{n-1} different diagrams for an n particles final state, all but one (the s, t planar one) contribute to the background component.

Since all the diagrams contribute equally to σ_n we find from eq. (25)

$$\sigma_n \propto 2^{n-1} g^4 \frac{(g^2 \ln s)^{n-2}}{(n-2)!} s^{2\bar{\alpha}-2} \tag{31}$$

if we neglect interference between various terms.

The total cross section is given by

$$\sigma_t = \sum_{n=2}^{\infty} 2^{n-1} g^4 \frac{(g^2 \ln s)^{n-2}}{(n-2)!} s^{2\bar{\alpha}-2} \tag{32}$$

$$= 2 g^4 s^{2\bar{\alpha}-2+2g^2} \tag{33}$$

Thus the total cross-section has only one pole at (making use of optical theorm)

$$\sigma_t = \frac{1}{s} \mathrm{Im}\{A^{2\to 2}\} = 2 g^4 \frac{1}{s} s^{2\bar{\alpha}-1+2g^2} \tag{34}$$

$$\Rightarrow \quad \alpha_P = 2\bar{\alpha} - 1 + 2g^2 \tag{35}$$

On the other hand, for each n (n is the number of produced particles) only one diagram contributes to reggeons

$$\sigma_t\,(\text{Reggeons}) = \sum_{n=2}^{\infty} g^4 \frac{(g^2 \ln s)^{n-2}}{(n-2)!}\, s^{2\bar{\alpha}-2}$$

$$= g^4\, s^{2\bar{\alpha}-2+g^2}$$

Thus the reggeons contribution to σ_t has a pole at

$$\alpha_R^{out} = 2\bar{\alpha} - 1 + g^2 \tag{36}$$

Similarly for the crossed diagrams (which presumably build up the pomeron) we get

$$\sigma_t\,(\text{non-planar diagrams}) = \sum_{n=2}^{\infty} \left(2^{n-1} - 1\right) \times g^4 \frac{(g^2 \ln s)^{n-2}}{(n-2)!}\, s^{2\bar{\alpha}-2} \tag{37}$$

$$= 2g^4\, s^{2\bar{\alpha}-2+2g^2} - g^4\, s^{2\bar{\alpha}-2+g^2} \tag{38}$$

which gives two poles, one is the usual pomeron pole at $\alpha = 2\bar{\alpha} - 1 + 2g^2$, the other one cancels the reggeon (which has the same quantum numbers

like the pomeron, i.e. the f_1) contribution to σ_t.

Now if we impose the self consistency condition on the reggeon $\alpha_R^{out} = \bar{\alpha}$, we get from eqs. 35 and 36

$$\alpha_R^{out}(0) = 1 - g^2, \quad \alpha_{IP}(0) = 1 \tag{39}$$

The above scheme for the pomeron is closely related to the interpretation of the pomeron in the topological expansion, namely the cylinder (as we shall see next chapter). However, the intercept of the pomeron is greater than that of the reggeons in the topological expansion, but here we are able to obtain an intercept of the pomeron, not only greater than that of the reggeons, but exactly at one (of course under some strict assumptions, namely (i) using chew-pignotti approximation, (ii) and imposing the self consistency condition on the reggeons.)

Figure captions

Fig. 1 : Representation of the unitarity equation, (d denotes diffractive intermediate states, including elastic).

Fig. 2 : Peripheral exchange in 2 ⟶ 2 amplitude.

Fig. 3 : Peripheral process 1 + 2 ⟶ (S_1) + (S_2) with exchange of X. The kinematics are specified by s, t, and the invariant masses S_1 and S_2.

Fig. 4 : Extension of Peripheral to multiperipheral process.

Fig. 5 : Multiperipheral graph.

Fig. 6 : Diagram for the production of n particle, showing the definition of sub-energies and momentum transfers.

Fig. 7 : The strong ordering limit, which occurs when the ordering of the particles in rapidity is the same as the ordering of their couplings, i.e. the same as in Fig. 6.

Fig. 8 : Symbolic version of multiperipheral bootstrap equation.

Fig. 9 : The s-t and t - u planar duality diagrams which provides the two contributions to the signature factor of a t-Channel Reggeon.

Fig. 10: The four signature contributions to the ab ⟶ 123 double Regge amplitude.

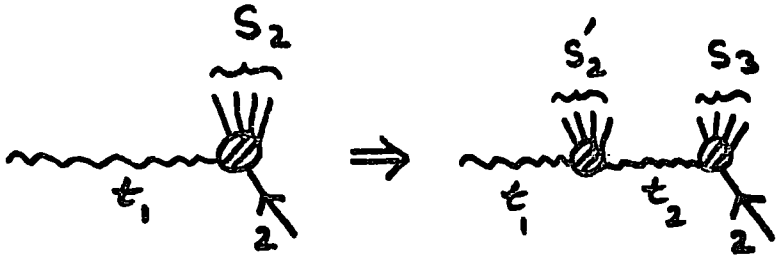

Fig. 4

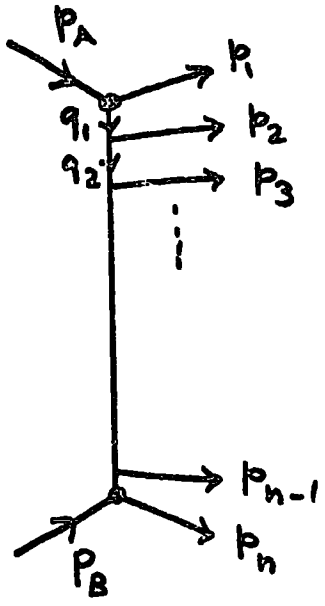

Fig. 5

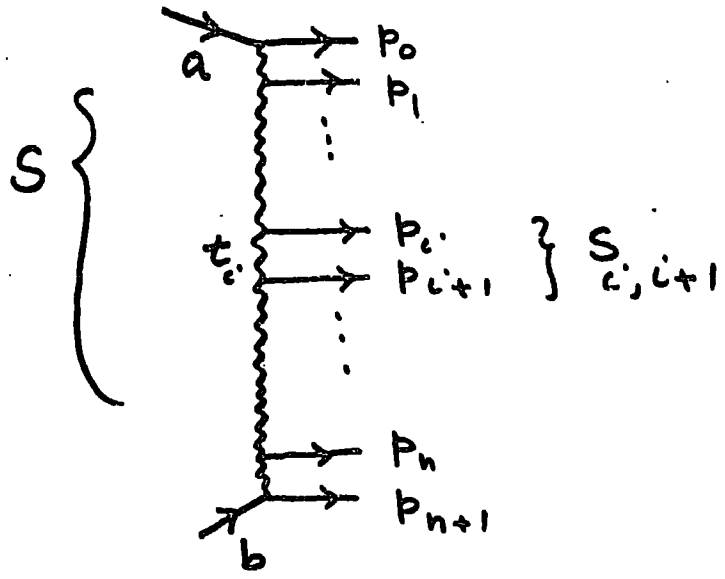

Fig. 6

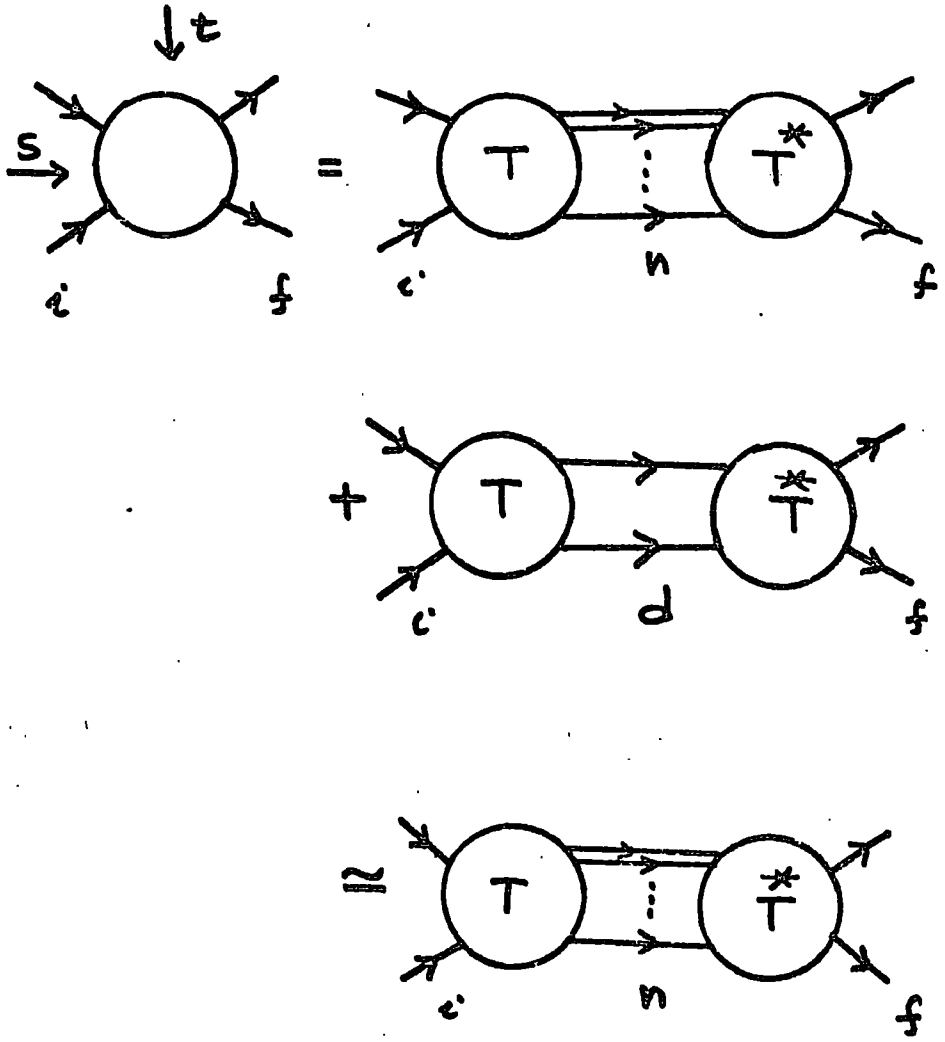

Fig. 1

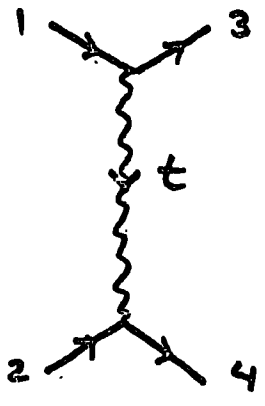

Fig.2

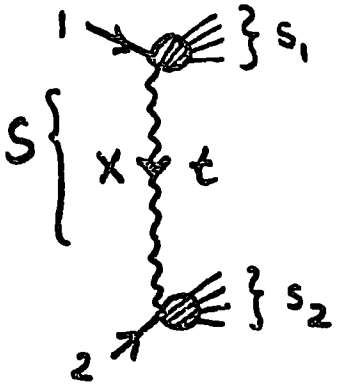

Fig.3

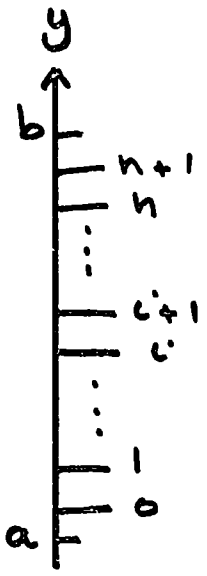

Fig.7

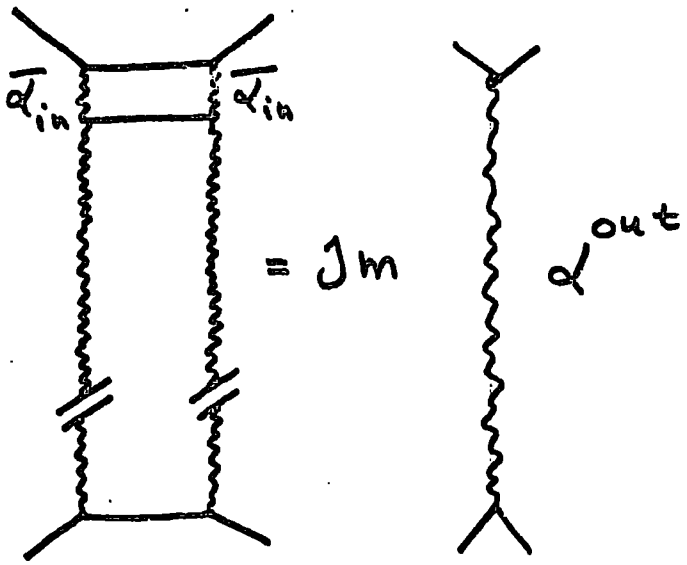

Fig.8

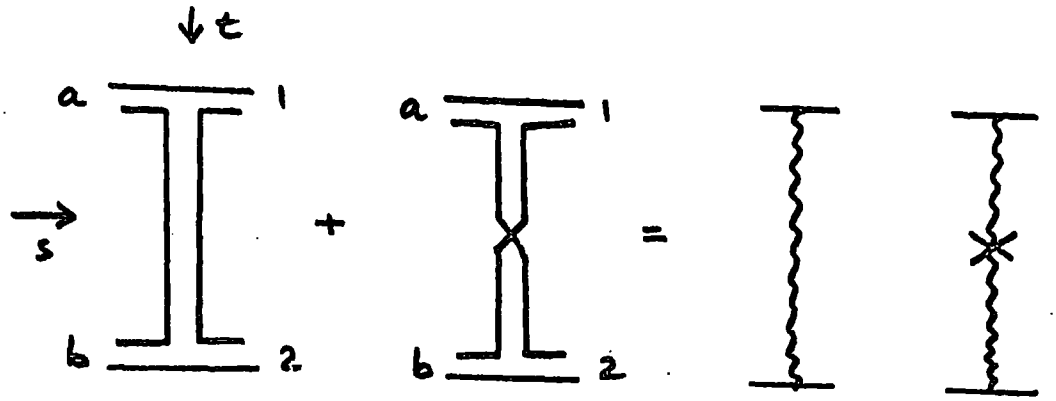

ab12 a2b1

Fig. 9

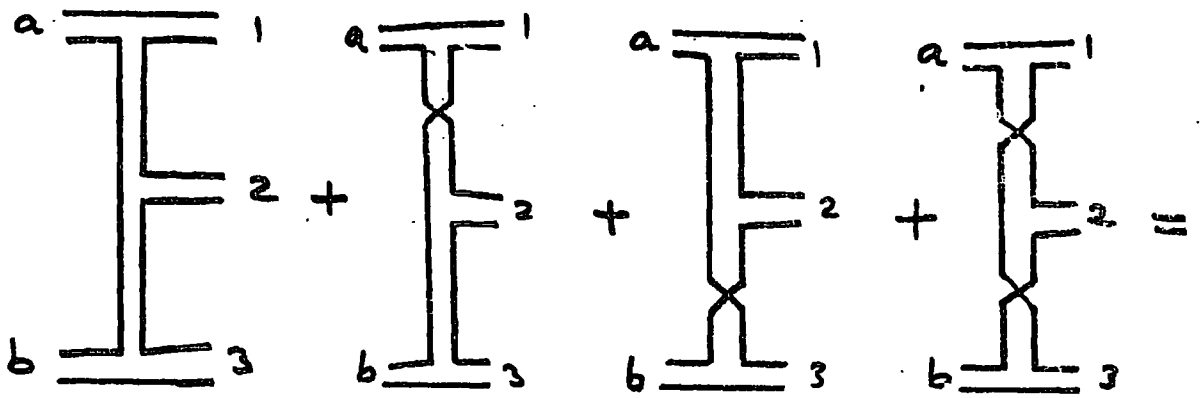

ab321 a23b1 a12b3 a2b31

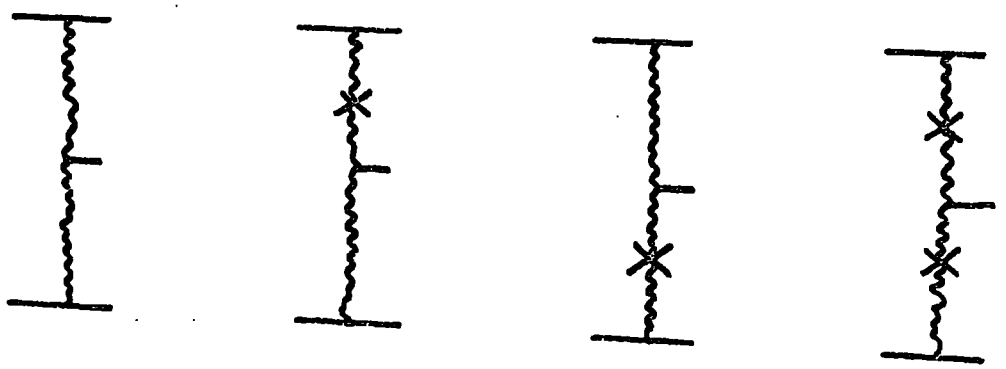

Fig. 10

CHAPTER II

Reggeons and Pomeron intercepts in dual Unitarization

1. Introduction

In this chapter we follow the newly proposed dual-unitarity scheme (or topological expansion) which makes use of the combined constraint of duality and unitarity ideas in the form of a multi-peripheral unitarity equation (see for example Veneziano;[18] Chan, Paton and Tsou;[25] Schmid and Sorensen)[13]. This approach seems to provide us with a systematic understanding of many aspects of strong interactions as the nature of the pomeron; the Okubo-Zweig-Iizuka[20] (OZI) rule and its violation; the suppression of exotic exchanges; and the breaking of exchange degeneracy among Regge poles with different quantom numbers. Our main purpose here is to get information concerning the output Regge-exchanges in the $2 \longrightarrow 2$ amplitude, when we insert a multiperipheral production amplitude $A_{2 \longrightarrow n}$ as input to the Unitarity equation

$$\mathrm{Im}\, A_{2\to 2} = \sum_n A_{2\to n} A^*_{2\to n} \qquad (1)$$

In the next section we calculate the output Regge exchanges in eq. (1) by solving the multiperipheral integral equation explicity, using the Chew-Pignotti approximation. In the third section we solve the unitarity equation for the first two terms in the topological expansion, namely the planar and the cylinder amplitudes. It will turn out that a serious difficulty of the dual unitary scheme is the problem of ω exchanges (the ω extinction). Another difficulty also is that the total contribution of the planar and the cylinder terms to f exchange vanishes, or stated differently the f trajectory is shifted upwards and is identical to the Pomeron. At this point we should

distinguish between two approaches to the planar bootstrap;

(i) In the approach where both the planar and the cylinder are generated.[3,13] In this approach the generation of the cylinder is related to the generation of the planar Reggeon through the bootstrap equation, $(1 - \alpha)/N = 2g^2$ (see sub-section 3.1). Using this approach, the total contribution of the planar and the cylinder terms to an SU(N) singlet with negative charge conjugation vanishes. This is because there is an exact concellation between the diagrams with even and odd number of twisted loops. With regard to f trajectory, it will be pushed up and its intercept at t = 0 in this approach is exactly at one (see Section 3).

(ii) The planar bootstrap is assumed, while the cylinder is generated. Since in this approach we do not have the above relation between the cylinder strength ($2g^2 = K$) and the planar parameter (α), the ω trajectory is shifted downwards but does not disappear, and the f trajectory is shifted upwards but not to one. This approach used in Ref. 28.

In section 4 we discuss some of the physical consequences of the inclusion of the higher order terms (the interference terms which have twists in the produced lines). It will turn out that the ω extinction happens only when these terms are excluded; when they are included, ω exchange is regenerated. We calculate in this section explicitly the $\rho - A_2$ splitting by solving the unitarity equation when the interference terms (at the two loops level) are included. We calculate also the residue and the intercept of exotic exchange by including all the higher order terms which generate exotic exchange and we compare this with the intercept and residue of planar Reggeons. Finally section 5 is devoted to some remarks.

2. Explicit S-matrix models

We start by writing the multiperipheral intehral equation for the amplitude A in the angular momentum plane, which takes the following form (using the Chew-Pignotti approximation)

$$A = V + VQV + \cdots$$
$$= V + VQA$$
$$= V + kA \qquad (1)$$

where the J-plane singularities are obtained by solving for det (1 - K) = 0. In eq. (1), $Q = 1/(x-\beta)$ and $\beta = 2\alpha(\bar{t}) - 1$, where we take $\bar{t} \approx -0.1$ (Gev/c)^2. The input Reggeons are assumed to be the exchange degenerate vector and tensor mesons (we neglect the unnatural parity exchange). V denotes the matrix representing the coupling of the produced objects to the exchanged reggeons, which is fixed by SU(3) and exchange degeneracy. We consider a world without strangeness (SU(2) symmetry). For the produced objects we consider several choices. We solve the unitarity equation at t = 0 and for positive G-parity (in the t-channel).

2.1 The pion production models

First we consider the model of Coulter and Snider[29] where only I-spin is conserved. In this case the relevant intermediate states in t-channel are (I= 1, I = 1) for both $I_t = 1$ and $I_t = 2$ (we do not consider here the $I_t = 0$ channel, since we are interested in comparing the output of $I_t = 0$, and $I_t = 2$), hence the matrix K has one element.

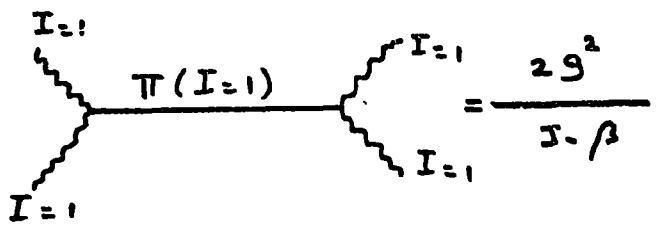

$$= \frac{2g^2}{J-\beta} \qquad (2)$$

$$k(I_t=1) = \frac{g^2}{J-\beta} \quad , \quad k(I_t=2) = \frac{-g^2}{J-\beta} \qquad (3)$$

which gives

$$\alpha_{I_t=1} = \beta + g^2$$

$$\alpha_{I_t=2} = \beta - g^2 \qquad (4)$$

which shows the desired suppression of $I_t = 2$.

Now if we consider the same model but we conserve both I-spin and G-parity. In this case the relevant intermediate states in t-channel are $(\rho\rho)$ and (A_2, A_2) for both $I_t = 1$ and $I_t = 2$. This gives

$$k(I_t=1) = \begin{bmatrix} 0 & \frac{g^2}{\pi-\beta} \\ \frac{g^2}{\pi-\beta} & 0 \end{bmatrix} \begin{matrix} \rho\rho \\ A_2A_2 \end{matrix}, \quad k(I_t=2) = \begin{bmatrix} 0 & \frac{-g^2}{\pi-\beta} \\ \frac{-g^2}{\pi-\beta} & 0 \end{bmatrix}$$

Solving for det (1 - k) = 0 we get

$$\alpha_{I_t=1} = \alpha_{I_t=2} = \beta \pm g^2 \qquad (5)$$

Thus the conservation of G-parity leads to an identical $I_t = 1$ and $I_t = 2$ in the output, a disastrous result in view of the experimental suppression of exotic. The origin of the difference between the above results (5) and (4) can be seen as follows:

The process 

contributes $+g^2$ to $I_t = 1$ channel and $-g^2$ to $I_t = 2$ channel (from the crossing matrix). Thus if we

produce n pions in the intermediate states, the contribution of $A_{in} A^*_{fn}$ is positive for both $I_t = 2$ and $I_t = 1$ channels, if n is even, and this contribution is positive (negative) for $I_t = 1$ ($I_t = 2$) if n is odd. In the I-Spin conserving model any number of the produced pions is allowed, and the sum $\sum_n A_{in} A^*_{nf}$ is an alternating series for $I_t = 2$. On the other hand when G-parity is conserved, either odd or even number of the produced pions is allowed and the sum $\sum_n A_{in} A^*_{nf}$ is no longer an alternating series.

2.2. The resonance production models ($\bar{1}$ and 2^+ production).

The above difficulties (eq. 5) are not avoided if we produce pions and η's. Here we will see how the production of $\bar{1}$ and 2^+ with equal strengths eliminate the exotic completely. Making use of SU(3) and exchange degeneracy we find that all the coupling of the produced $\bar{1}$ and 2^+ to the exchanged reggeons are equal. Since however 2^+ are higher mass resonances we associate a suppression factor x, when 2^+ are produced.

The coupling matrices K are given by

$$k(I_t=2) = k_V + k_T = \frac{g^2}{J-\beta}\begin{bmatrix} -1 & +1 \\ +1 & -1 \end{bmatrix} + \frac{xg^2}{J-\beta}\begin{bmatrix} +1 & -1 \\ -1 & +1 \end{bmatrix} \qquad (6)$$

$$k(I_t=1) = k_V + k_T = \frac{g^2}{J-\beta}\begin{bmatrix} +1 & +1 \\ +1 & +1 \end{bmatrix} + \frac{xg^2}{J-\beta}\begin{bmatrix} +1 & +1 \\ +1 & +1 \end{bmatrix} \qquad (7)$$

$$K\left(I_t=0\right) = K_V + K_T = \frac{g^2}{3-\beta}\begin{bmatrix} 2 & 1 & -\sqrt{3} & 0 \\ 1 & 2 & 0 & -\sqrt{3} \\ -\sqrt{3} & 0 & 0 & 1 \\ 0 & -\sqrt{3} & 1 & 0 \end{bmatrix} + \frac{x\hat{g}^2}{3-\beta}\begin{bmatrix} 1 & 2 & -\sqrt{3} & 0 \\ 2 & 1 & 0 & -\sqrt{3} \\ -\sqrt{3} & 0 & 0 & 1 \\ 0 & -\sqrt{3} & 1 & 0 \end{bmatrix} \quad (8)$$

if we produce $\bar{1}$ and $\overset{+}{2}$ with the same strength (x = 1), the exotic exchange will be eliminated completely. However, in $I_t = 0$ channel we have only one leading pole and the exchange degeneracy between ρ and f is lost (this is the same result of H. Lee model CH. I § 5). If on the other hand we take x = 0, we maintain the exchange degeneracy between f and ρ (in $I_t = 0$ we have non-leading pole which is exchange degenerate with the $I_t = 1$ leading pole). For the exotic we get

$$\alpha_{I_t=2} = \beta - 2g^2 \quad (9)$$

Although this intercept for the exotic seems to be reasonable, the residue of the exotic is such that it gives large exotic cross-section when compared with experiment.

Finally we note that in the above models, ω pole in the output is not generated. This is because the relevant intermediate states in the t-channel (for W quantum nunbers exchange in t-channel) are (ω, f) and (ρ, A_2). But because of the assumption of exchange degeneracy between Vector and Tensor trajectories and the standard signature factors, these terms do not contribute to the overlap function in the unitarity equation.

3. The topological expansion

3.1 The motivations and the parameter N

Consider first the quark-duality diagrams of Figs. 1 & 2. The Chan-Paton factors of Fig. 2 is N (where N is the types of quarks) times that of Fig. 1. The reason for this is that in Fig. 2 we have a closed loop and one should sum over the types of quarks in this loop. Similarly the Chan-Paton factors for the Figs. 3, 4 & 5 respectively give N^2, N, and 1. On the other hand the most evident difference between these diagrams is their different topological structure (planar, cylinder, and torus). Thus we see that when the topological structures of the diagrams get more complicated, the contribution of certain diagram will be suppressed by a factor $1/N$ (to some power) compared to the planar ones. (In fact there are other dynamical suppression factors in most cases, as we shall see later, which make this expansion converge more rapidly).

Now, in dual perturbation theory, a general term in the perturbation series involves powers of g^2 and g^2N. In this theory every orientable loop (for the loop to be orientable it should have two twist, since every quark line has an arrow, i.e. baryon number) can be classified (in terms of few numbers namely; b: the number of boundaries where the external particles are attached, w: the number of windows which are boundaries without legs attached to them, and h: the number of handles) by the topological structure of the two-dimensional surface on which it can be embedded, so that every part of this surface is covered by a planar diagram. In this language the unitarized n point function is given by

$$A_{b,w,h}(g,N) \propto g^{n-2} (g^2)^{b-1+2h} (g^2N)^w \qquad (10)$$

In the conventional expansion, the number N is irrelevant and the expansion is in the loop number

$$\ell = b - 1 + 2h + W \tag{11}$$

On the other hand in the topological expansion, we collect the graphs which have the same topological structure. It is thus expansion in g^2 (or $\frac{1}{N}$) at g^2N fixed. The starting point in this expansion is the sum of all planar graphs with arbitrary number of windows. In this case we have b = 1, h = 0, and the corresponding topology is a sphere with one boundary with the external particle attached to it. The other terms in this expansion which have more complicated topological structure, have an order of magnitude (compared to the planar one) which is given by

$$\left(\frac{1}{N}\right)^{b-1+2h} = (g^2)^{b-1+2h} \tag{12}$$

The second term in this expansion is the sum of all diagrams where both exchanged reggeons in one loop at least are crossed. The sum of these diagrams gives the amplitude which has vacuum quantum number exchanges in t-channel (the cylinder, see Fig. 6), which usually is identified with the (bare) Pomeron. In this case we have b = 2, h = 0, and the corresponding topology is a sphere with two boundaries. The order of magnitude is

$$g^2 \simeq 1/N$$

To go to higher order terms one must allow for the produced object to be crossed. Fig. 5 is an example. The corresponding topology is a sphere with one boundary and one handle (b = 1, h = 1). This class of diagrams are responsible for the breaking of exchange degeneracy between

ρ and A_2 as we shall see in Section 4. The order of magnitude of Fig. 5. is $g^4 \simeq 1/N^2$.

3.2. The properties of quark-diagrams

For any given quark diagram whether it is planar or not, we attach to it three properties.

(i) Quark line flow (i.e. the t-channel quantum numbers). For the planar diagrams we have always $q\bar{q}$ in t-channel. Thus these diagrams contribute to the N^2 plet. Reggeons in t-channel, (In fact we define in terms of $q\bar{q}$ pairs, the Pomeron, the Reggeons, and the exotic, to be the Zero, the one, and the two pairs of $q\bar{q}$). On the other hand all the diagrams which give the cylinder topology, have vacuum quantum number exchange in t-channel and they contribute only to SU(N) singlet. Finally, the interference terms can have zero or one or two pairs of $q\bar{q}$ in t-channel, as we shall see in section 4.

(ii) The orientation of the quarks at both ends of the diagram. If the diagram has the same quarks orientations at both ends of the multiperipheral chain, it gives a positive contribution for both $C_t = +$ and $C_t = -$ where C_t is the charge conjugation in t-channel. On the contrary, if the diagram has opposite orientations at the ends of the multiperipher chain, it gives positive contribution to $C_t = +$ and negative contribution to $C_t = -$. For the planar diagrams we have always the same orientation at both ends of the diagram. For the diagrams which build up the cylinder, if a certain diagram has even number of crossed loops it gives positive contribution to both $C_t = +$ and $C_t = -$, but if the diagram has an odd number of crossed loops it gives positive (negative) contribution to $C_t = +$ ($C_t = -$). The interference terms have both properties depending on the way we arrange the crosses on the Reggeons and on the produced lines. For example in Fig. 8 where we have three particles in the intermediate

states; Fig. 8a gives positive contribution for both $C_t = +$, and $C_t = -$, while Fig. 8b gives positive contribution t. $C_t = +$ and negative contribution to $C_t = -$.

(iii) The phases which are associated with the reggeons signatures. Only the interference terms have phases, the reason for this is that since uncrossed reggeon has phase $\exp(-i\pi\alpha)$ while crossed reggeon has phase 1, it turns out that all the planar diagrams and all the diagrams which contribute to the cylinder have phase 1.

The (ω) extinction

From the above properties it is easy to see how the total contribution of the planar and the cylinder terms to W exchange vanishes. Consider for example a diagram where we have n produced objects. The total number of quark diagrams is 2^n $(= 2^{n-1} \cdot 2)$, 2^{n-1} diagrams because every reggeon can either be crossed or not and 2 accounts for the two different orientation of quarks for every diagram). Half of these diagrams $2^n/2$, have even number of twisted loops (the planar diagram has zero number of twisted loops and it is one of these) and they give positive contribution to w exchange. The other half have odd number of twisted loops and it gives negative contribution to w. Thus the total contribution to W exchange vanishes for each n, and after summation over n, no w trajectory is generated in the L.H.S. of the unitarity equation.

3.3. The planar and the cylinder amplitudes.

The planar amplitude is the sum of all planar diagrams with arbitrary number of windows. At this level of the expansion "the Born term"; the exchange degeneracy is exact, the IOZ rule is exact, there is no Pomeron and no exotic. In terms of quark diagrams we write the planar amplitude M in the case of SU(N) as,

$M =$ 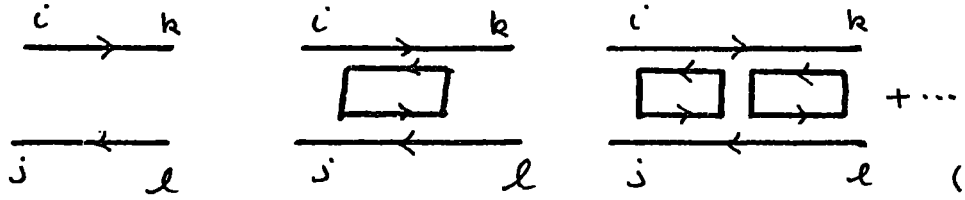

(13)

$$= \sum_{n=0}^{\infty} \left(\frac{2g_N^2}{J-\beta}\right)^n \delta_{ik}\delta^{jl}$$

$$= \frac{J-\beta}{J-\alpha}\,\delta_{ik}\delta^{jl}$$

where (14)

$$\alpha = \beta + 2g^2N, \qquad \beta = 2\bar{\alpha} - 1, \qquad \alpha = \alpha(\bar{t})$$

From eq. (14) we obtain the planar bootstrap condition (assuming $\bar{t} = 0$ and the self consistency between the input and the output Reggeons).

$$\alpha = \bar{\alpha} \Rightarrow \quad 1 - \alpha = 2g^2N \tag{15}$$

From eq. (15) we read the following interesting results.

(i) The leading Reggeon intercept must be below one.

(ii) The effective coupling $\lambda^2 = 2g^2N$ is fixed. This in fact is one of the motivation to the topological expansion.

The next term in the topological expansion is the sum of all diagrams where both reggeons in the loop are crossed. This term has the cylinder properties and it is communicate with states of zero <u>additive</u> quantum numbers. The cylinder correction is given by

$C =$ 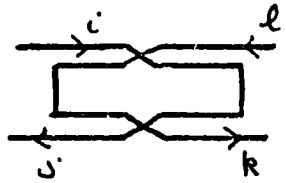

$$= \pm \frac{2g^2}{J-\beta}\,\delta^j_i\,\delta^l_k \tag{16}$$

The $\pm$ here refers to the Charge Conjugation in t-channel $C_t = \pm$.

The total amplitude A after the cylinder correction is given by

$A =$ 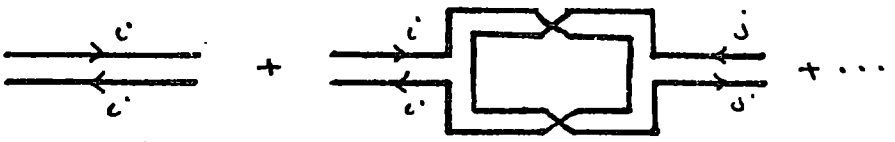 $+ \cdots$

(17)

$$= M + MCM + \cdots = \frac{1}{M^{-1} - C}$$

It is easy to solve eq. (17) in the case of SU(2). In this case the planar poles are two for each C. We associate each trajectory with different quark index, the trajectories are exchange degenerate, we lable their common trajectory by α. Thus we have

$$M = \begin{bmatrix} \frac{J-\beta}{J-\alpha} & 0 \\ 0 & \frac{J-\beta}{J-\alpha} \end{bmatrix} \tag{18}$$

$$C = \pm \begin{bmatrix} \frac{2g^2}{J-\beta} & \frac{2g^2}{J-\beta} \\ \frac{2g^2}{J-\beta} & \frac{2g^2}{J-\beta} \end{bmatrix} \tag{19}$$

Solving for $\det (M^{-1} - C) = 0$ we get

$$\begin{aligned} C_t = + \qquad & J_f = \alpha + 4g^2 \\ C_t = - \qquad & J_\omega = \alpha - 4g^2 \end{aligned} \tag{20}$$

Substituting eq. (15) in eq. (20) in the case of SU(2) we get

$$J_f = \alpha + 1 - \alpha = 1 \qquad \text{; the Pomeron of H. Lee}$$

$$J_\omega = \alpha - \alpha + \beta = \beta \tag{21}$$

The Residue of W pole is given by

$$\text{Res } \underset{\sim}{A}(J=\beta) = \lim_{J\to\beta} (J-\beta)\, \frac{1}{\bar{M}^{-1} - C} \tag{22}$$

$$= \lim_{J\to\beta} (J-\beta) \begin{bmatrix} \frac{J-\alpha+2g^2}{J-\beta} & \frac{-2g^2}{J-\beta} \\ \frac{-2g^2}{J-\beta} & \frac{J-\alpha+2g^2}{J-\beta} \end{bmatrix} \times \frac{(J-\beta)^2}{(J-\alpha)^2 + 4g^2(J-\alpha)} \tag{23}$$

For the first diagonal element we get

$$\text{Res } \underset{\sim}{A}^{11} = \lim_{J\to\beta} (J-\beta)\, \frac{J-\alpha+2g^2}{(J-\beta)} \times \frac{(J-\beta)^2}{(J-\alpha)^2 + 4g^2(J-\alpha)} \tag{24}$$

$$= \lim_{J\to\beta} \frac{2(J-\beta)(J-\alpha+2g^2) + (J-\beta)^2}{2(J-\alpha) + 4g^2}$$

$$= 0 \tag{25}$$

and we get the same result for the other elements of the matrix. Similarly we have calculated the Residue of f pole and we found it equal to $4g^2$.

Next consider the case when $\bar{t} \neq 0$ and write

$$\alpha = \bar{\alpha} + \Delta \tag{26}$$

eq. (21) now is given by (making use of eq. 26 and eq. 14);

$$\begin{aligned} J_f &= 1 + 2\Delta \\ J_\omega &= \beta \end{aligned} \tag{27}$$

From eq. (27) we conclude that for a reasonable value of Δ we get a pomeron intercept which is much above one. On the other hand the w Residue, vanishes independent of both Δ and $\bar{\alpha}$ (see eq. 25).

A similar calculation can be done in the case of SU(3), in this case the matrices of eqs. (18, 19) have three rows and three columns ($p\bar{p}$, $n\bar{n}$ and $\lambda\bar{\lambda}$). In the limit of exact SU(3) symmetry the three trajectories associated with the three types of quarks are exchange degenerate. Solving for det $(M^{-1} - C) = 0$ we get

$$\begin{aligned} J_f &= \alpha + 6g^2, \qquad J_\omega = \alpha \\ J_\phi &= \alpha - 6g^2, \qquad J_{f'} = \alpha \end{aligned} \tag{28}$$

The w and f' are not shifted by the cylinder correction because in the limit of exact SU(3) they become members of octets that do not

communicate with the cylinder. If, however, SU(3) symmetry is broken in the sense that the trajectory associated with the strange quarks is lower than the others, the four I = 0 trajectories will be shifted (Chew and Rosenzweig[28]).

4. The interference terms

As we mentioned earlier, the interference terms are those which have twists in the produced lines. The number of these terms is given by $(2^n.2^n-2^n)$ where n is the number of the produced objects in the intermediate states, the factor (-2^n) takes account of the sum of the planar and the cylinder terms. If we produce objects with positive and negative charge conjugation (e.g. vector and tensor mesons) we write

$$\varepsilon = \frac{\text{a twisted produced line}}{\text{an untwisted produced line}} = \frac{g_+^2 - g_-^2}{g_+ + g_-^2} \qquad (29)$$

where g_+ (g_-) refer to the couplings of objects with positive (negative) Charge Conjugation.

From eq. (29) we see that $-1 < \varepsilon < 1$, it will turn out, however, through the calculation in this section that a small negative value for ε is favourable.

4.1. Exotic exchange in the t-Channel.

Exotic exchange arises from diagrams where all produced lines are twisted, whether the exchanged reggeons are twisted or not. Thus we have

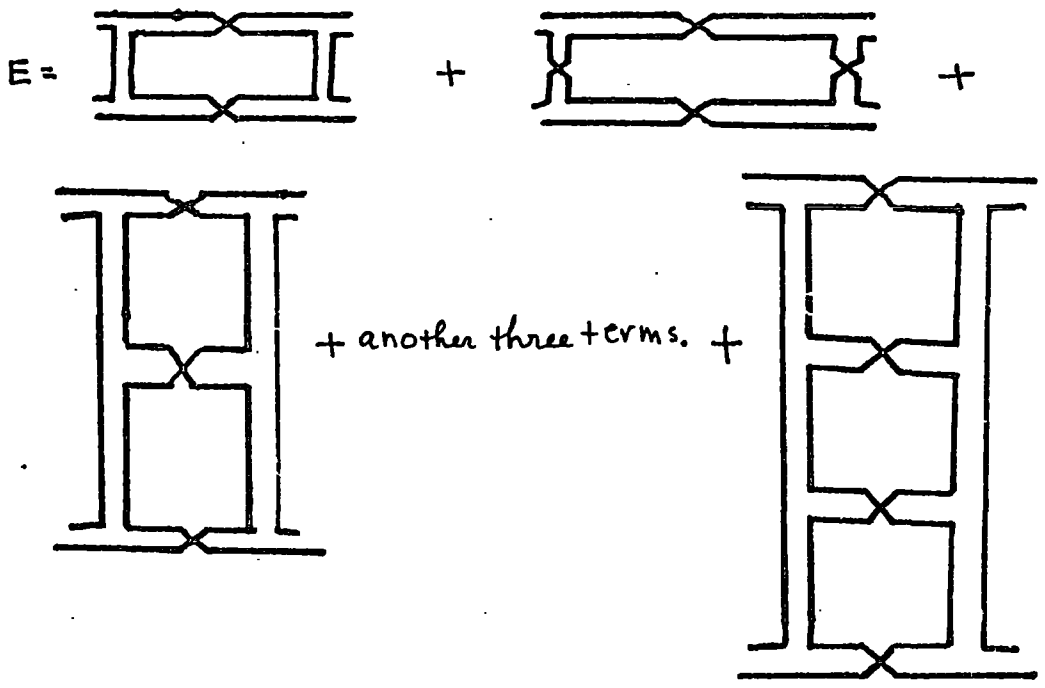

$$E = 2\frac{(2\hat{g}\epsilon)^2}{s-\beta} + 2^2\frac{(2\hat{g}\epsilon)^3}{(s-\beta)^2} + 2^3\frac{(2\hat{g}\epsilon)^4}{(s-\beta)^3} + \cdots$$

$$= 2\hat{g}\epsilon\left[\frac{4\hat{g}\epsilon}{s-\beta} + \frac{(4\hat{g}\epsilon)^2}{(s-\beta)^2} + \frac{(4\hat{g}\epsilon)^3}{(s-\beta)^3} + \cdots\right] = \frac{(2\hat{g}\epsilon)(4\hat{g}\epsilon)}{s-\beta-4\hat{g}\epsilon} \quad (30)$$

Hence

$$\alpha_E^{out} = \beta + 4\hat{g}\epsilon$$

$$\text{Residue} = 8g^4\epsilon^2 \quad (31)$$

It is worth mentioning that if we calculate the exotic exchange to lowest order in ϵ, i.e. taking the diagrams which have two produced lines only, we get

$$E = \frac{8g^4\epsilon^2}{s-\beta} \quad (32)$$

to be compared with eq. (30).

Finally we note that according to the second property of quark diagrams discussed in sub-section 3.2, the total contribution of the above series of diagrams to $I_t = 2$, $C_t = -$ Channel vanishes for each n. Since $G = (-1)^I C$, we have no output pole for the $I_t = 2$, $G_t = -$ - Channel.

4.2. The ρ - A_2 Splitting

To calculate the breading of exchange degeneracy between g and A_2 one must take into account all the quark diagrams which generate in the L.H.S. of the unitarity equation (1) the following U - t diagram

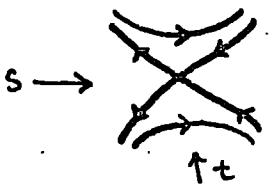

this is because this diagram contribute to N^2 plet of reggeons exchange in t-Channel, and it gives positive (negative) contribution to C_t=+(-) Channels.

We consider here the two loops diagram (lowest order in ϵ) which generate the above u-t diagram. The topology of these diagrams are that of the torus (b = 1, h = 1)

T = 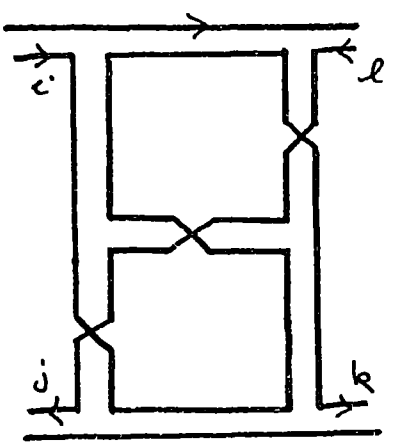

+ Complex Conjugate

the phase = 1

$$= 2\,(\pm 2g^2)(2g^2\epsilon)\,\frac{1}{(s-\beta)^2}\,\delta_{ik}\,\delta^{jl} \tag{33}$$

The amplitude F after the torus correction is given by

$$F = \sum_{n=0}^{\infty} (TA)^n A = \frac{1}{M^{-1} - C - T} \tag{34}$$

Since for ρ and A_2 the cylinder kernel vanishes (C = 0), det. $(M^{-1} - T) = 0$ gives

$$\frac{s-\alpha}{s-\beta} \pm \frac{2g^2(2g^2\epsilon)^2}{(s-\beta)^2} = 0 \quad \Rightarrow$$

$$s_\rho = \alpha - \frac{4\epsilon g^2}{N}, \qquad s_{A_2} = \alpha + \frac{4\epsilon g^2}{N}$$

$$\Rightarrow \qquad \alpha_\rho - \alpha_{A_2} = -\frac{8g^2\epsilon}{N} \tag{35}$$

Let us now see how we can arrive at the same result of eq. (35) by considering the two loops diagram (lowest order in ϵ) which generate the U-t diagram and the S-t diagram, these are

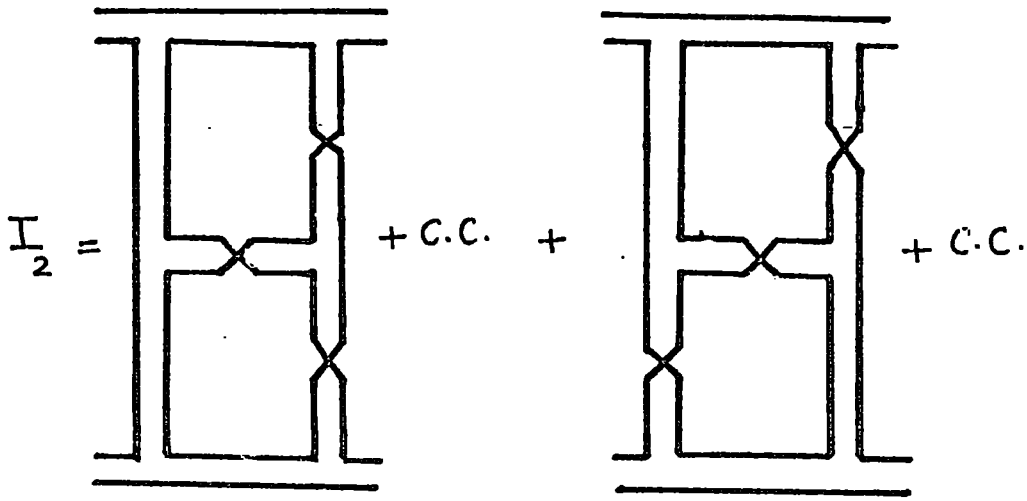

The phase = $e^{-2i\pi\alpha}$ The phase = 1

$$I_2 = (2g^2)^2 \in \frac{1}{(s-\beta)^2} \; 2\,(\cos 2\pi\alpha \pm 1)\, \delta_{c\cdot k}\, \delta^{jl} \tag{36}$$

The amplitude F including the interference terms of two loops (I_2) is given by

$$F = \sum_{n=0}^{\infty} (I_2 A)^n A = \frac{1}{M^{-1} - C - I_2} \tag{37}$$

For ρ and A_2 exchange in t-Channel the cylinder kernel vanishes, then det $(M^{-1} - I_2) = 0$ gives

$$\frac{J-\alpha}{J-\beta} - \frac{(2\tilde{g}^2)^2 \in 2(\cos 2\pi\alpha \pm 1)}{(J-\beta)^2} = 0 \qquad (38)$$

which gives

$$J_\rho = \alpha - \frac{8 \in \tilde{g}^2}{N} \sin^2 \alpha$$

$$J_{A_2} = \alpha + \frac{8 \in \tilde{g}^2}{N} \cos^2 \alpha \qquad (39)$$

hence

$$J_\rho - J_{A_2} = -\frac{8 \in \tilde{g}^2}{N}$$

4.3. The regeneration of W

The contribution of the interference terms with two loops only i.e. I_2, to W exchange in t-channel is given by (eq. 36)

$$I_2(\omega) = (2\tilde{g}^2)^2 \in \frac{1}{(J-\beta)^2} 2(\cos 2\pi\alpha - 1) \qquad (40)$$

$$= -4 \in \sin^2 \pi\alpha \left(\frac{2\tilde{g}^2}{J-\beta}\right)^2$$

On the other hand the amplitude A (the planar amplitude with the cylinder correction) vanishes for W exchange in t-channel, i.e.

$$A(\omega) = \frac{s-\beta}{J-\beta} \tag{41}$$

Thus the full amplitude F (the amplitude A with the interference terms I_2) gives for w exchange

$$F(\omega) = \frac{\text{Res.}}{J-\alpha_\omega} = A(\omega) + A(\omega)\, I_2(\omega)\, A(\omega) + \cdots$$

$$= 1 + \left(-4\epsilon \sin^2 \pi\alpha \frac{4g^2}{(J-\beta)^2}\right)$$

$$= \frac{1}{1 - \left[-4\epsilon \sin^2 \pi\alpha \frac{4g^2}{(J-\beta)^2}\right]}$$

$$= \frac{(J-\beta)^2}{(J-\beta)^2 - \left(-4\epsilon \sin^2 \pi\alpha \cdot (4g^2)\right)} \tag{42}$$

eq. (42) implies that we have two poles given by

$$F(\omega_1) = \frac{(J-\beta)^2 \Big/ \left[(J-\beta) + (-4\epsilon \sin^2 \pi\alpha \cdot 4\hat{q}^2)^{1/2}\right]}{(J-\beta) - (-4\epsilon \sin^2 \pi\alpha \cdot 4\hat{q}^2)^{1/2}} \tag{43}$$

$$F(\omega_2) = \frac{(J-\beta)^2 \Big/ \left[(J-\beta) - (-4\epsilon \sin^2 \pi\alpha \cdot 4\hat{q}^2)^{1/2}\right]}{(J-\beta) + (-4\epsilon \sin^2 \pi\alpha \cdot 4\hat{q}^2)^{1/2}} \tag{44}$$

hence

$$\alpha_\omega^{out} = \beta \pm 4\hat{q}^2 (-\epsilon)^{1/2} \sin \pi\alpha \tag{45}$$

4.4. The Violation of the IOZ rule.

In order to get a reggeon coupling which violates the IOZ rule, the first or/and the last produced line must be crossed (Fig. 7a, 7b). From Fig. 7a we see that the process which violates the IOZ rule is (to lowest order in ϵ) suppressed by a factor ϵ/N compared to the process which are given for example by Fig. 3 and which do not violate the IOZ rule. Hence from the experimental suppression of the IOZ rule violating process (Fig. 7a) we can estimate the strength of the coupling which violate the IOZ rule.

For the decay processes like $\phi \to \rho\pi$ or $\psi \to \rho\pi$ we are however in the time like region ($t = m_\rho^2$) and we have dynamical enhancements factors depending on the masses (asymptotic planarity). To see this consider for example the above decaying process, which by making use of semi-local duality and factorization gives

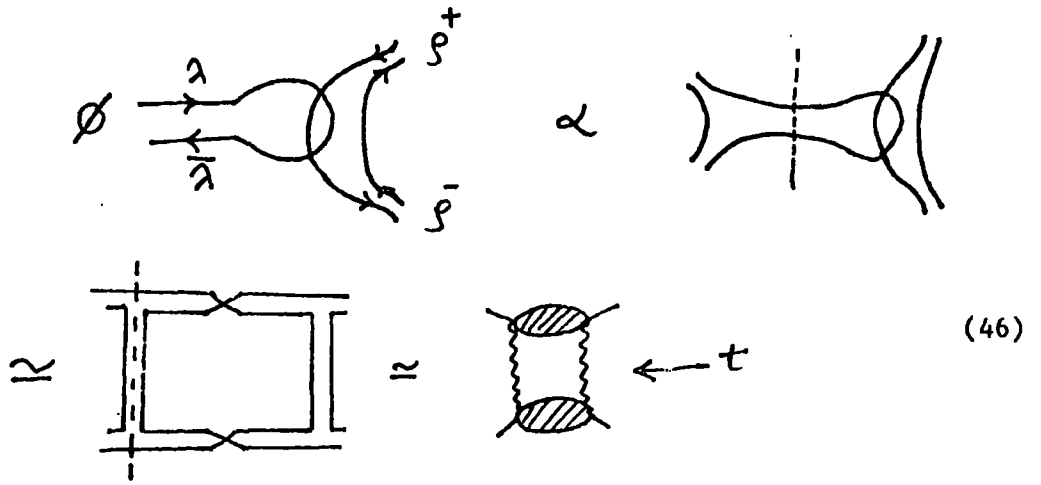

(46)

Thus the above type of decay has a Regge cut-like dependence on the masses of the decaying particles, which as $t \longrightarrow \infty$ is $\propto t^{-d}$ where d is positive. This explains for example why $\Gamma(\psi \rightarrow \rho\pi)$ is suppressed compared to $\Gamma(\phi \longrightarrow \rho\pi)$.

4.5. Numerical estimation of ϵ

From the previous calculations we see that the sign and the magnitude of the suppression factor ϵ is sensitive to many physical quantities. For example if ϵ is positive we get a positive intercept of the exotic exchange (eq. 31), a Complex ω pole (from eq. 45) and a wrong sign for the $\rho - A_2$ splitting (from eq. 35), three undesirable results. On the other hand if one assumes the production of vector and tensor mesons, a negative value for ϵ is a welcome result in view of the dynamical suppression of higher mass resonances, i.e. tensor mesons, (see eq. 29). Schmid, Webber and Sorensen[34] have used the experimentally measured suppression of exotic exchange reactions to determine ϵ by considering only the lowest order diagrams which give exotic exchange, i.e. eq. 32. Since, however, the cross-section of these processes is proportional to ϵ^4, the sign of ϵ is irrelevant. They found that $\epsilon \approx |0.25|$. From the above considerations we take the negative sign. With $\epsilon \simeq -0.25$ we have the following interesting results.

(1) The ρ - A_2 splitting

Since $\alpha_\rho - \alpha_{A_2} = -8g^2\epsilon/N$, making use of the bootstrap condition

$2g^2N = 1-\alpha \simeq 0.5$, we get

$$\alpha_\rho - \alpha_{A_2} = 0.125 \quad \text{for } N=2 \tag{47}$$

$$\alpha_\rho - \alpha_{A_2} = 0.08 \quad \text{for } N=2.5$$

(2) The Residue and intercept of W pole

For obvious reason we consider eq. (43) for the ω pole. The intercept is given by (we take N = 2),

$$\alpha_\omega = \beta + 4g^2(-\epsilon)^{1/2} \sin \pi\alpha$$

$$\Delta\alpha_\omega = 4g^2(-\epsilon)^{1/2} \sin\pi\alpha \simeq 0.25 \tag{48}$$

the Residue is given by (from eq. 43)

$$\text{Res.} = \frac{[4g^2(-\epsilon)^{1/2} \sin\pi\alpha]^2}{2[4g^2(-\epsilon)^{1/2}\sin\pi\alpha]} = \frac{1}{2}[4g^2(-\epsilon)^{1/2}\sin\pi\alpha]$$

$$= 0.13 \tag{49}$$

to be compared with the Residue of the planar W (from eq. 13)

$$\text{Res.}_{\omega}\ (\text{planar}) = (\mathbb{J}-\beta) = 2\hat{g}N \simeq 0.5 \tag{50}$$

Where we have taken $\alpha \simeq 0.5$, since it satisfies the consistency condition $\alpha = \alpha(\bar{\epsilon})$ if $\bar{\epsilon}$ is not too large.

(3) The exotic exchange

The intercept of Exotic exchange is (from eq. 31)

$$\alpha_E = \beta + 4g^2\epsilon = -0.13 \tag{51}$$

and The Residue

$$\text{Res.}_{E} = 8g^4\epsilon^2 = 0.008 \tag{52}$$

Notice, however, that it is wrong to compare this result with the planar residue $2g^2N = 0.5$. The reason for this is that, in writing eq. (13), the external legs were amputated. If they were included, the planar Reggeon residue would be $2g^2(2g^2N)$, instead of $(2g^2N)$. Thus the Exotic residue which is comparable with the planar residue is given by

$$\text{Res.}_{E} = \frac{8g^4\epsilon^2}{2g^2} = 4g^2\epsilon^2 = 0.03 \tag{53}$$

5. Remarks

(i) The Pomeron f identity.

In sub-section 3.3 we discussed the effect of the cylinder correction to the planar approximation. No new poles were generated at the cylinder level, and the effect of the cylinder is to shift the I = 0 planar poles. The planar f is shifted upwards and is identified near t = 0 with the bare pomeron. This picture which was suggested by Chew and Rosenzweig[28] is in contrast with the standard picture in Reggepole models, where there is an f, exchange degenerate with the ω, and a pomeron whose intercept is about 0.5 higher. Although the Chew-Rosenzweig scheme did pass some experimental tests,[31,32] the recent data on Vector Meson production (D.W. DUKE[35]) Cannot be described by this scheme. On the other hand the standard picture, i.e. ω-f EXD model, can adequately describe the data.

(ii) Two-Vacuum trajectories

Having seen from the recent data on Vector Meson Production, the need for two Vacuum trajectories, one would like to ask whether the existence of such two Vacuum trajectories are consistent with the topological expansion. In Ref. (36) Veneziano showed that the unitarity condition for h = 0 (no-handles) implies that factorizable poles appear in $\bar{C}$ (= p + C, the plane plus the Cylinder) and not in C alone. The Chew-Rosenzweig scheme not only satisfies this requirement but also makes the total number of poles in $\bar{C}$ the same as in P. Veneziano[36] suggested an alternative scheme which satisfies the above requirement, and which ends up with two Vacuum trajectories.

(iii) The Regenerated ω.

The intercept of the regenerated ω is still low (eq. 48) but perhaps not very far from the physical ω. The residue, however, is too small compared to the planar one (see eqs. 49, 50).

Figure captions

Fig. 1 : The four point function planar dual diagram

Fig. 2 : The one planar loop.

Fig. 3 : The two planar loop diagram

Fig. 4 : A two non-planar loop diagram which is suppressed by a factor $1/N$ compared to Fig. 3.

Fig. 5 : A two-non planar loop diagram which is suppressed by a factor $1/N^2$ compared to Fig. 3.

Fig. 6 : The topological equivalence between the cylinder and a non-planar one loop with vacuum Q.N. in t-channel.

Fig. 7 : Lowest order diagrams violating IOZ rule, 7a single disconnected 7b double disconnected.

Fig. 8 : The two-loop interference kernel H_2 which gives the $g - A_2$ splitting.

(a) The quarks have the same orientation at both ends of the diagram.

(b) The quarks have opposite orientation at the ends of the diagram.

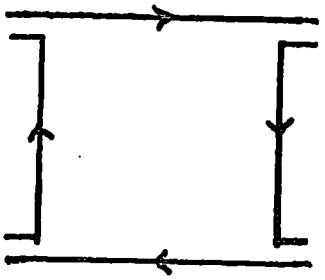

Fig. 1

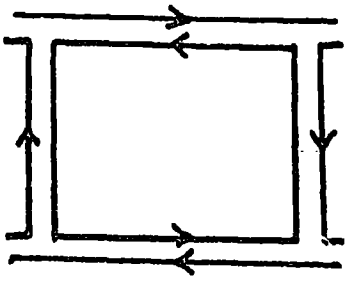

Fig. 2

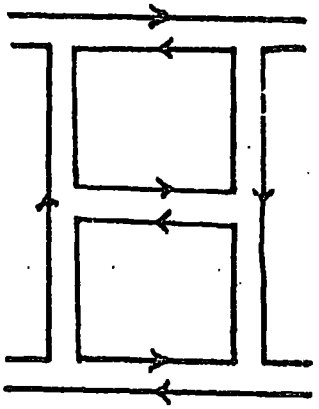

Fig. 3

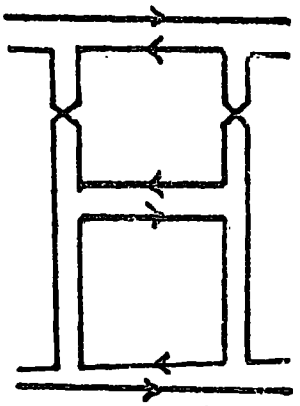

Fig. 4

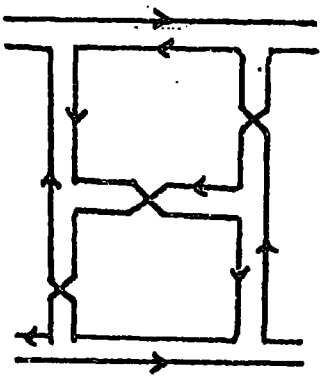

Fig. 5

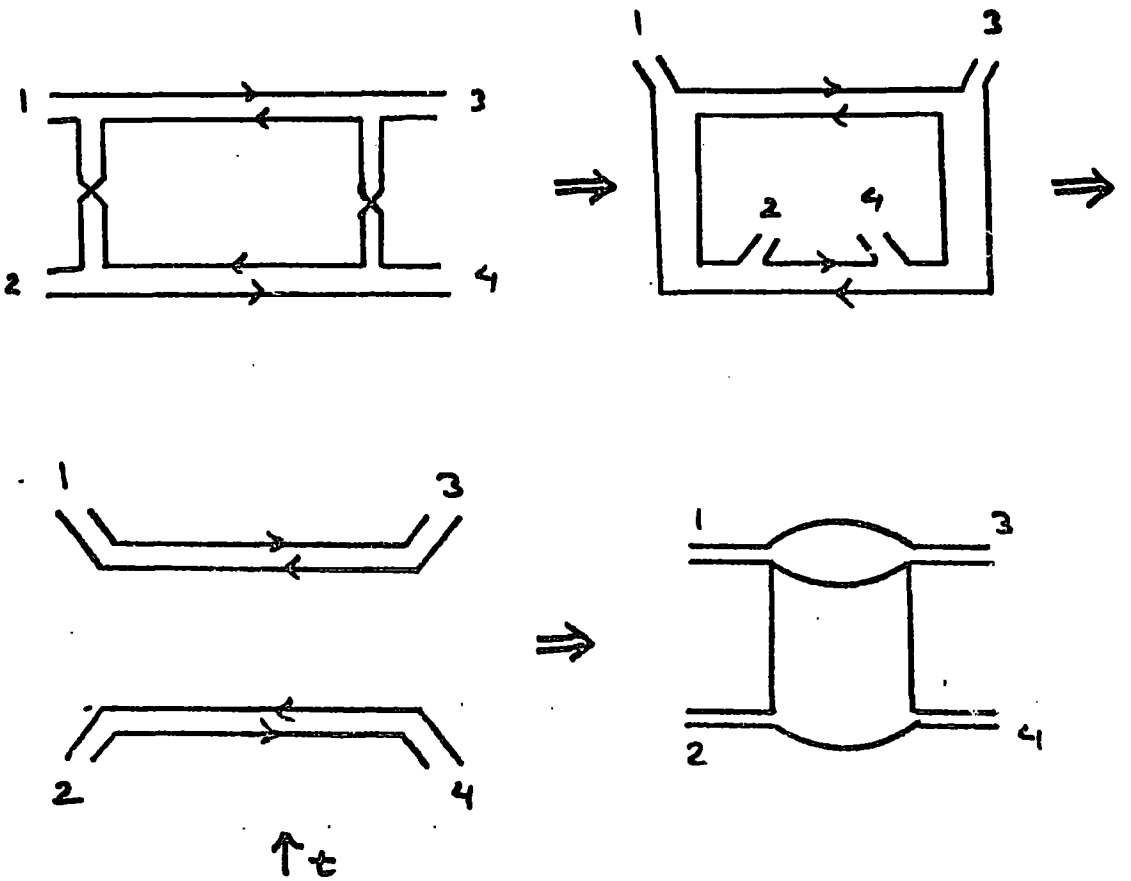

Fig. 6

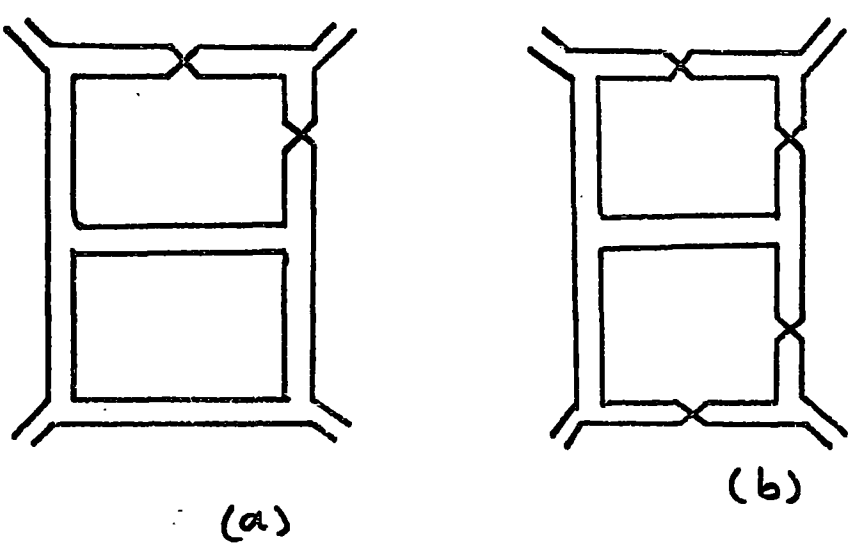

Fig. 7

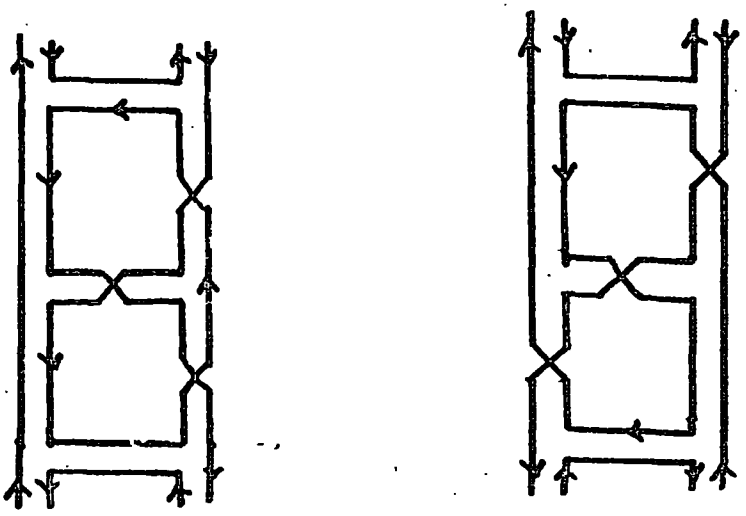

(a) (b)

Fig. 8

CHAPTER III

Unitarity, Pion Production and Exotic Trajectories[39]

1. Introduction

In the previous chapter we discussed several attempts to construct t-channel Regge trajectories from multi-particle s-channel unitarity both in the framework of the topological expansion and explicit s-matrix models.

We found from both approaches that, in order to get a suppressed exotic in the output, some sort of an incomplete cancellation should take place between the contributions of the produced objects of positive and negative C-parity, e.g. vector and tensor mesons. In addition to this, the assumption that vector and tensor mesons dominate multi-particle unitarity is justified experimentally[37] where about 60% - 80% of the produced pions are estimated to come from the decay of non strange vector and tensor mesons.

It is well known, however, that the exact unitarity equation includes only stable particles in the intermediate states, and attempts to rewrite the unitarity equation in terms of resonances or "clusters" lead to problems of double counting, etc. Some of these problems are discussed by Freeman, Zarmi and Veneziano,[38] who avoid them only by ignoring the resonances and working in an approximation in which pions are directly produced.

In this chapter we will consider a model with only pions as produced particles (in fact we should consider the production of $O^-(\pi, \eta)$ quartet. Since, however, η production is suppressed due to its high mass, we ignore η production here. In the next chapter the effect of η production will be taken into account). In our work we endeavour to see how the pion production model of CH. II, section 2 can be improved so that a more reasonable output is obtained. In one sense our problem must have a solution since if

we know the amplitude $ab \longrightarrow n$, where n is a state of n pions then Im ($ab \longrightarrow ab$) is completely determined by unitarity and will inevitably yield the experimentally observed trajectories. However it is not clear whether a satisfactory result can be obtained with a reasonably simple (i.e. multi-Regge type) description of the $ab \longrightarrow n$ amplitudes. We shall assume a multi-Regge form for $ab \longrightarrow n$ amplitudes; i.e. we order the produced pions in rapidity and approximate each sub-energy by its Regge form (see Fig. 1). The t-integrations are performed by the simple expedient of replacing functions of t by suitable averages.[13] For the exchange reggeons we consider only vector and tensor trajectories, we neglect sister trajectories and the unnatural parity exchanges. The exchange degeneracy of the input trajectories (ρ, ω, f, A_2) is not assumed. As a result of this the Pomeron exchange is not neglected completely in the input, its contribution comes through the inclusion of f which is higher than the others. In addition to vector and tensor trajectories, we include I = 2 trajectories in the input. It will turn out that both of these effects (i.e. the inclusion of I_2 = exchange and breaking of EXD) improves the output spectrum.

In the next section we introduce our model. The coupling and signature matrices are given in Section 3. Section 4 contains the results when I = 2 input is neglected. Its lowest order contribution is discussed in Section 5. Finally Section 6 is devoted to conclusions and some remarks.

2. The Model

We use the simplified form of the multi-Regge model of reference (13). The contribution to unitarity of the diagram depicted in Fig. 2, summed over the number of rungs (pions), is denoted by $A_{(i_1 i_2)(j_1 j_2)}$. In matrix notation we write

$$\underset{\sim}{A} = \underset{\sim}{V} + \underset{\sim}{V}\,\underset{\sim}{Q}\,\underset{\sim}{V} + \cdots \qquad (1)$$

$$= \underset{\sim}{V} + \underset{\sim}{V}\,\underset{\sim}{Q}\,\underset{\sim}{A}$$

where V has elements given by

$V_{(i_1 i_2)(j_1 j_2)}$ =

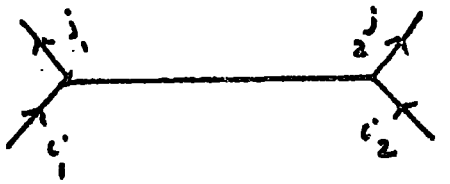

(2)

and Q is a diagonal matrix with elements

$$Q_{(i_1 i_2)(i_1 i_2)} = \frac{\xi^*_{i_1}\ \xi_{i_2}}{J - \bar{\alpha}_{i_1} - \bar{\alpha}_{i_2} + 1} \qquad (3)$$

Here ξ_{i} is the signature factor of the i^{th} trajectory

$$\xi_{i} = e^{-i\pi\bar{\alpha}_i} \pm 1 \qquad (4)$$

with $\pm$ corresponding to even/odd signature, and $\bar{\alpha}_i$ is the i^{th} trajectory taken at a suitable value of t. In fact we choose $t = -0.1\ \text{Gev}^2$.

It is convenient to define

$$\tilde{\underset{\sim}{A}} = \underset{\sim}{Q}^{1/2}\, \underset{\sim}{A}\, \underset{\sim}{Q}^{1/2}$$

$$\tilde{\underset{\sim}{V}} = \underset{\sim}{Q}^{1/2}\, \underset{\sim}{V}\, \underset{\sim}{Q}^{1/2} \qquad (5)$$

So that eq. (1) becomes

$$\tilde{\underset{\sim}{A}} = \tilde{\underset{\sim}{V}} + \tilde{\underset{\sim}{V}}\, \tilde{\underset{\sim}{A}} \qquad (6)$$

$$\tilde{\underset{\sim}{A}} = (\underset{\sim}{1} - \tilde{\underset{\sim}{V}})^{-1}\, \tilde{\underset{\sim}{V}} \qquad \text{(see Fig. 3)} \qquad (7)$$

The leading output Regge trajectory (at t = 0) is then the highest value of J for which det $(\underset{\sim}{1} - \tilde{\underset{\sim}{V}}) = 0$. We calculate this for I = 0,1,2,3 and for even and odd G - parity.

3. The Coupling and Signature Matrices

For the sake of completeness we write down here the matrices $\tilde{\underset{\sim}{V}}$ of eq. (5). In fact because of the redefinition of $\tilde{\underset{\sim}{V}}$ in eq. (5); these matrices are symmetric. Since we have six exchanged trajectories (f, w, ρ, A_2, x, y; x is an exotic state with positive G-parity and positive signature, y is an exotic state with negative G-parity and negative signature), it turns out that we will have in general 36 pairs intermediate states (1_1 and 1_2 in Fig. 3). Since however we exclude (I = 2, I = 2) intermediate states and since we conserve I-spin and G-parity in the model, the relevant intermediate states are:

i) for the f - exchange amplitude in t - channel,

$$(\ell_1, \ell_2) = (\rho, \rho), (A_2, A_2), (f, f), (\omega, \omega).$$

ii) for the w - exchange amplitude in t - channel,

$$(\ell_1, \ell_2) = (f, \omega), (\omega, f), (A_2, \rho), (\rho, A_2).$$

iii) for theρ - exchange amplitude in t - channel

$$(\ell_1, \ell_2) = (\rho, \rho), (A_2, A_2), (\rho, f), (f, \rho), (\rho, x), (x, \rho), (A_2, y), (y, A_2).$$

iv) for the A_2 - exchange amplitude in t - channel,

$$(\ell_1, \ell_2) = (\rho, \omega), (\omega, \rho), (f, A_2), (A_2, f), (A_2, \rho), (\rho, A_2), (x, A_2), (A_2, x), (y, \rho), (\rho, y).$$

v) for the x - exchange amplitude in t - channel,

$$(\ell_1, \ell_2) = (\rho, \rho), (A_2, A_2), (\omega, y), (y, \omega), (f, x), (x, f), (\rho, x), (x, \rho), (A_2, y), (y, A_2).$$

vi) for the y - exchange amplitude in t - channel,

$$(\ell_1, \ell_2) = (A_2, \rho), (\rho, A_2), (x, A_2), (A_2, x), (y, \rho), (\rho, y), (x, \omega), (\omega, x), (y, f), (f, y).$$

For the residue we put

$$G_1 = G^{\pi^+}_{A_2^+ \rho^0} \tag{8}$$

$$G_2 = G^{\pi^+}_{A_2^+ f} = G^{\pi^+}_{\rho^+ \omega} \tag{9}$$

$$g = \bar{G}^{\pi}_{x A_2} = \bar{G}^{\pi}_{y g} \tag{10}$$

$$g' = \bar{G}^{\pi}_{x y} \tag{10^1}$$

The equality in eq. (9) would follow from exchange degeneracy. We assume it here to reduce the number of input parameters - relaxing it would allow some improvement of the output but since it already reasonable we do not consider this necessary at this stage. Notice also that in eqs. (10) and (10^1) we have defined what we call "the reduced coupling" which is independent of I_3 of the particles, and it is related to the couplings when we have definite I_3 for the particles by

$$G(a \to b+c) = \langle I_b, I_c, I_{3b}, I_{3c} \mid I_a, I_{3a} \rangle \bar{G}(a \to b+c)$$

Finally for the I-spin crossing matrices, we follow reference (14) and we calculate them in terms of 6-j symbol; (see appendix A). The $\underset{\sim}{\tilde{V}}$ matrices are:

f : I=0, G(+), τ=+1

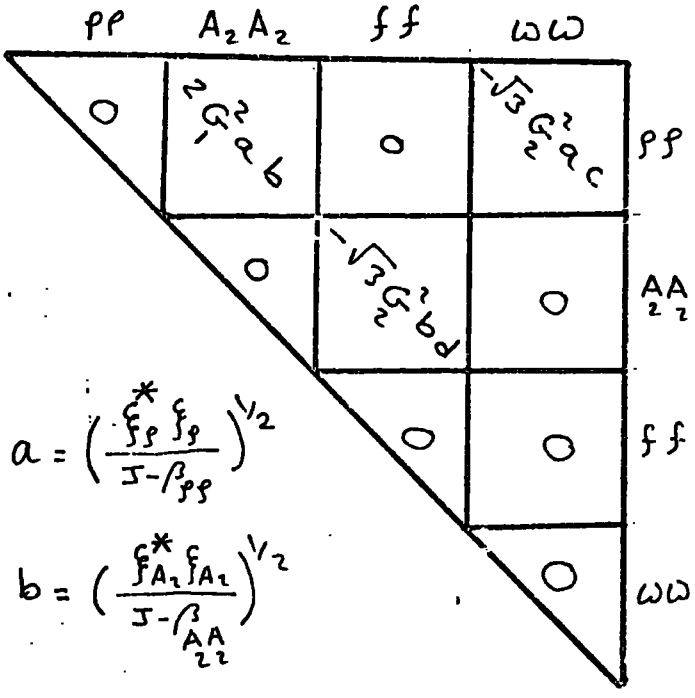

where for example $a = \left(\frac{f_\rho^* f_\rho}{I - \beta_{\rho\rho}}\right)^{1/2}$

$b = \left(\frac{f_{A_2}^* f_{A_2}}{I - \beta_{A_2A_2}}\right)^{1/2}$

ω : I=0, G(−), τ=−1

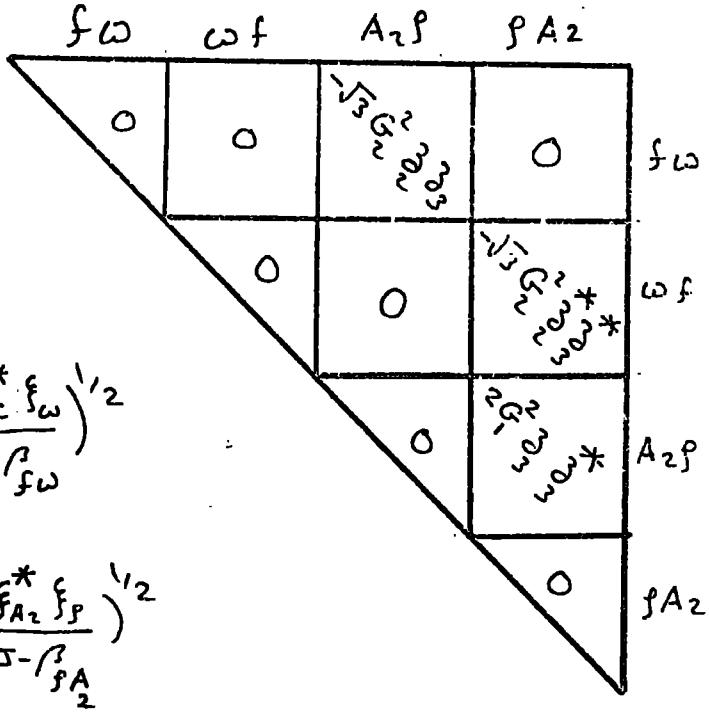

where $g_2 = \left(\frac{f_f^* f_\omega}{I - \beta_{f\omega}}\right)^{1/2}$

$g_3 = \left(\frac{f_{A_2}^* f_\rho}{I - \beta_{\rho A_2}}\right)^{1/2}$

ρ: $I=1$, $G(+)$, $\tau=-1$

	$\pi\pi$	A_2A_2	ρf	$f\rho$	$\rho\chi$	$\chi\rho$	$A_2\gamma$	γA_2
$\pi\pi$	0	$\frac{1}{2}g_{\rho\pi\pi}^2$	0	0	0	0	$\frac{1}{\sqrt{2}}g_{\rho\pi\pi}g_{\rho\pi\gamma}$	$\frac{1}{\sqrt{2}}g_{\rho\pi\pi}g_{\rho\pi\gamma}^*$
A_2A_2		0	$-\frac{1}{\sqrt{2}}g_{\rho\pi\pi}g_{f\pi\pi}$	$-\frac{1}{\sqrt{2}}g_{\rho\pi\pi}g_{f\pi\pi}^*$	$\frac{1}{\sqrt{2}}g_{\rho\pi\pi}g_{\chi\pi\gamma}$	$\frac{1}{\sqrt{2}}g_{\rho\pi\pi}g_{\chi\pi\gamma}^*$	0	0
ρf			0	0	0	0	0	$g_{f\pi\gamma}g_{\rho\pi\pi}$
$f\rho$				0	0	0	$g_{f\pi\gamma}g_{\rho\pi\pi}$	0
$\rho\chi$					0	0	$\frac{1}{\sqrt{10}}g_{\chi\pi\gamma}g_{\rho\pi\pi}$	$\frac{1}{\sqrt{10}}g_{\chi\pi\gamma}g_{\rho\pi\pi}$
$\chi\rho$						0	$\frac{1}{\sqrt{10}}g_{\chi\pi\gamma}g_{\rho\pi\pi}$	$\frac{1}{\sqrt{10}}g_{\chi\pi\gamma}g_{\rho\pi\pi}$
$A_2\gamma$							0	0
γA_2								0

E.G. $Z_2 = \left(\frac{f_{A_2}^* f_\gamma}{1-\beta_{A_2\gamma}}\right)^{1/2}$

and so on..

A_2 : $I=1$, $G(-)$, $\tau=+1$

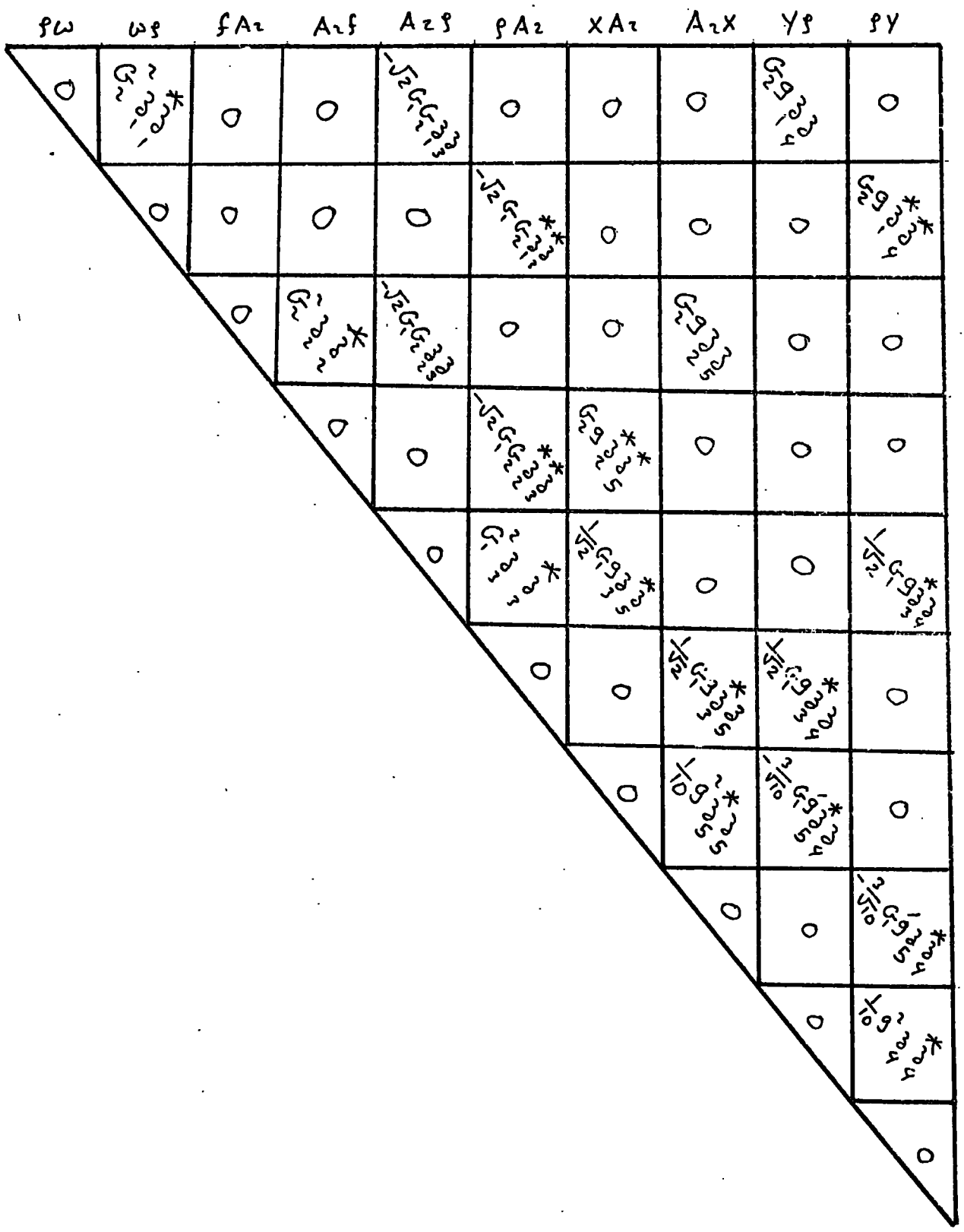

X : $I=2,\ G(+),\ \mathcal{C}=+1$

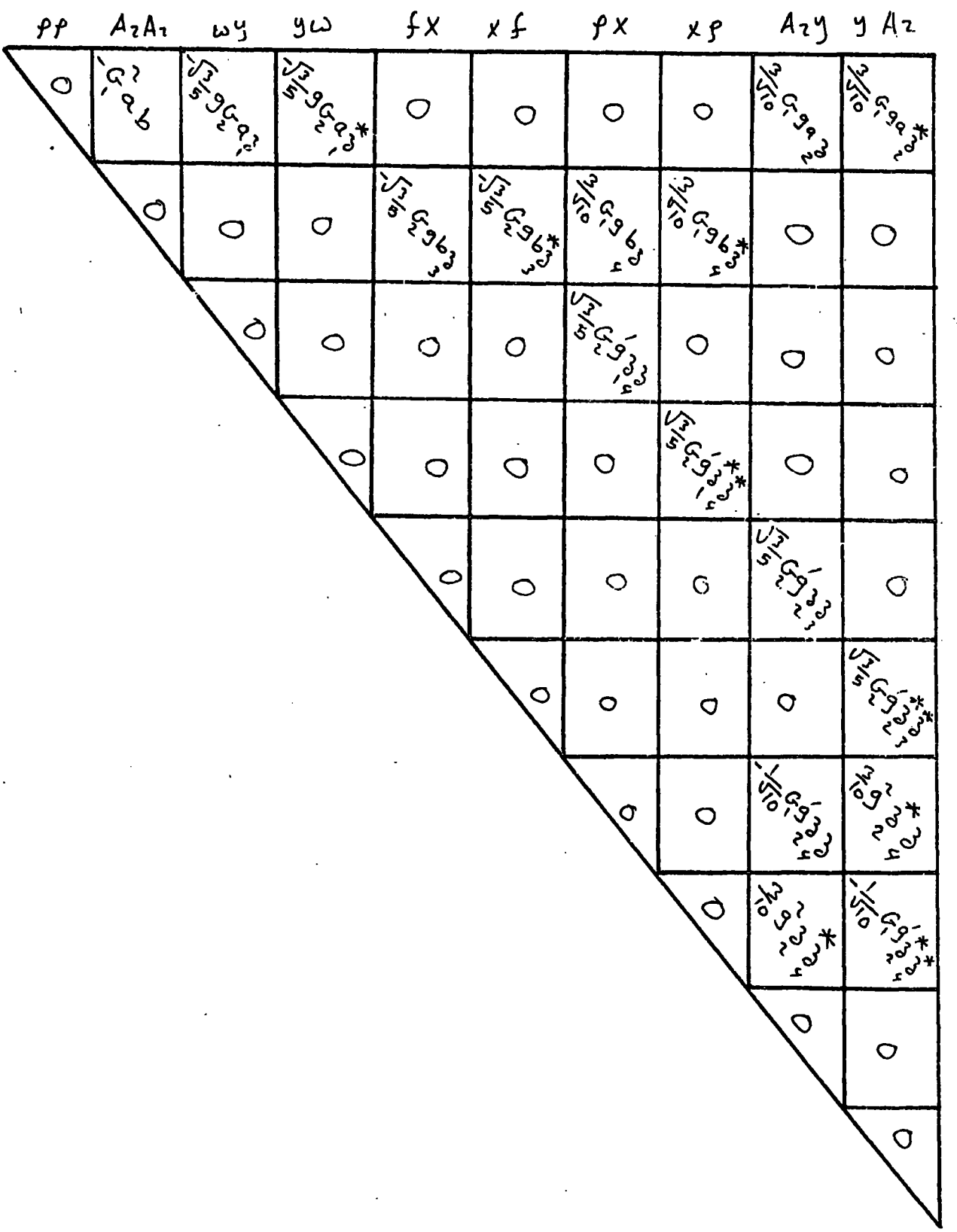

$Y: I=2, G(-), \tau=-1$

Z: I=3, G(+)

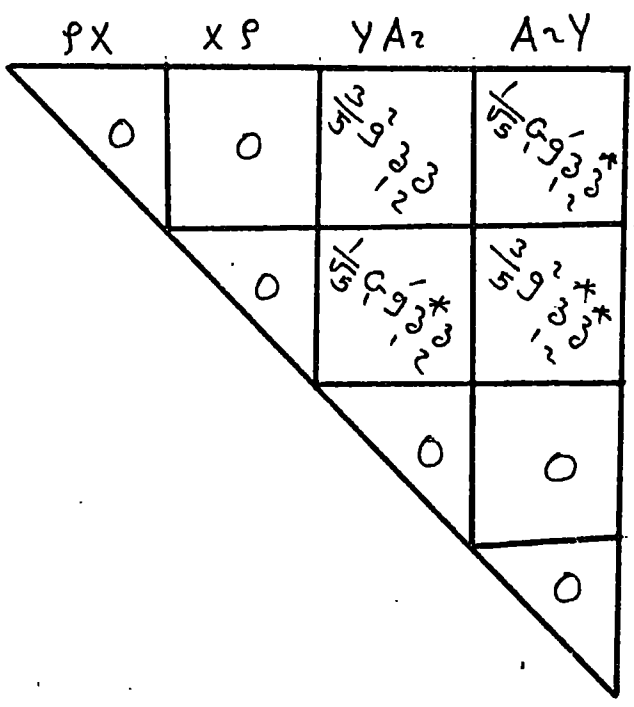

W: I=3, G(-)

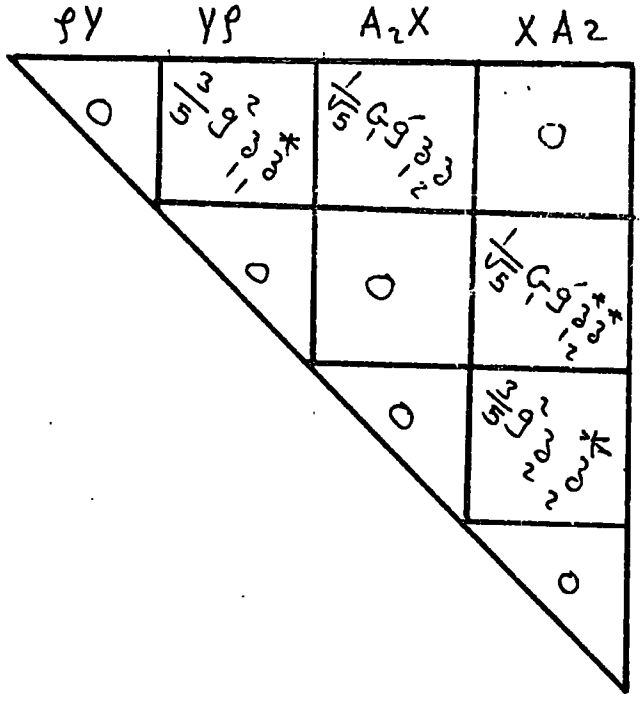

The small letters a, b, c, d and z^0s which appear in the preceding $\underset{\sim}{\tilde{V}}$ matrices represent the appropriate elements of the $Q^{\frac{1}{2}}$ matrices (see eq. 3). To illustrate the calculation of the $\underset{\sim}{\tilde{V}}$ matrices elements, we do this here for the element which appears in the first row and third column in Y matrix. For this element, we have in s-channel the I = 1 process;

$$X A_2 \longrightarrow A_2 \rho$$

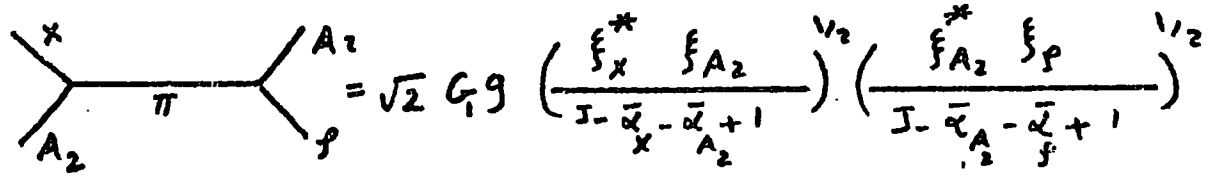

$$= \sqrt{2}\, G_1 g \left(\frac{\xi_X^* \xi_{A_2}}{J - \bar{\alpha}_X - \bar{\alpha}_{A_2} + 1}\right)^{1/2} \left(\frac{\xi_{A_2}^* \xi_\rho}{J - \bar{\alpha}_{A_2} - \bar{\alpha}_\rho + 1}\right)^{1/2}$$

$$= \sqrt{2}\, G_1 g\, \delta_5^*\, \delta_3 \qquad (8)$$

Notice that because π^+ is linear combination of $(A_2^+ \rho^0$ and $A_2^0 \rho^+)$ and because we did not include this effect in the definition of G_1, we have an additional $\sqrt{2}$ in front of G_1.

But the crossing matrix element for the above process when X is exchanged $(I^t = 2)$ is given by

$$\left(X\right)_{t,S\ \ 2,1} = 3/2\sqrt{5} \qquad (9)$$

hence

$$A(X\bar{A}_2 \xrightarrow[I=2]{X} \bar{A}_2 \rho) = \frac{3}{2\sqrt{5}}\, A(X A_2 \xrightarrow[I=1]{\pi} A_2 \rho)$$

$$= \frac{3}{2\sqrt{5}} \sqrt{2}\, G_1 g\, \delta_5^*\, \delta_3 = \frac{3}{\sqrt{10}}\, G_1 g\, \delta_5^*\, \delta_3$$

4. Evaluation of Regge trajectories without exotic input

In this section we calculate the leading output Regge trajectories (at t = 0) by solving the equations $\det\left(\underset{\sim}{1} - \underset{\sim}{\tilde{V}}_0\right) = 0$ for the highest value of J. The input to the calculation is the values of $\bar{\alpha}$ for ρ, A_2, ω and f. We take these to be reasonable experimental values of the trajectories at $t = -0.1\ (\text{Gev})^2$. For the f we take a value midway between the "pomeron" at $\alpha(0) = 1$ and the exchange degenerate f at $\alpha(0) \simeq 0.5$. This is either the "unflavoured" $\mathbb{P} = f$ of dual unitarisation theory, or it is a phenomenological "average" of the $\mathbb{P}$ and the f. We take

$$\bar{\alpha}_\omega = \bar{\alpha}_{A_2} = 0.3 \tag{10}$$

$$\bar{\alpha}_\rho = 0.4 \tag{11}$$

$$\bar{\alpha}_f = 0.7 \tag{12}$$

Since the extra effects (the exotic exchange effects) do not affect the w and f trajectories (because we do not consider $(I = 2,\ I = 2)$ intermediate states), we choose G_1^2 and G_2^2 to give the correct experimental output for $\alpha_\omega = 0.4$ and $\alpha_f = 0.8$. This requires

$$\begin{aligned} G_1^2 &= 0.216 \quad , \quad G_2^2 = 0.13 \\ G_1 &= 0.46 \quad , \quad G_2 = 0.36 \end{aligned} \tag{13}$$

The resulting output trajectories are shown in the first column of table (1). We see that the results are encouraging. In particular we obtain a reasonable value for the ρ output, the correct sign and magnitude for the $\rho - A_2$ splitting and values of α_x and α_y which show considerable suppression of exotics.

Before we close this section we would like to mention that in order to generate an output w - trajectory, it is necessary not only to break exchange degeneracy between the trajectories, but also between the couplings. First of all in the models where one assumes the degeneracy of the trajectories; the interference terms of trajectories with opposite signatures do not contribute to the overlap function. Since the two corresponding Regge exchanges for the w-exchange amplitude in t-channel are (w, f) and (ρ, A_2), the above assumption prevents the generation of an output w - trajectory. In the model we are considering we are able to generate w - pole because we do not assume exchange degenerate trajectories However from w matrix the equation $\det(\underset{\sim}{1} - \underset{\sim}{\tilde{V}}) = 0$ gives (after putting $J = \alpha_w^{out} = 0.4$)

$$1 + 33.11\, G_2^4 + 342.72\, G_2^8 = 8.97\, G_1^4 \qquad (14)$$

which shows that G_1 must be different from G_2 in order to obtain physically acceptable values for these coupling constants. E.g. if we take $G_1 = G_2 = G$, eq. (14) gives:

$$G^4 = -0.07 \pm i\,0.08 \qquad (14')$$

5. The effect of I = 2 exchange

We allow the possibility of X and Y exchange by introducing the vertices g of equation (10). We do not of course have experimental information on the trajectories $\bar{\alpha}_X$ and $\bar{\alpha}_Y$ so we take values which agree reasonably well with our output, i.e.

$$\bar{\alpha}_X = \bar{\alpha}_Y = -0.2 \tag{15}$$

The method we have used to calculate the effect of these exchange is discussed in details in Appendix B (in fact we evaluate, to lowest order in g^2, the effect of X and Y exchange on our ρ, A_2, X and Y trajectories).

It turns out that, due to the size of the matrix $\tilde{V}$ for A_2 (previous section) this procedure would be very complicated in this case, for this reason we have calculated the effect of ρ A_2 splitting in the $\tilde{V}$ matrix of A_2 in two ways. First; we ignore the ρ A_2 splitting in the unperturbed calculation "the calculation of section 4", thereby obtaining an output

$$\alpha_{A_2} = 0.21 \tag{16}$$

Now if we include the effect ρ A_2 splitting in the exact calculation of section 4, we obtain

$$\alpha_{A_2} = 0.36 \tag{17}$$

On the other hand, the contribution of ρ A_2 splitting calculated in the perturbation method of this section is 0.17, whereas equations (16), (17) show that its contribution calculated exactly is 0.15. We conclude that this effect, for the A_2, may be treated in lowest order (effectively this means that we ignore cross-terms between (ρ A_2) splitting effects and X/Y effects).

The Final results are shown in the second column of table (1). We note that g^2 has a much greater effect on X, Y than on ρ, A_2. For $g^2 > 0$ the effect is to lower the exotic trajectories. Values similar to those given in eq. (13) take both α_X and α_Y below zero - which is probably adequate for this type of calculation. The value of α_{A_2} is excellent but α_ρ comes out too small by approximately 0.1. Tentatively we attribute this to the fact that we have ignored the pion trajectory in the input, since it is well known that the (2π) state makes some contribution to the physical ρ.

Finally, we have calculated the positive and negative G, I = 3 trajectories (Z & W) which we now obtain

$$\alpha_Z^{out} \simeq -0.85 + \left[0.89^4 + 0.6 g^2 g'^2\right]^{1/2} \qquad (18)$$

$$\alpha_W^{out} \simeq -0.9 + \left[2.19^4 + 0.6 g^2 g'^2\right]^{1/2} \qquad (19)$$

With reasonable values of g^2 and g'^2, there does not seem to be any danger of these trajectories rising too high.

6. Conclusion and final remarks

As we have mentioned in the introduction an exact description of the $ab \longrightarrow n$ amplitudes will inevitably lead, through unitarity, to the observed Regge trajectories. We have used a very simplified form of the multi-Regge form for the amplitudes, with realistic input trajectories and obtained reasonable values for the output $I = 0, 1, 2, 3$. From the table of the results we see that;

(i) The Breaking of Exchange degeneracy plays an important role in making a significant difference between the $I = 1$ and $I = 2$ output (see the first column of the table).

(ii) The exotic exchange (see the second column of the table) has much greater effect on X, Y than on ρ, A_2. This effect (for $g^2 > 0$) is in the right direction (apart from ρ !). e.g. the lowest order calculation of this effect pushes Y down by $(-1.76\ g^2)$ and A2 up by $(+\ 0.1\ g^2)$. However one may well ask whether this suppression of exotics is sufficient. The data (see the discussion in ref. 13) for example may well require much smaller values of α_{exotic}. In fact in refs. (13, 17) (see also Ch. 2, § 2) it is shown that a complete cancellation in the unitarity sum for exotic exchange requires the production of $\bar{1}$ and 2^+ with equal strength, and it is unlikely that these cancellations would arise from the type of calculation performed here.

(iii) The sign of ρ A_2 splitting is right, but the amount of ρ A_2 splitting is small (e.g. for $g^2 = 0.1$ $\quad \alpha_\rho - \alpha_{A_2} \simeq 0.05$).

(iv) The pomeron of the model is the f. we have only one vacuum trajectory lying above the others. In fact with G_1^2 and G_2^2 given by eq. (13), the equation $\det (\underset{\sim}{1} - \underset{\sim}{\tilde{V}}(f)) = 0$ gives

$$J^4 + 0.6J^3 - 1.09J^2 - 0.176J + 0.126 = 0$$

From which we find that the highest root is $J = 0.8$, and the second one is at $J = 0.3$

Supplement: Repeating the calculation with $\alpha_f^{out}(0) = 0.6$

Since in Ch. V, we will find that the one ladder vacuum trajectory is capable to reproduce the experimentally observed multiplicity and charge exchange ratios at energies $S < 40$ Gev^2, and at high energy one needs the multi-ladder vacuum trajectory to explain these effects. We use these multi-ladder diagrams to create a new high lying vacuum singularity (the Pomeron) in which case we do not have the $\mathbb{P} = f$ relation so we expect the f to be lower.

For this reason we take e.g. $\alpha_f^{out}(0) = 0.6$. With regard to $\bar{\alpha}_f$ we still consider it at 0.7, this is because both f and some of the promoted f (The $\mathbb{P}$) are expected to contribute to the input vacuum trajectory. If we repeat the calculation of section 4 Now, we obtain;

$$G_1^2 = 0.2 \qquad G_2^2 = 0.11$$
$$G_1 = 0.45 \qquad G_2 = 0.33 \tag{20}$$

to be compared with those of eq. (13).

Finally, with the values of G_1 and G_2 given in (20), we repeat the calculation of sections 4 & 5 and the results are shown in table 2. The effect is to reduce α^{out} in the first column by approximately 0.03 (apart from f), while the values of the second column stay almost the same.

TABLE 1

Trajectory	Calculation without X&Y	Final results
W	0.4	0.4 (fitted)
f	0.8	0.8 (fitted)
ρ	0.44	$0.44 - 0.2g^2$
A_2	0.36	$0.38 + 0.1g^2$
X	0.17	$0.17 - 1.11g^2$
Y	0.15	$0.15 - 1.76g^2$

TABLE 2

Trajectory	Calculation without X&Y	Final results
W	0.4	0.4 (fitted)
f	0.6	0.6 (fitted)
ρ	0.4	$0.4 - 0.23g^2$
A_2	0.33	$0.33 + 0.12g^2$
X	0.147	$0.147 - 1.2g^2$
Y	0.12	$0.12 - 1.9g^2$

Figure captions

Fig. 1 : The produced pions are ordered in rapidity, and each sub-process is approximated by its Regge form.

Fig. 2 : The contribution to unitarity of the diagram with n pion produced.

Fig. 3 : Symbolic representation to eq. (6).

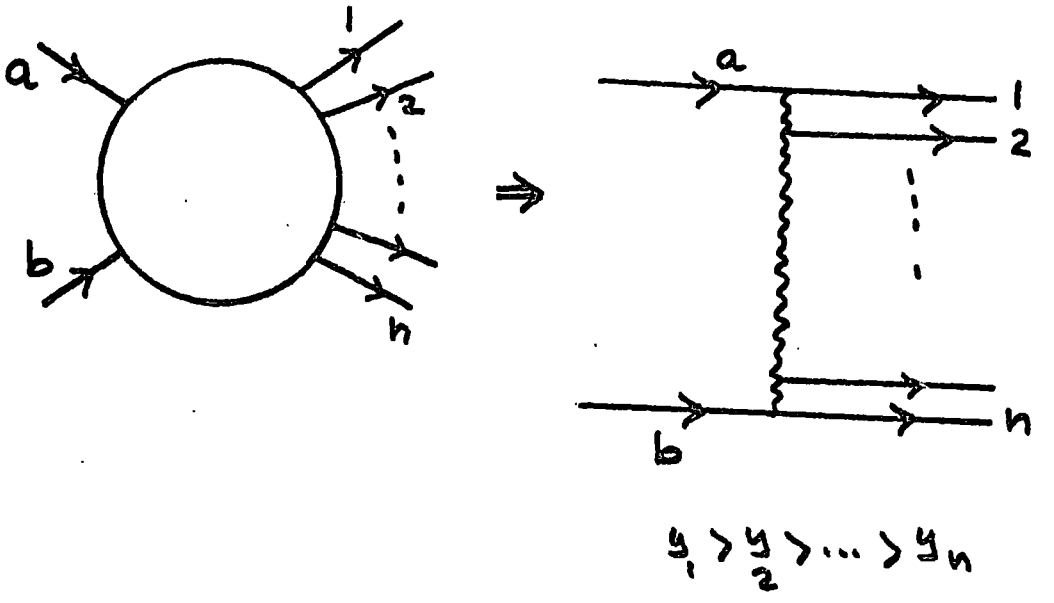

Fig. 1

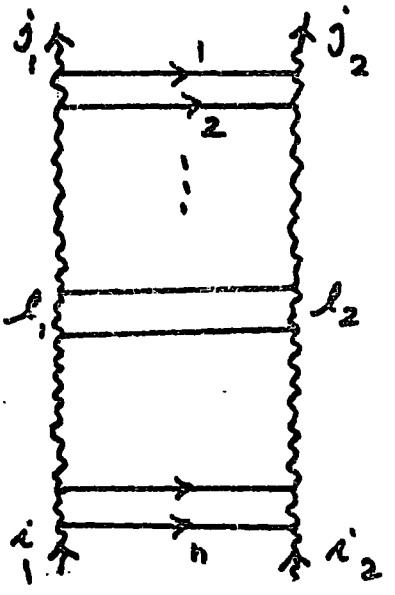

Fig. 2

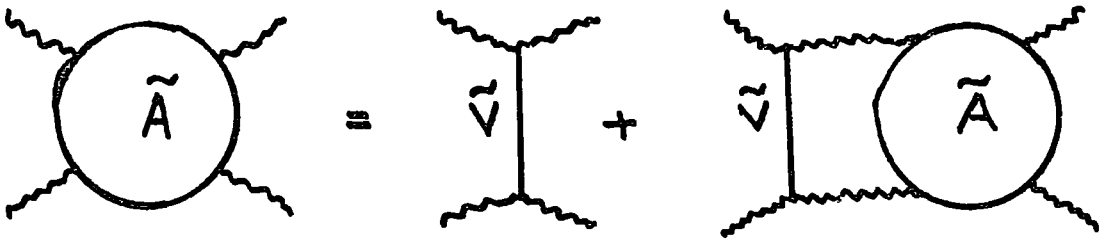

Fig. 3

CHAPTER IV

Unitarity with only Stable Particle Production

Introduction

This chapter is a continuation to Ch.III., where as we mentioned earlier that since the exact unitarity equation includes only stable particle in the intermediate states, and since in our model we ignore baryons and we consider a world without strangeness, this means that we should only include pions and η's. Since, however, η's are much heavier than pions, we do not expect η's to be produced with the same strength as pions; therefore we associate a suppression factor x when η is produced. We consider a few instructive examples;

($x = 0.5$, $x = 0.25$, and $x = 0.125$).

In the next section we discuss the coupling scheme. The coupling and signature matrices are given in section 3. The results of the calculation and the conclusions are given in section 4.

The Coupling Scheme

The relative coupling strengths of $0^-(\pi,\eta)$ to $1^-(\rho,\omega)$ and $2^+(A_2,f)$ can be calculated from the expression;

$$Tr(M_1 \bar{M}_2 M_3) + c_1 c_2 c_3 Tr(M_1 M_3 \bar{M}_2) \qquad (1)$$

where M_i and 2 x 2 matrices and represent our SU(3) multiplets (0^-, 1^- and 2^+) in the absence of strangeness, e.g. for the $0^-(\pi,\eta)$ we have

$$M_p = \text{Psuedoscalar} = \begin{bmatrix} \frac{1}{\sqrt{2}}(\eta+\pi^0) & \pi^+ \\ \pi^- & \frac{1}{\sqrt{2}}(\eta-\pi^0) \end{bmatrix} \qquad (2)$$

$$\bar{M}_\rho = \begin{pmatrix} \frac{1}{\sqrt{2}}(\bar{\eta} + \bar{\pi}^0) & \bar{\pi}^- \\ \bar{\pi}^+ & \frac{1}{\sqrt{2}}(\bar{\eta} - \bar{\pi}^0) \end{pmatrix} \tag{3}$$

and similar matrices for $\bar{1}$ and $\bar{2}^+$. C_i which appear in eq. (1) are the charge conjugation quantum numbers of the nutral members of M_i multiplet. If $C_1C_2C_3 = +\ (-)$, we say that the coupling is symmetric (anti-symmetric). Thus, for example for the vertex

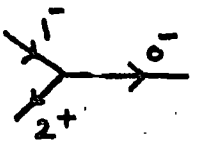

(4)

we have:

$$\begin{aligned} & Tr\,(M_\rho \bar{M}_\nu M_T) + C_\rho C_\nu C_T\, Tr\,(M_\rho M_T \bar{M}_\nu) \\ \Longrightarrow\quad & Tr\,(M_\rho \bar{M}_\nu M_T) - Tr\,(M_\rho M_T \bar{M}_\nu) \end{aligned} \tag{5}$$

which gives;

$$\begin{aligned} & \sqrt{2}\,\pi^0\left[\bar{\rho}^-A_2^- - \bar{\rho}^+A_2^+\right] + \sqrt{2}\,\pi^+\left[\rho^+A_2^0 - \bar{\rho}^0A_2^-\right] \\ & + \sqrt{2}\,\pi^-\left[\bar{\rho}^0A_2^+ - \bar{\rho}^-A_2^0\right] \end{aligned} \tag{6}$$

Thus "as it should be the case" η does not couple to 1^- and 2^+ because the conservation of I-spin and G-parity forbid that.

On the other hand for the vertex 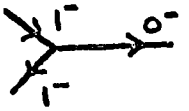 we have

$$Tr\,(M_p \bar{M}_v M_v) + c_p c_v c_v\, Tr(M_p M_v \bar{M}_v)$$

$$\Rightarrow \quad Tr\,(M_p \bar{M}_v M_v) + Tr(M_p M_v \bar{M}_v) \tag{7}$$

which gives

$$\sqrt{2}\,\eta\,[\bar{\omega}\omega + \bar{\rho}^0\rho^0 + \bar{\rho}^+\rho^+ + \bar{\rho}^-\rho^-] + \sqrt{2}\,\pi^+[\bar{\rho}^+\omega + \bar{\omega}\rho^-]$$

$$+\sqrt{2}\,\pi^-[\bar{\rho}^-\omega + \bar{\omega}\rho^+] + \sqrt{2}\,\pi^0[\bar{\rho}^0\omega + \bar{\omega}\rho^0] \tag{8}$$

and for the vertex 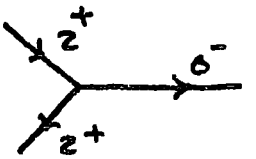 we obtain

$$\sqrt{2}\,\eta\,[\bar{f}f + \bar{A}_2^0 A_2^0 + \bar{A}_2^+ A_2^+ + \bar{A}_2^- A_2^-] + \sqrt{2}\,\pi^+[\bar{A}_2^+ f + \bar{f}A_2^-]$$

$$+\sqrt{2}\,\pi^-[\bar{A}_2^- f + \bar{f}A_2^+] + \sqrt{2}\,\pi^0[\bar{A}_2^0 f + \bar{f}A_2^0] \tag{9}$$

Now if we make use of the assumption used in Ch.III (eq. (9))

$$G_2 = G^{\pi^+}_{A_2^+ f} = G^{\pi^+}_{\rho^+\omega}$$

we obtain that all the couplings of eqs. (8) and (9) are equal and equal to G_2.

On the other hand, following eq.(8) of Ch.III,

$$G_1 = G^{\pi^+}_{A_2^+ \rho^0}$$

We find that the couplings of eq. (6) are equal, and equal to G_1 and finally for the exotic we write as before;

$$g = G^{\pi}_{x A_2} = G^{\pi}_{y \rho}$$

$$g' = G^{\pi}_{xy}$$

Notice that the above coupling scheme is equivalent to the Zweig rules for quark graphs, where one can obtain the above coupling using the pictorial techniques discussed in ref. (20).

3. The Couplings and Signatures Matrices:

In the model of Ch.III, because we produce only pions we have off-diagonal matrix elements, as a result of G-parity conservation. Here, the effect of producing η's (in addition to pions) is to full completely the diagonal elements, (it adds nothing to the other elements of the matrices). Thus we have:

f : I = 0, G(+), τ = +1

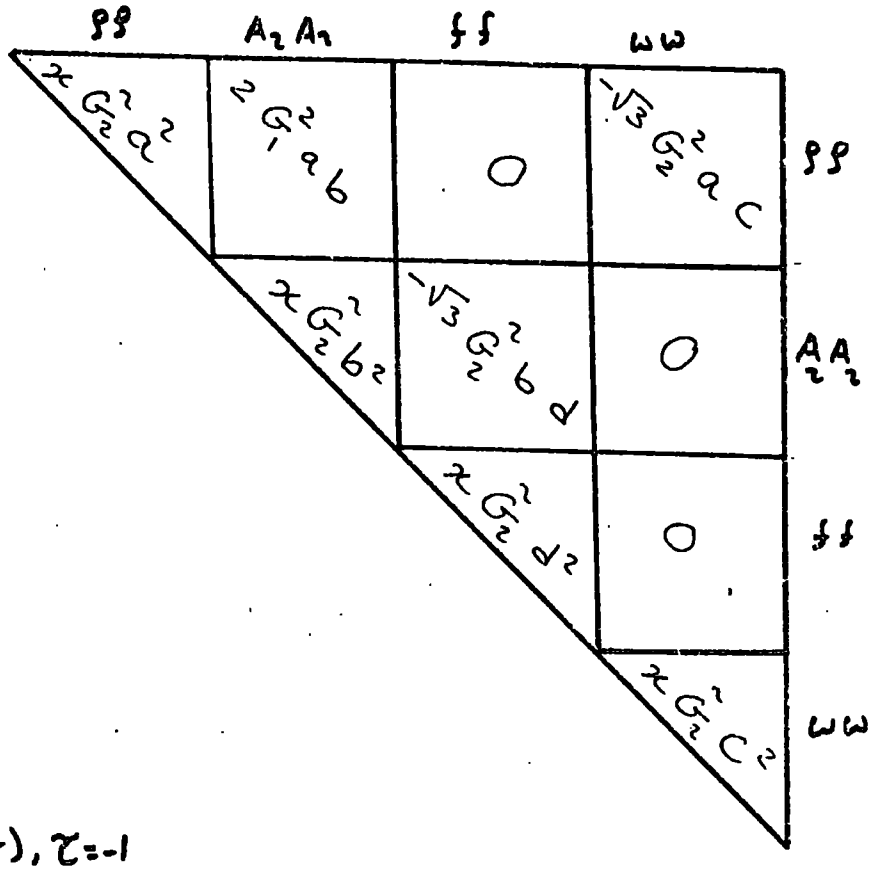

ω: I = 0, G(−), τ = −1

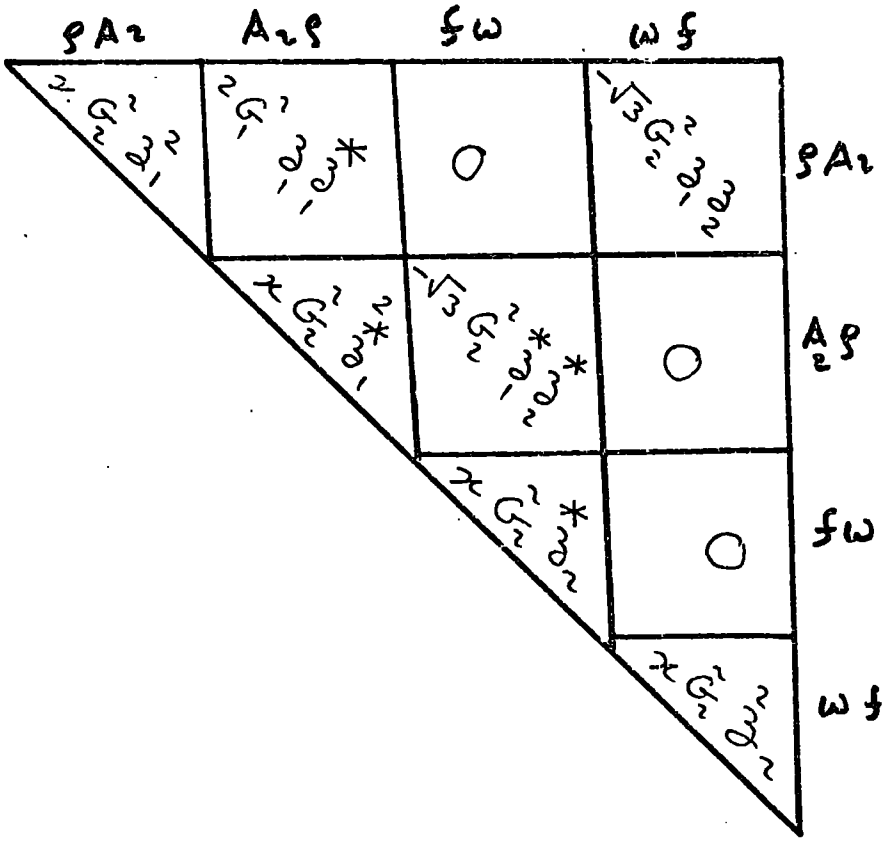

A_2: $I=1$, $G(+)$, $\tau=+1$

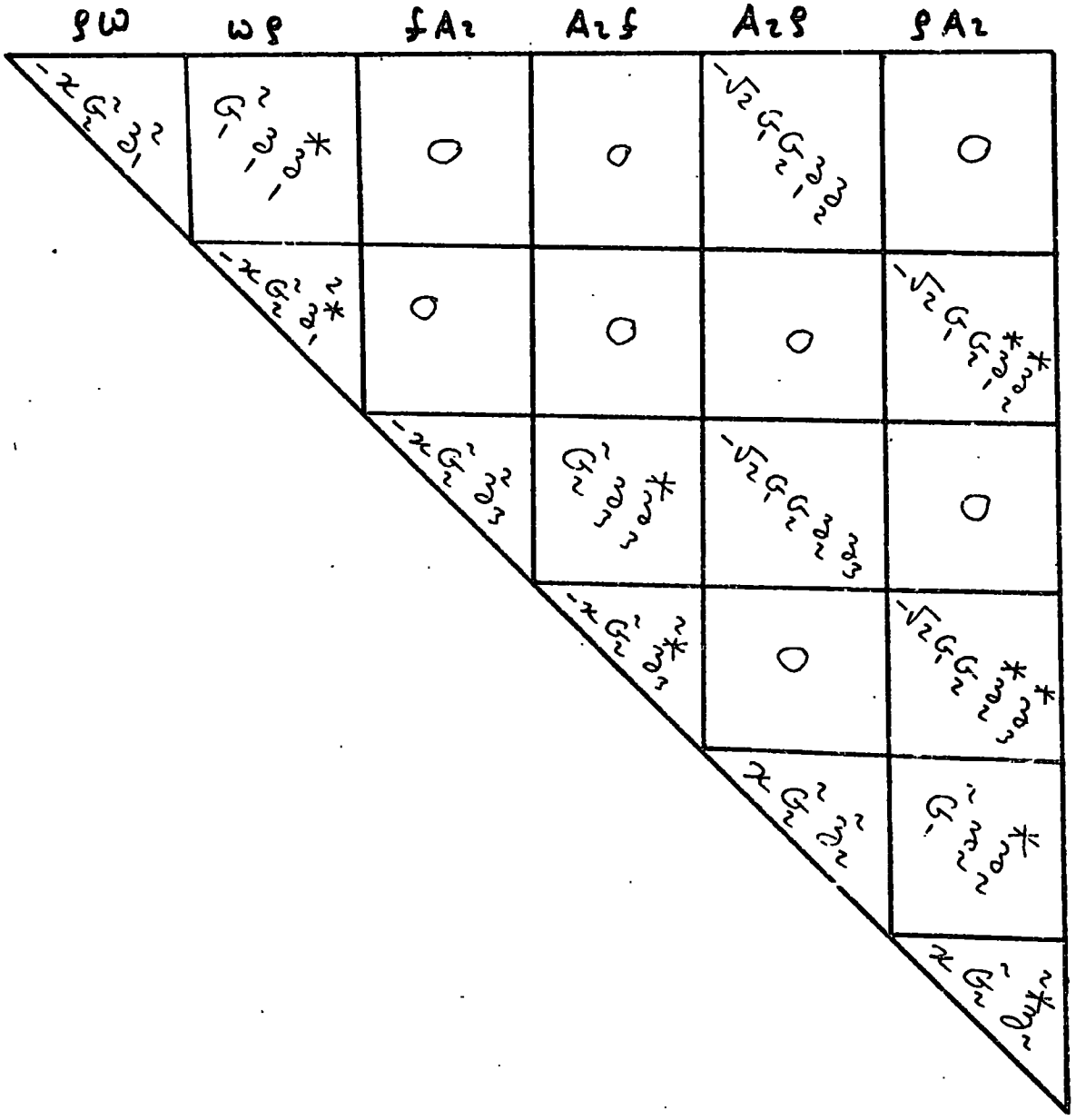

ρ: $I=1$, $G=+$, $\tau=-1$

X: $I=2$, $G(+)$, $\tau=+1$

Y: $I=2$, $G(-)$, $\tau=-1$

4. Evaluation of Regge trajectories

We calculate here the leading output Regge trajectories (at t = 0) by solving the equations det $(1 - \tilde{V}_o) = 0$ for the highest value of J. The input to the calculation are as before:

$$\bar{\alpha}_\omega = \bar{\alpha}_{A_2} = 0.3$$

$$\bar{\alpha}_g = 0.4 \qquad (10)$$

$$\bar{\alpha}_f = 0.7$$

We determine G_1^2 and G_2^2 from ω and f matrices by requiring the leading output to be equal to 0.4 and 0.8 respectively. This implies:

x	G_1^2	G_2^2
½	0.2	0.1
¼	0.21	0.12
⅛	0.21	0.123
0	0.216	0.13

(11)

The reason why the strength of the coupling G^2_2 decreases with increasing x (more than G_1^2 does) is because:

(i) the inclusion of η production comes through the coupling G_2 only (see section 2) and (ii) the strength of G_1 and G_2 are determined in such a way to give the correct experimental output for α_f and α_ω. Thus because of (i) when x increases the contribution of G_2 to the matrices increases, but because of the constraint (ii), the value of G_2 decreases.

The results of the calculation are shown in the table below for x = 0.5, 0.25 and 0.125. We give also in the table the effect of exotic

exchange calculated as before, for x = 0.25.

Trajectory	Calculation without exotic	Final results
ω	0.4	0.4 (fitted)
f	0.8	0.8 (fitted)
ρ	0.47	
	0.47	$0.47 - 0.26\,g^2$
	0.46	
	0.23	
x	0.21	$0.21 - 1.05g^2$
	0.19	
	0.26	
A_2	0.32	$0.32 + 0.1g^2$
	0.35	
	0.09	
y	0.12	$0.12 - 1.7g^2$
	0.13	

From this table we see that the effect of the inclusion of η is to push up (down) the positive G-parity poles (negative G-parity poles). As a result of that we get approximately the correct ρ A_2 splitting in sign and magnitude. However for a reasonable values of x, this effect seems to be quite small compared to the original results. We have calculated (with x = 0.25) the multiplicities for π's and η's production in the $I_t = 0$, C(+) amplitude (i.e. the f), and we found that the ratio of η's production to pions is about $^1/17$. Details of these calculations and other calculations of multiplicities are given in the next chapter.

CHAPTER V

THE CALCULATION OF MULTIPLICITIES

1. Introduction

This chapter is devoted to the calculation of multiplicities. We do this in the $I_{t=0}$, $G=+$ amplitudes, i.e. the f, which dominate at high S. In the next section we calculate the average multiplicities of I = 0, 1, and 2 exchanges in the context of the pion production model of Chapter III, from which we deduce the total multiplicity and the average multiplicities of charge transfers, $\langle n_{\Delta Q=0} \rangle$, $\langle n_{\Delta Q=\pm 1} \rangle$, $\langle n_{\Delta Q=\pm 2} \rangle$ It will turn out that these results are in good agreement with the data at energies $S \lesssim 40$ $(\text{Gev})^2$, but are incompatible with the data at higher energies. This leads us to the suggestion that at higher energies a new effect takes place, namely the two and more ladder contribution that was predicted in the dual-model,[23] and which will be the subject of Chapter VI. Finally, we calculate in section 3 the average multiplicity of pion and η production in the context of the stable particle production model of Chapter IV, in the case when the suppression factor $\alpha = 1/4$

2. The total and change transfers multiplicities

2.1. The method

To calculate the I = 0, 1, and 2 exchanges, we put a factor $\sqrt{\lambda_0}$, $\sqrt{\lambda_1}$, $\sqrt{\lambda_2}$, in each I = 0, 1, 2 propagators. Since we are considering ladders with equal I-Spin in both sides

(f exchange in t channel), we insert a factor λ_I into Q of eq. (3) Chapter III.

Then we have

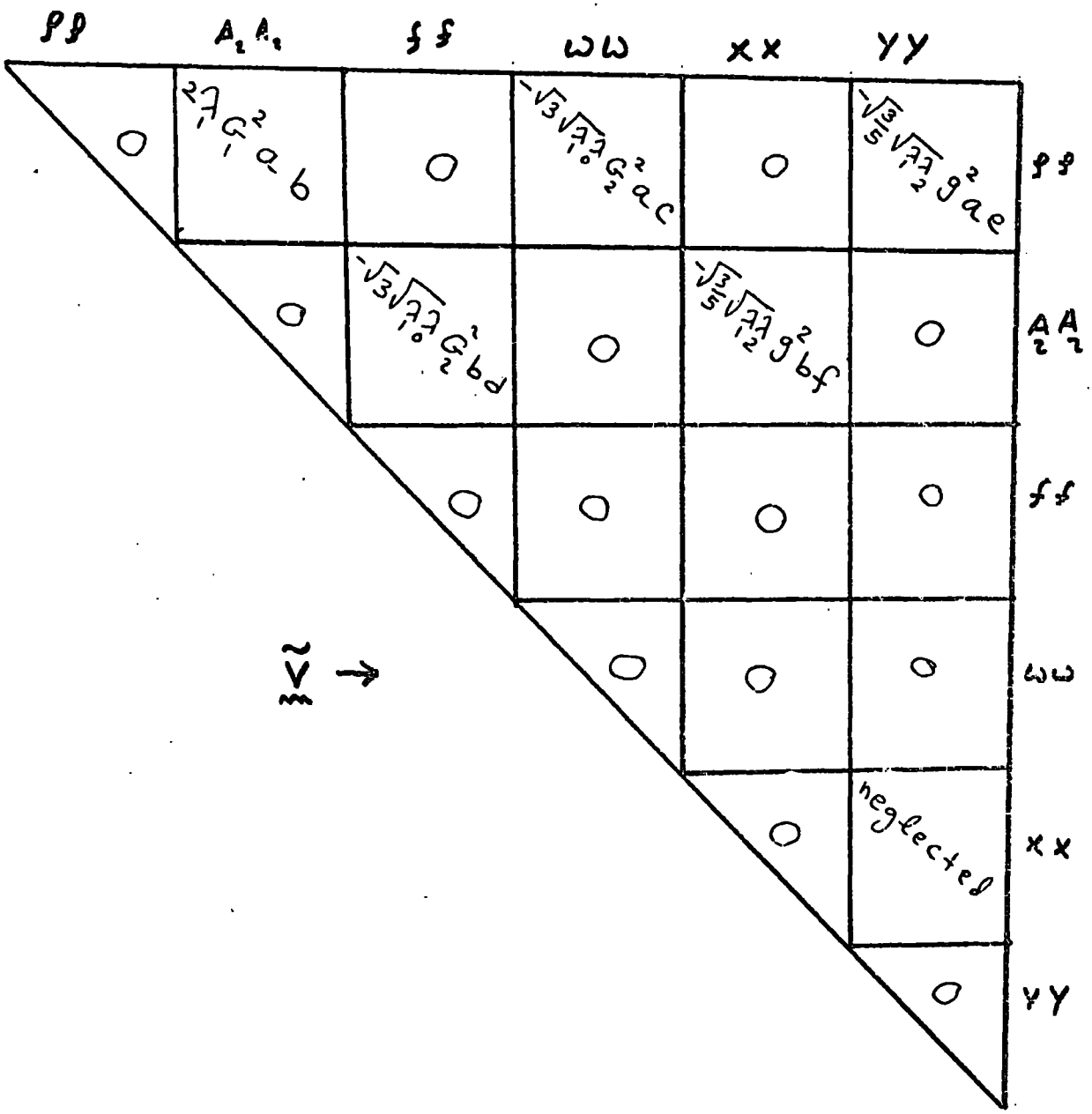
ρρ
A₂A₂
ff
ωω
xx
yy
$\frac{2}{15}G_1^2 q^2 b$
$-\sqrt{3}\sqrt{\frac{2}{15}}G_2^2 q^2 c$
$-\sqrt{\frac{3}{5}}\sqrt{\frac{2}{15}}g_2^2 q^2 e$
$-\sqrt{3}\sqrt{\frac{2}{15}}G_0^2 G_2^2 p^2 d$
$\sqrt{\frac{3}{5}}\sqrt{\frac{2}{15}}g_2^2 f^2 g$
neglected
$\tilde{\tilde{V}} \rightarrow$

Then we write

$$\underset{\sim}{\tilde{A}} = (\underset{\sim}{1} - \underset{\sim}{\tilde{V}})^{-1} \underset{\sim}{\tilde{V}} \tag{1}$$

at $J = \alpha^{out}$ where α^{out} is the leading pole (the f), $\underset{\sim}{\tilde{A}}$ has a pole. The residue is given by

$$\text{Res}\ \underset{\sim}{\tilde{A}}(J=\alpha^{out}) = \lim_{J \to \alpha_{out}} (J - \alpha_{out})\, \underset{\sim}{\tilde{A}}(J) \tag{2}$$

If we write the matrix $\underset{\sim}{\tilde{V}}$ in the following abbreviated form (neglecting X and Y contribution)

$$\underset{\sim}{\tilde{V}} = \begin{pmatrix} 0 & A & 0 & B \\ A & 0 & D & 0 \\ 0 & D & 0 & 0 \\ B & 0 & 0 & 0 \end{pmatrix}$$

equation 2 gives

$$\text{Res}\ \underset{\sim}{\tilde{A}}(\alpha_{out}) = \lim_{J \to \alpha_{out}} \begin{pmatrix} A^2+B^2-B^2D^2 & A & AD & B-BD^2 \\ A & A^2+D^2-B^2D^2 & D-DB^2 & AB \\ AD & D-DB^2 & D^2-D^2B^2 & ABD \\ B-BD^2 & AB & ABD & B^2-B^2D^2 \end{pmatrix} \times \frac{J-\alpha_{out}}{\det(\underset{\sim}{1} - \underset{\sim}{V}(J))} \tag{3}$$

$$= \lim_{J \to \alpha_{out}} \underset{\sim}{L}(J) \times \frac{J-\alpha_{out}}{\det(\underset{\sim}{1} - \underset{\sim}{\tilde{V}}(J))}$$

Expanding det $(\underline{\underline{1}} - \underline{\underline{\tilde{V}}}(J))$ about $J = \alpha_{out}$ and noticing that det $(\underline{\underline{1}} - \underline{\underline{\tilde{V}}}(\alpha_{out})) = 0$, equation 3 becomes

$$\text{Res}\, \underline{\underline{\tilde{A}}}(\alpha_{out}) \equiv R = \frac{\underline{\underline{L}}(\alpha_{out})}{\left.\frac{\partial [\det(\underline{\underline{1}} - \underline{\underline{\tilde{V}}}(J))]}{\partial J}\right|_{J=\alpha_{out}}} \tag{4}$$

Now we write

$$\underline{\underline{\tilde{A}}}(s) = \underline{\underline{\tilde{R}}}\, s^{\alpha} \tag{5}$$

If we take a particular component e.g. the first diagonal element of the matrix $\underline{\underline{L}}$ (denoting $\underline{\underline{\tilde{A}}}$ and $\underline{\underline{\tilde{R}}}$ for this component by $\tilde{A}_{11}$ and $\tilde{R}_{11}$) equation (5) gives

$$\tilde{A}_{11}(s) = \tilde{R}_{11}(s)\, s^{\alpha} \tag{5'}$$

The mean multiplicity of I - Gap is given by

$$\langle n \rangle_I = \left(\frac{\partial \tilde{A}_{11}}{\partial \lambda_I}\right) \Big/ \tilde{A}_{11} = \frac{1}{\tilde{R}_{11}} \left.\frac{\partial \tilde{R}_{11}}{\partial \lambda_I}\right|_{\lambda_I = 1} + (\log s) \left.\frac{\partial \alpha}{\partial \lambda_I}\right|_{\lambda_I = 1} \tag{6}$$

Since the constant term in eq. (6) depends on the particular component of the matrix $\underline{\underline{L}}$ which we are considering, we calculate

this term for all the diagonal elements of $\underset{\sim}{L}$ and then we take the average.

2.2. The calculation of logs coefficient

We have done these calculations in two cases: first, when X and Y contribution to the matrix $\underset{\sim}{\tilde{V}}$ is neglected, second, when this contribution is taken into account.

In the first case the equation $\det\left(\underset{\sim}{1} - \underset{\sim}{\tilde{V}}\right) = 0 \Rightarrow$

$$J^4 + 0.6J^3 - J^2(0.82\lambda_1^2 + \lambda_1\lambda_0 0.19 + 0.08)$$
$$-J(0.1 + \lambda_1\lambda_0 0.08) + 0.13\lambda_1^2 + 0.008\lambda_1^2\lambda_0^2 - 0.013 = 0 \qquad (7)$$

When $\lambda_1 = \lambda_0 = 1$ the highest root of eq. (7) is $J = \alpha_{out} = 0.8$. But when we keep λ_1 and λ_0 as parameters we have

$$J = J(\lambda_1, \lambda_0) \qquad (8)$$

Since, however, λ_1 and λ_0 are artificial parameters (in eq. (6) we put $\lambda_1 = \lambda_0 = 1$ after the derivative) we write:

$$\lambda_1 = 1 + \varkappa_1 \qquad \lambda_0 = 1 + \varkappa_0 \qquad (9)$$

and we expand about $\lambda_i = 1$ to a first order. Thus we have:

$$\lambda_1^2 = 1 + 2x_1$$

$$\lambda_0^2 = 1 + 2x_0$$

$$\lambda_1 \lambda_0 = 1 + x_1 + x_0$$

$$J^4 = J_0^4 + 4J_0^3 \left[x_1 \frac{\partial J}{\partial x_1} + x_0 \frac{\partial J}{\partial x_0} \right] \qquad (10)$$

$$J^3 = J_0^3 + 3J_0^2 \left[x_1 \frac{\partial J}{\partial x_1} + x_0 \frac{\partial J}{\partial x_0} \right]$$

$$J^2 = J_0^2 + 2J_0 \left[x_1 \frac{\partial J}{\partial x_1} + x_0 \frac{\partial J}{\partial x_0} \right]$$

$$J = J_0 + \left[x_1 \frac{\partial J}{\partial x_1} + x_0 \frac{\partial J}{\partial x_0} \right]$$

where $$J_0 = J(x_1 = 0, x_0 = 0) = 0.8$$

putting the approximations of eq. (10) in eq. (7) we get,

$$1.26 \left[x_1 \frac{\partial J}{\partial x_1} + x_0 \frac{\partial J}{\partial x_0} \right] - 0.95 x_1 - 0.16 x_0 = 0 \qquad (11)$$

Since eq. (11) holds for arbitrary x_1 and x_0 we have

$$1.26\, x_1 \frac{\partial J}{\partial x_1} = 0.95\, x_1 \Longrightarrow \frac{\partial J}{\partial x_1} = 0.75$$

$$1.26\, x_0 \frac{\partial J}{\partial x_0} = 0.16\, x_0 \Longrightarrow \frac{\partial J}{\partial x_0} = 0.13 \qquad (12)$$

To calculate the mean multiplicity of I-gaps, when X and Y contribution to the matrix $\underset{\sim}{\tilde{V}}$ is taken into account, we need first to solve the eq. $\det(1 - \underset{\sim}{\tilde{V}}) = 0$ for the highest root of J. In order to do that we need to give the coupling, g^2 a reasonable numerical value. Putting $g^2 = 0.1$ we get

$$J = 0.81 \quad \text{(exact solution)}$$

$$J = 0.815 \quad \text{(perturbation method)} \qquad (13)$$

From equation (13) we conclude that (i) the effect of exotic exchange pushes (f) up and (ii) This effect calculated by the perturbation method (see app. B) is quite close to its exact value. This proves the validity of the perturbation method (this result in fact reminds us with a similar one, namely the effect of δA_2 splitting in the $\underset{\sim}{\tilde{V}}$ matrix of A_2 "CH.III § 5" where we found that the value of this effect calculated exactly (by the perturbation method) is 0.15 (0.17)).

Taking the exact solution (J = 0.81) and proceeding as before we get finally:

$$\partial J/\partial x_0 = 0.13$$

$$\partial J/\partial x_1 = 0.78 \qquad (14)$$

$$\partial J/\partial x_2 = 0.03$$

Comparing eqs. (14) and (12) we see that the effect of exotic exchanges is to increase the total multiplicity by a small amount.

$$\langle n\rangle_{tot.} = 0.8 \log s \longrightarrow \langle n\rangle_{tot} = 0.94 \log s$$

2.3. The Calculation of the residue term

We calculate the constant term in the case when the X and Y contribution to $\underset{\sim}{\tilde{V}}$ is neglected. From eqs. (3), (4) and (6) we write

$$\frac{1}{\tilde{R}_{11}}\frac{\partial \tilde{R}_{11}}{\partial \lambda_I}\bigg|_{\lambda_I=1} = \frac{\partial (A^2+B^2-B^2D^2)/\partial \lambda_I}{(A^2+B^2-B^2D^2)}\bigg|_{\lambda_I=1} - \frac{\partial\left[\frac{\partial[\det(1-V(J))]}{\partial J}\Big|_{J=\alpha}\right]\Big/\partial\lambda_I}{\frac{\partial[\det(1-V(J))]}{\partial J}\Big|_{J=\alpha}}\Bigg|_{\lambda_I=1} \qquad (15)$$

which gives:

$$\frac{1}{\tilde{R}_{11}}\frac{\partial \tilde{R}_{11}}{\partial \lambda_1} = 1.93 - 1.52 = 0.41$$

$$\frac{1}{\tilde{R}_{11}}\frac{\partial \tilde{R}_{11}}{\partial \lambda_0} = 0.01 - 0.38 = -0.37 \qquad (16)$$

The residue terms which corresponds to the other diagonal elements of $\underset{\sim}{L}$ can be calculated in the same way, and they are given in the following table:

The channel;	gg	A_2A_2	ff	$\omega\omega$
	$\tilde{R}_{11}$	$\tilde{R}_{22}$	$\tilde{R}_{33}$	$\tilde{R}_{44}$
$I=1$	0.41	-0.96	-0.12	-0.32
$I=0$	-0.37	0.18	0.54	0.15

$$\Longrightarrow \quad \langle \tilde{R} \rangle_{I=1} = -0.32 , \quad \langle \tilde{R} \rangle_{I=0} = 0.131$$

and thus finally we have;

$$\begin{aligned} \langle n \rangle_{I=0} &= 0.13 \log S + 0.13 \\ \langle n \rangle_{I=1} &= 0.78 \log S - 0.32 \\ \langle n \rangle_{I=2} &= 0.03 \log S \end{aligned} \tag{17}$$

which gives

$$\langle n \rangle_{\text{tot. rungs}} = -0.2 + 0.94 \log S \tag{18}$$

In comparing with experiment we have to consider data on pp scattering. Clearly the coefficient of the Ln term will be unaffected by the nature of the colliding particles but there is uncertainty in the value of the constant. To fix our parameters we take the average value given above and add one to it. The one takes account of the ease with which either proton can excite to, for example, $\omega\,\Delta$ which will then produce an extra pion.

$$\langle n \rangle_{\text{tot. Produced Particles}} = 0.8 + 0.94 \log S \tag{19}$$

2.4. Comparison with the data

For pp scattering the total multiplicity of charged particles is well described by[6]

$$\langle n \rangle_{ch.} = -1.1 + 1.4 \log S \tag{20}$$

Assuming the number of neutrals equals the number of positive or negative charged particles and allowing for the necessary excess of two positive particles we write;

$$\langle n_{ch} - 2_{\text{Protons}} \rangle = 1.4 \log S - 3.1 \tag{21}$$

$$\Rightarrow \quad \langle n \rangle_{\text{neutral}} = 0.7 \log S - 1.6$$

hence eqs. (22) and (20) give:

$$\langle n \rangle_{tot.} = 2.1 \log S - 2.7 \tag{23}$$

To be compared with the total multiplicity predicted by our model, eq. (19). Clearly the prediction is too small at high energies by a factor of about two. On the other hand for $S \lesssim 40$ Gev^2 the fit is quite reasonable. In view of the fact that we have not included η production in the model (we will do that in the next section) and also the fact that we cannot calculate the pp process (notice that the constant term in eq. (19) is somewhat uncertain. It is determined as the average of the values obtained in $\rho\rho$, A_2A_2, $\omega\omega$ and ff scattering), we regard the agreement at low energy as satisfactory.

Next we consider the charge transfer along the rungs. Assuming that $I = 1$ in eq. (17) gives $Q = +1, -1, 0$ in equal proportions, we get

$$\langle n \rangle_{\Delta Q=0} = 0.39 \log S + 0.02$$

$$\langle n \rangle_{\Delta Q=+1} = \langle n \rangle_{\Delta Q=-1} = 0.26 \log S - 0.11 \qquad (24)$$

At $S \simeq 20$ Gev^2 we find $\Delta Q = 0, +1, -1$ in the ratio 1:1:1.8 compared with the experimental[22] values 1:1:2. Bearing in mind the sources of error noted above the agreement is excellent.

Finally we compare the ratio $|\Delta Q|=2 \,/\, \Delta Q=0$ predicted by our model with the data. The data compilation of ref. (22) shows this ratio in the central region around zero rapidity. For $\pi^- P$ the ratio is about 2% at 16 Gev/c and for pp it increases from about 7% at 12 Gev/c to about 14% at 205 Gev/c. The increase with energy is more apparent if we compare this data with the newer data of Lamsa et al.[16] who show the ratio for $\pi^- P$ at 200 Gev/c as a function of rapidity gap y. At the mean charged rapidity gap (they only include charged particles)

of 0.7 the ratio is about two-thirds. Our model is again satisfactory at low energies but it clearly cannot accommodate the large amount of $|\Delta Q| = 2$ at high energy. We, therefore, have to explain (i) the origin of the additional $|\Delta Q| = 2$ exchange, (ii) its energy dependence and (iii) its dependence on Y. We defer the discussion of these questions and others to the next chapter.

3. The average multiplicity of π's and η's production

To calculate the average multiplicity of pions and η's we insert a factor λ_1 (λ_0) into V of eq. (2) Chapter III when π (η) is produced;

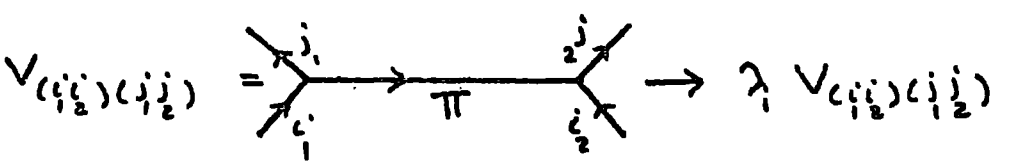

(25)

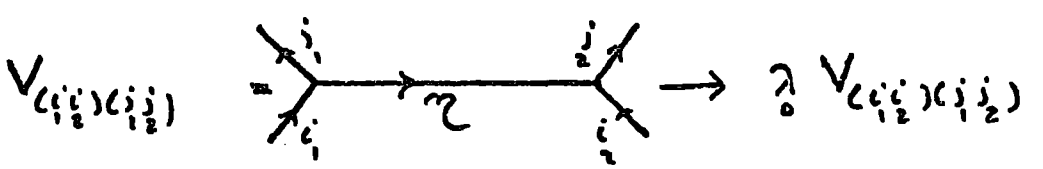

(26)

Then we have (we take x = ½)

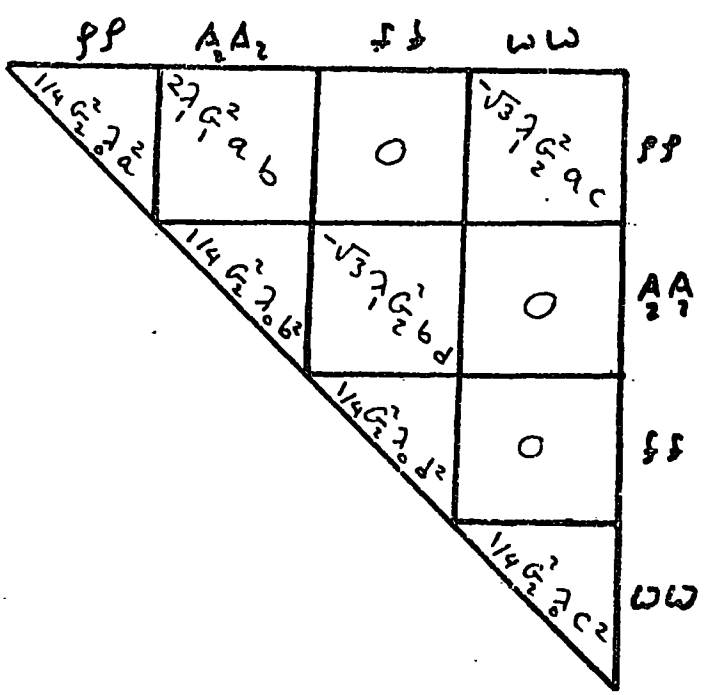

The equation det ($\underline{1} - \underline{\tilde{V}}$) = 0 gives

$$1.12 \left[x_1 \frac{\partial J}{\partial x_1} + x_0 \frac{\partial J}{\partial x_0} \right] = 1.2\, x_1 + 0.07\, x_0 \tag{27}$$

which gives

$$\frac{\partial J}{\partial x_1} = 1.07 \qquad \frac{\partial J}{\partial x_0} = 0.063 \tag{28}$$

hence

$$\langle n \rangle_\pi = 1.07 \log S + \text{Constant.}$$
$$\langle n \rangle_\eta = 0.063 \log S + \text{Constant.} \tag{29}$$

which gives the ratio (30)

$$\langle n \rangle_\pi \,/\, \langle n \rangle_\eta = 17/1$$

for large S

The total multiplicity of eq. (29) shows some improvement compared to that of eq. (19).

CHAPTER VI

Charge Exchange and the Nature of the Pomeron[40]

1. Introduction

The main conclusion which we have drawn from the calculations of the preceding chapter is that; while the single ladder model gives a good description of low energy data ($s \lesssim 40$ Gev^2), it is not satisfactory at higher energies, e.g. the predicted relative probabilities $|\Delta Q|=2 / \Delta Q=0$ and $|\Delta Q|=3 / |\Delta Q|=1$, where ΔQ is the charge exchange across a rapidity gap, is too small compared with the new data of Lamsa et al,[16] but in agreement with the data at low energy.[22] Our main task here is to explain the additional $|\Delta Q| = 2$ exchange, and its Y and S dependence (see Fig. 5).

Before we introduce our model we mention a possible explanation considered by Lamsa et al.[16] In the strong ordering limit one would not expect the occurrence of $|\Delta Q| > 1$ gaps (see Fig. 1a). However, for small Δy the strong ordering would be violated. Consequently the single cross-over or multiple cross-over phenomena might occur, leading to $|\Delta Q| > 1$ gaps (see Figs. 1B, 1c, and 1d). Given that the observed rapidity gaps are small we should not be surprised to see such terms. However we would expect

them to fall off faster with y (exponentially in $\Delta s = e^y$)* and more important, since this effect is local in rapidity space it does not have a high threshold and should not be energy dependent. If the energy dependence which appears to occur in the data is confirmed then we must look elsewhere for an explanation.

---

*Consider the process 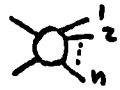 we order the particles by their rapidity, i.e. $y_1 > y_2 > \cdots > y_n$. If we take a sub-process in the ladder diagram  ; this sub-process has in general contributions from both t-channel and u-channel.

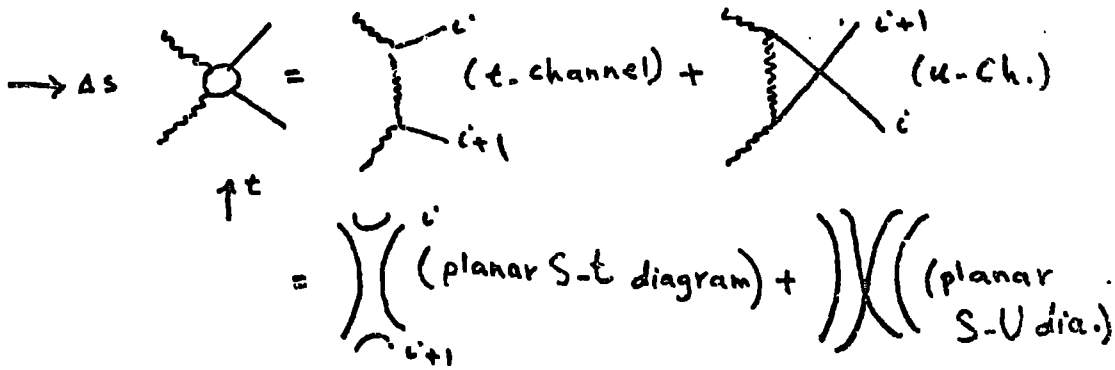

In the strong ordering limit $y_{i} \gg y_{i+1}$, we don't have the second diagram. But when $\Delta y = y_{i} - y_{i+1}$ is small, the second diagram might occur, leading to $|\Delta Q| > 1$ gaps (2 $q\bar{q}$ pairs in t - channel). The contribution of this diagram is roughly given by

$$\sim (\Delta s)^{\alpha(u)} = e^{\alpha(u) \ln \Delta s}$$

Since $s + t + u = \Sigma$ for t small and fixed we get

$$\sim e^{-ye^y} \quad \text{where } y = \ln \Delta s$$

Thus if the occurrence of $|\Delta Q| > 1$ gaps to be attributed to the above cross-over phenomena, we would expect them to fall off exponentially in e^y. On the other hand the data points of Fig. 5 seem to fall on a Gaussian Curve.

We suggest that what is being observed at high energies is the decay of two (and more) heavy $(M \sim \sqrt{s})$ clusters which are approximately at rest in the centre-of-mass system and which decay independently. Thus instead of having one ladder, we have several over-lapping ladders in rapidity space (Fig. 2).

Such contribution is expected, for example, in the Dual models[23] and it arises from the diagram shown in Fig. (3). Notice however that if we approximate the production amplitude in Fig. 3 by the leading Regge exchanges then t_{min} effects would restrict M_1^2 and M_2^2 to be $\ll S$, in the large S limit $[\, t_{min} \approx -M_1^2 M_2^2 / S \,]$ and this would then merely yield the single ladder multi-Regge contribution (Fig. 4). On the other hand, if we use a Dual model to describe the production amplitude we effectively include lower lying trajectories which do not have the same t dependence in their residues so that t_{min} effect does not operate and we have an extra contribution from $M_1^2 \sim M_2^2 \sim S$. In fact the M_1^2, M_2^2 integral diverges at this point and yield a new (pomeron) singularity. In the language of the topological expansion; the cylinder itself has a singularity. Although in the present Dual models this singularity is at 2, there is arguments for believing that this singularity is at 1 (see Chapter I, § 5), and so will dominate over the promoted f at high energies. Also it only occurs in the Pomeron sector. In the next section we introduce our model and we compare its predictions with the high energy data.

2. The Model, Comparison with the Data

We consider a simple model in which we permit contributions from one, two or three ladders, ignoring possible interference terms. At a given energy we denote the relative probability of these diagrams by $1 : \gamma_2 : \gamma_3$. We assume that the available energy is divided equally

amongst the two or three ladders, i.e. if we have an event with k ladders produced simultaneously, and if the total available energy is S, then the average multiplicity for each ladder is given by,

$$\langle n \rangle_k = a + b \log \frac{S}{k^2} \qquad (1)$$

of course for a given S, there is a maximum number $k_{max}(s)$ of the ladders which can be produced simultaneously such that $\langle n \rangle_k$ is large (at least of order two or three).

Now the total multiplicity of the produced particles is given by

$$\left\langle \text{the total multiplicity} \right\rangle = \frac{\text{the total number of particles}}{\text{the total number of events}} \qquad (2)$$

From eqs. (1) and (2) we get

$$\langle n(s) \rangle = \frac{\langle n_1(s) \rangle + 2\gamma_2 \langle n_1(\frac{s}{4}) \rangle + 3\gamma_3 \langle n_1(\frac{s}{9}) \rangle}{1 + \gamma_2 + \gamma_3} \qquad (3)$$

where $\langle n_1(s) \rangle$ is the average number of pions produced in a single ladder of energy S. We take this from our previous calculations

$$\langle n(s) \rangle^{(1)}_{tot.} = 0.8 + 0.94 \log S \qquad (4)$$

Since in the analysis of Lamsa et al. only charged particles are included we take two thirds of equation 4. This gives

$$\langle n(s) \rangle^{(1)}_{Ch.} = 0.53 + 0.63 \log S \qquad (5)$$

The two and three ladders contributions are given respectively by;

$$\langle n\rangle^{(2)}_{ch.} = 2\gamma_2\,[\langle n_1(s/4)\rangle] = 2\gamma_2\,[0.53 + 0.63\log\tfrac{s}{4}] \tag{6}$$

$$\langle n\rangle^{(3)}_{ch.} = 3\gamma_3\,[\langle n_1(s/9)\rangle] = 3\gamma_3\,[0.53 + 0.63\log\tfrac{s}{9}] \tag{7}$$

It is convenient to rewrite the above equations in the following form,

$$\langle n\rangle^{(1)}_{ch.} = \lambda_1 \log s \tag{8}$$

$$\langle n\rangle^{(2)}_{ch.} = 2\gamma_3\,[\lambda_2 \log\tfrac{s}{4}] \tag{9}$$

$$\langle n\rangle^{(3)}_{ch.} = 3\gamma_3\,[\lambda_3 \log\tfrac{s}{9}] \tag{10}$$

At S 400 Gev^2 (we take this value because the analysis of Lamsa et al. are done in 200 - Gev/c interactions), we find

$$\lambda_1 = 0.72\,,\quad \lambda_2 = 0.747\,,\quad \lambda_3 = 0.77 \tag{11}$$

The fact that these values are not equal is a reflection of the presence of the constant term in $\langle n \rangle = \lambda \ \mathrm{Log} S + C$.

The known multiplicity (eq. 3) gives a relation between γ_2 and γ_3, so we have one degree of freedom which is restricted by the fact that γ_2 and γ_3 are positive.

We turn now to the question of charge-exchange. If the individual ladders have rungs with $\Delta Q = 0, +1$ and -1 with equal probability then when the ladders overlap, we have for the probability of $|\Delta Q| = 2$ gap

$$P_2^{(2)} = 0.4 \quad \text{for two ladders} \qquad (12)$$

and

$$P_2^{(3)} = 0.46 \quad \text{for three ladders} \qquad (13)$$

Here we normalise (following Lamsa et al.) so that $P_2 + P_0 = 1$. Similarly for a $|\Delta Q| = 3$ gap, we have

$$P_3^{(3)} = 0.14 \qquad (14)$$

where this is normalised so that $P_3 + P_1 = 1$

We assume a poisson distribution in each ladder. Thus for one ladder production, the probability of length y having n particle is given by

$$R_n^{(1)} = e^{-\lambda' y} (\lambda' y)^n / n! \qquad (15)$$

$$\sum_{n=0}^{\infty} R_n^{(1)} = 1$$

and the probability of a gap having length y is

$$R^{(1)} = \lambda_1' e^{-\lambda_1' y} \quad , \quad \lambda_1' \int_0^\infty e^{-\lambda_1' y} dy = 1 \tag{16}$$

where

$$\lambda_1' = \langle n(s) \rangle^{(1)}_{\text{tot. rungs}} \Big/ \text{Log } S \tag{16'}$$

For the simultaneous production of two and three ladders, the corresponding relations are

$$R_n^{(2)} = e^{-2\lambda_2' y} (2\lambda_2' y)^n / n! \tag{17}$$

$$R^{(2)} = (2\lambda_2') \; e^{-2\lambda_2' y} \tag{18}$$

$$R_n^{(3)} = e^{-3\lambda_3 y} (3\lambda_3 y)^n / n! \tag{19}$$

$$R^{(3)} = (3\lambda_3') \; e^{-3\lambda_3' y} \tag{20}$$

where λ_1', λ_2', λ_3' are calculated from equations 8 - 10 as follows:

From eq. 8 we write

$$\langle n(s) \rangle^{(1)}_{\text{tot.run.}} = \langle n(s) \rangle^{(1)}_{\text{ch.}} - 2/3$$

$$= \lambda_1 \log s - 2/3 = \lambda_1' \log S \tag{21}$$

similarly for the production of two and three ladders we have;

$$\langle n \rangle^{(2)}_{rungs} = \gamma_2 \left[2\lambda_2 \log \frac{s}{q} - 2/3 \right]$$

$$= \gamma_2 \left[2\lambda'_2 \log \frac{s}{q} \right] \qquad (22)$$

$$\langle n \rangle^{(3)}_{rungs} = \gamma_3 \left[3\lambda_3 \log \frac{s}{9} - 2/3 \right] \qquad (23)$$

$$= \gamma_3 \left[3\lambda'_3 \log \frac{s}{9} \right]$$

At $S \simeq 400$ Gev^2, we get (24)

$$\lambda^2_1 = 0.61 \qquad \lambda'_2 = 0.67 \qquad \lambda'_3 = 0.72$$

From the above consideration we obtain for the probability that a gap has $|\Delta Q| = 2$

$$P_2(y) = \frac{P_2^{(1)} \lambda'_1 e^{-\lambda'_1 y} + P_2^{(2)} (2\gamma_2 \lambda'_2) e^{-2\lambda'_2 y} + P_2^{(3)} (3\gamma_3 \lambda'_3) e^{-3\lambda'_3 y}}{\lambda'_1 e^{-\lambda'_1 y} + 2\lambda'_2 \gamma_2 e^{-2\lambda'_2 y} + 3\lambda'_3 \gamma_3 e^{-3\lambda'_3 y}} \qquad (25)$$

Similarly for the probability that a rapidity gap y has $|\Delta Q| = 3$ we obtain

$$P_3(y) = \frac{P_3^{(2)} (2\lambda'_2 \gamma_2) e^{-2\lambda'_2 y} + P_3^{(3)} (3\lambda'_3 \gamma_3) e^{-3\lambda'_3 y}}{\lambda'_1 e^{-\lambda'_1 y} + 2\lambda'_2 \gamma_2 e^{-2\lambda'_2 y} + 3\lambda'_3 \gamma_3 e^{-3\lambda'_3 y}} \qquad (26)$$

In Fig. 5a we show the resulting $P_2(y)$ and $P_3(y)$ for values $\gamma_2 = 0.50$ and $\gamma_3 = 2.2$. Similar fits can be obtained with other values. We see that the model gives a good description of the data. The principle defect of the fit is that P_2 and P_3 are small near $y = 0$. This is very likely because we have ignored the small amount of $|\Delta Q| = 2$ which will inevitabiy occur in the one ladder terms. Our model does not readily allow us to include these since they will have a very different y - dependence than $|\Delta Q| = 0, \pm 1$ gaps. However, to illustrate the effect we ignore this and suppose that one-ladder gaps have $|\Delta Q| = 0, 1, 2$ in the ratio 34, 64, 2. This gives

$$P_2^{(1)} = 0.0556 \quad , \quad P_2^{(2)} = 0.41 \quad , \quad P_2^{(3)} = 0.48$$

$$P_3^{(2)} = 0.0278 \quad , \quad P_3^{(3)} = 0.15 \qquad (27)$$

The resulting $P_2(y)$ and $P_3(y)$ are shown as in Fig. 5b, where γ_2 and γ_3 are given the same values as in Fig. 5a.

There is also another important remark related to $P_2(0)$. Since the 2-prong events (which are mainly $\Delta Q = 0$) are not included in the analysis of Lamsa et al., one expects $P_2(0)$ to be smaller, and close to that predicted by the model.

There are two further quantities which we can calculate with our model. The two particle correlation is given by

$$\langle n^2 \rangle / \langle n \rangle^2 = 1.24 \qquad (28)$$

which agrees with the experimental value[24] of 1.28. In view of the fact that we have ignored the diffractive component, which is well known to contribute positively to the correlation, this agreement should not be taken very seriously. Also we can estimate α_f by the following method. We assume that at "low" energy, say $S \approx 20$ Gev^2, the single ladder (f) term dominates.

Then at $S \simeq 400$ Gev^2 it contributes a fraction

$$\exp(\alpha_f - 1)(\log 400 - \log 20) = 1/(1+\gamma_2+\gamma_3)$$

or

$$\alpha_f \simeq 1 - \frac{1}{3}\log(1+\gamma_2+\gamma_3)$$

$$= 0.56 \qquad (29)$$

This is not the best evaluation of α_f but it is an original one.

Finally we note a qualitative prediction of the model which is independent of the details. Since the contribution of the single ladder diagrams will reduce with energy we expect $P_2(y)$ curve to fall off less rapidly with y as the energy increases. Such a phenomenon if observed would be very hard to explain in any "single ladder model".

Figure captions

Fig. 1 : (a) Charges exchanged are restricted to

(b) No restriction on

(c) The single cross-over phenomenon.

(d) Multiple cross-over.

Fig. 2 : Two-overlapping ladders.

Fig. 3 : The dual model "two-ladder" contribution to the Pomeron.

Fig. 4 : A term in the single ladder contribution to the Pomeron.

Fig. 5 : The calculated $P_2(y)$ and $P_3(y)$ compared to the data points. In (a) there is no $|\Delta Q| = 2$ in the single ladder. In (b) a small amount of $|\Delta Q| = 2$ is included in the single ladder.

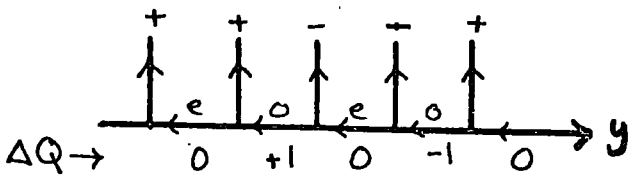

e: even ΔQ
o: odd ΔQ

(a)

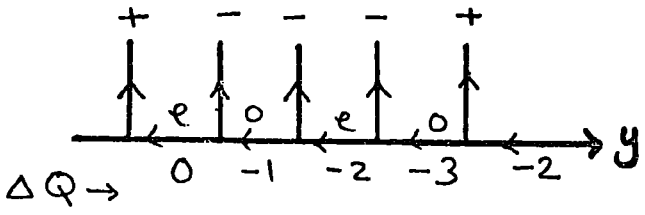

(b)

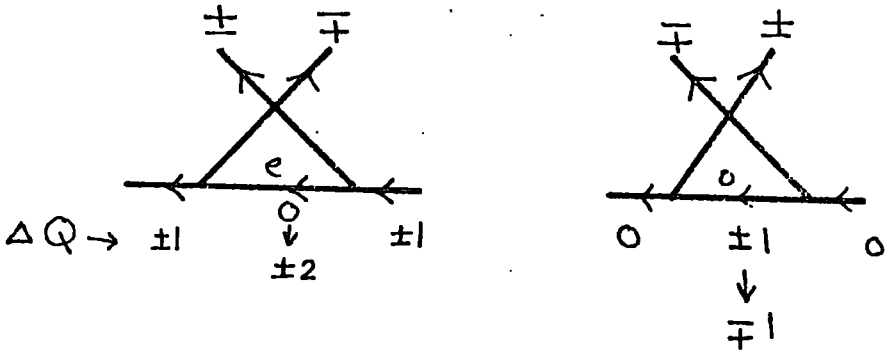

(c)

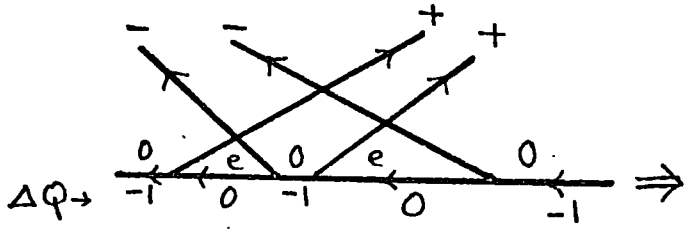

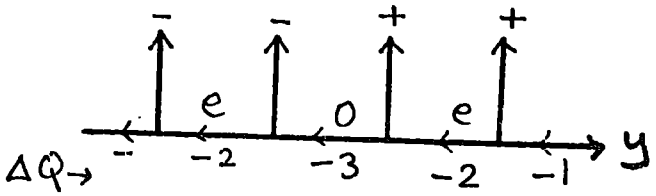

(d)

Fig. 1

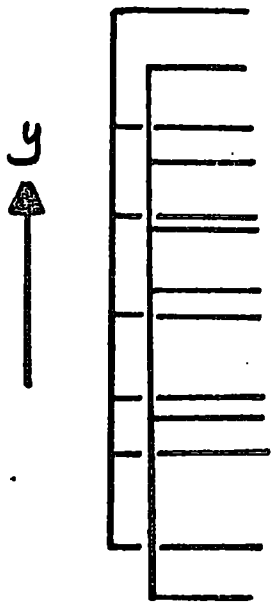

Fig.2

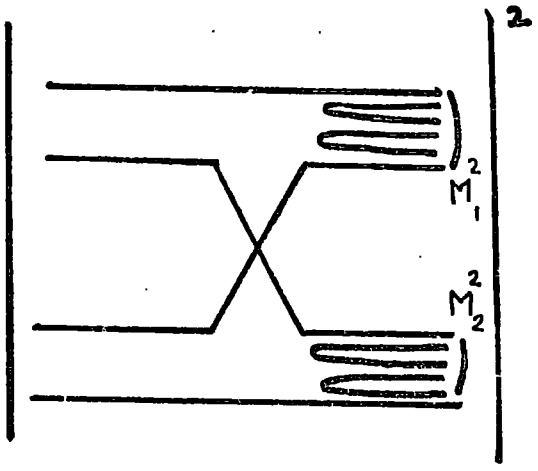

Fig.3

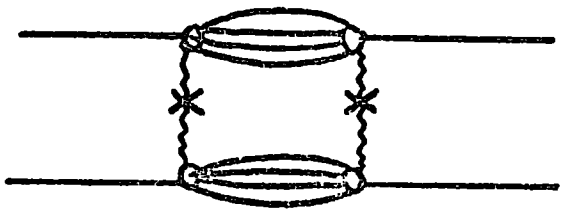

Fig.4

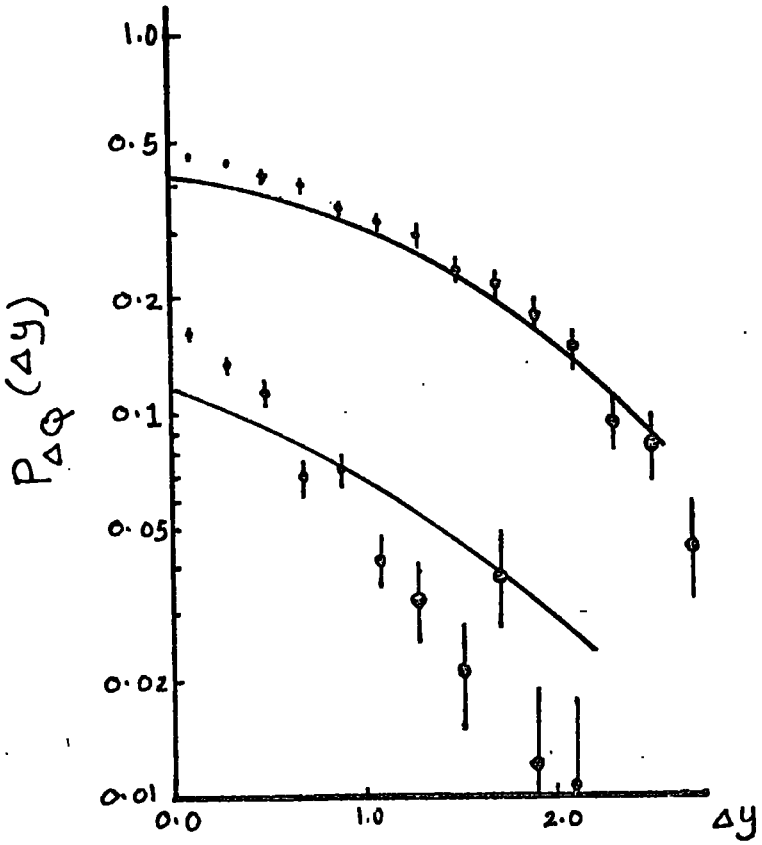
1.0
0.5
0.2
0.1
0.05
0.02
0.01
$P_{\Delta Q}(\Delta y)$
0.0
1.0
2.0
Δy

(a)

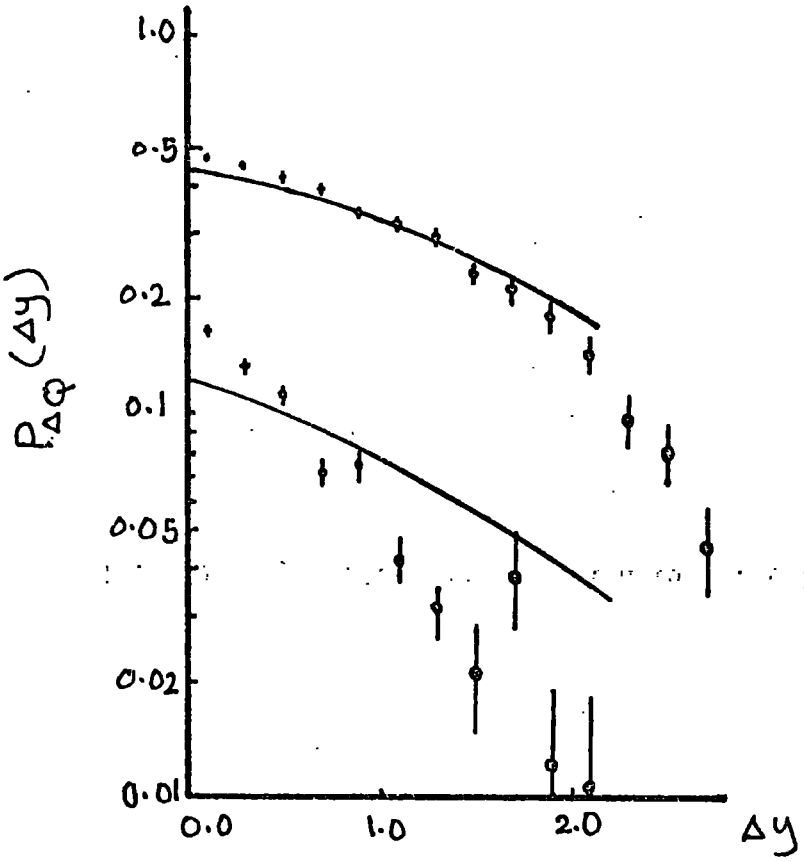
1.0
0.5
0.2
0.1
0.05
0.02
0.01
$P_{\Delta Q}(\Delta y)$
0.0
1.0
2.0
Δy

(b)

Fig. 5

APPENDIX A

The Crossing Matrices

In this appendix we calculate the relevent elements of the crossing matrices which we need to write down the matrices $\underset{\sim}{\tilde{V}}$; (Ch. III, § 3). Since in ref. (14) tables are provided for SU(2) and SU(3) crossing matrices, we concentrate here only on those channels where one or more of the involved particles are exotic. Following the method of ref. (14) we write;

$$A^{(I_a)} + B^{(I_b)} \xrightarrow{I} C^{(I_c)} + D^{(I_d)} \qquad \text{(s - Channel)}$$

$$A^{(I_a)} + \bar{C}^{(I_c)} \xrightarrow{I'} \bar{B}^{(I_b)} + D^{(I_d)} \qquad \text{(t - Channel)}$$

the crossing matrix X_{st} is given by

$$(X_{st})_{I,I'} = \xi_{st}(2I'+1) \begin{Bmatrix} I_a & I_b & I \\ I_d & I_c & I' \end{Bmatrix} \qquad \text{(A.1)}$$

and

$$(X)_{I,I} = \frac{2I+1}{2I'+1} (X_{st})_{I,I'} \qquad \text{(A.2)}$$

where the phase factor is given by

$$\xi_{st} = (-1)^{I+I'} \tag{A.3}$$

When I_b and I_c both are integer, which is always the case in the processes we are considering. The 6.j symbol is related to Racah coefficient;

$$\begin{Bmatrix} j_1 & j_2 & j_3 \\ \ell_1 & \ell_2 & \ell_3 \end{Bmatrix} = (-1)^{j_1+j_2+\ell_1+\ell_2} W(j_1 j_2 \ell_2 \ell_1 ; j_3 \ell_3) \tag{A.4}$$

which can be calculated from the tables and symmetry relations given in ref. (15) "App. 1".

$1+0 \longrightarrow 2+2$ $\quad \rho\omega \longrightarrow XY$ (s - Channel)

$1+2 \longrightarrow 0+2$ $\quad \rho\bar{X} \longrightarrow \bar{\omega}Y$ (t - Channel)

$$A_{I_t=2} = (X)_{t\,s\,2,1}\, A_{I_s=1} = \sqrt{3/5}\; A_{I_s=1}$$

$1+1 \longrightarrow 2+2$ $\quad \rho A_2 \longrightarrow XY$ (s - channel)

$1+2 \longrightarrow 1+2$ $\quad \rho\bar{X} \longrightarrow \bar{A}_2 Y$ (t - channel)

$$A_{I_t=1} = (X_{tS})_{1,1}\ A_{I_s=1} = -3/2\sqrt{5}\ A_{I_s=1}$$

$$A_{I_t=2} = (X_{tS})_{2,1}\ A_{I_s=1} = -1/2\sqrt{5}\ A_{I_s=1}$$

$$A_{I_t=3} = (X_{tS})_{3,1}\ A_{I_s=1} = 1/\sqrt{5}\ A_{I_s=1}$$

$1+2 \longrightarrow 2+1 \qquad \rho Y \longrightarrow X A_2$ (s - Channel)

$1+2 \longrightarrow 2+1 \qquad \rho \bar{X} \longrightarrow \bar{Y} A_2$ (t - Channel)

$$A_{I_t=1} = (X_{tS})_{1,1}\ A_{I_s=1} = 1/10\ A_{I_s=1}$$

$$A_{I_t=2} = (X_{tS})_{2,1}\ A_{I_s=1} = 3/10\ A_{I_s=1}$$

$$A_{I_t=3} = (X_{tS})_{3,1}\ A_{I_s=1} = 3/5\ A_{I_s=1}$$

$1+2 \longrightarrow 1+2$ $\qquad \rho\gamma \longrightarrow \rho\gamma$ (s - Channel)

$1+1 \longrightarrow 2+2$ $\qquad \rho\bar{\rho} \longrightarrow \bar{\gamma}\gamma$ (t - Channel)

$$A_{I_t=0} = (X_{ts})_{0,1}\, A_{I_s=1} = -\sqrt{3/5}\, A_{I_s=1}$$

$1+2 \longrightarrow 0+1$ $\qquad \rho\gamma \longrightarrow \omega\rho$ (s - Channel)

$1+0 \longrightarrow 2+1$ $\qquad \rho\omega \longrightarrow \bar{\gamma}\rho$ (t - Channel)

$$A_{I_t=1} = (X_{st})_{1,1}\, A_{I_s=1} = 1 \cdot A_{I_s=1}$$

$1+2 \longrightarrow 1+0$ $\qquad \rho\gamma \longrightarrow \rho\omega$ (s - Channel)

$1+1 \longrightarrow 2+0$ $\qquad \rho\bar{\rho} \longrightarrow \bar{\gamma}\omega$ (t - Channel)

$$A_{I_t=2} = (X_{ts})_{2,1}\, A_{I_s=1} = -\sqrt{3/5}\, A_{I_s=1}$$

$1+1 \longrightarrow 1+2$ $\qquad \rho A_2 \longrightarrow \rho\gamma$ (s - Channel)

$1+1 \longrightarrow 1+2$ $\qquad \rho\bar{\rho} \longrightarrow \bar{A}_2\gamma$ (t - Channel)

$$A_{I_t=1} = (X_{ts})_{1,1}\, A_{I_s=1} = 1/2\, A_{I_s=1}$$

$$A_{I_t=2} = (X_{ts})_{2,1}\, A_{I_s=1} = 3/2\sqrt{5}\, A_{I_s=1}$$

APPENDIX B

A Perturbation Method for Calculating the Exotic Effect

In the models of Ch.II, because we assume exchange degeneracy between the trajectories and the couplings; we have a common factor between all the elements of the matrix $\underset{\sim}{V}$, namely $g^2/(s-\beta)$. On the contrary, in the Model we consider in Ch.III, we do not assume neither strong nor weak Exchange degeneracy. Hence the coupling constant g^2 and the dynamical factor $1/(s-\beta)$ is different from element to another. Add to this the large size of our matrices, this makes the direct way of solving the equation $\det(\underset{\sim}{1} - \underset{\sim}{\tilde{V}}) = 0$ for the highest root J impracticable. For this reason the following perturbation method is suggested instead.

We want values of J such that

$$[\underset{\sim}{1} - \underset{\sim}{V}(s)]|\lambda\rangle = |0\rangle \tag{B.1}$$

Let $$\underset{\sim}{V} = \underset{\sim}{V_0} + \underset{\sim}{V_1} \quad \begin{cases} 0 = \text{lowest order} \\ 1 = \text{first order} \end{cases} \tag{B.2}$$

Then suppose
$$[\underset{\sim}{1} - \underset{\sim}{V_0}(s_0)]|\lambda_0\rangle = |0\rangle \tag{B.3}$$

and put
$$|\lambda\rangle = |\lambda_0\rangle + |\lambda_1\rangle + |\lambda_2\rangle + \cdots \tag{B.4}$$

$$J = J_0 + J_1 + J_2 + \cdots \tag{B.5}$$

where 1 denotes first order, 2 denotes second order, ...

Then we write
$$V_0(J) = V_0(J_0) + \Delta J \dot{V}_0(J_0) + \frac{\Delta J^2}{2!} V_0''(J_0) + \cdots \tag{B.6}$$

$$V_1(I) = V_1(I_0) + \Delta I\, V_1'(I_0) + \frac{\Delta I^2}{2!} V_1''(I_0) + \cdots \qquad (B.7)$$

then (1) becomes

$$\left[1 - V_0(I_0) - \Delta I\, V_0'(I_0) - \cdots - V_1(I_0) - \Delta I\, V_1'(I_0) - \cdots\right) \left| |\lambda_0\rangle + |\lambda_1\rangle + \cdots \right\rangle \qquad (B.8)$$

$$= |0\rangle$$

Computing each order:

zeroth order (B.9)

$$(1 - V_0(I_0))\,|\lambda_0\rangle = |0\rangle$$

first order $$(1 - V_0(I_0))\,|\lambda_1\rangle - I_1 V_0'(I_0)\,|\lambda_0\rangle - V_1(I_0)\,|\lambda_0\rangle = |0\rangle \qquad (B.9')$$

If we take the scalar product with $\langle \lambda_0 |$ and noticing B.3 we get

$$-I_1 \langle \lambda_0 | V_0' | \lambda_0 \rangle = \langle \lambda_0 | V_1(I_0) | \lambda_0 \rangle \qquad (B.10)$$

Since $V_1(I_0)\,|\lambda_0\rangle$ is perpendicular to $|\lambda_0\rangle$ (as we shall see in the example below), we get

$$I_1 = 0 \qquad (B.11)$$

Second order

$$(1 - V_0(I_0))\,|\lambda_2\rangle - I_2 V_0'(I_0)\,|\lambda_0\rangle - V_1(I_0)\,|\lambda_1\rangle = |0\rangle \qquad (B.12)$$

If we take scalar product with $\langle \lambda_0 |$ we get

$$-I_2 \langle \lambda_0 | V_0' | \lambda_0 \rangle = \langle \lambda_0 | V_1(I_0) | \lambda_1 \rangle \qquad (B.13)$$

By making use of (B.9') we get

$$-I_2 = \frac{\langle \lambda_0 | V_1(I_0) \left[1 - V_0(I_0)\right]^{-1} V_1(I_0) | \lambda_0 \rangle}{\langle \lambda_0 | V_0'(I_0) | \lambda_0 \rangle} \qquad (B.14)$$

The Calculation of $\alpha_\rho^{out}(0)$.

To illustrate the perturbation method which we have just discussed, in calculating the exotic effect (Ch. III, § 5), we calculate here J_0^ρ and J_2^ρ. For this purpose we write $\underset{\sim}{V}^{(\rho)}$ matrix in the following abbreviated form:

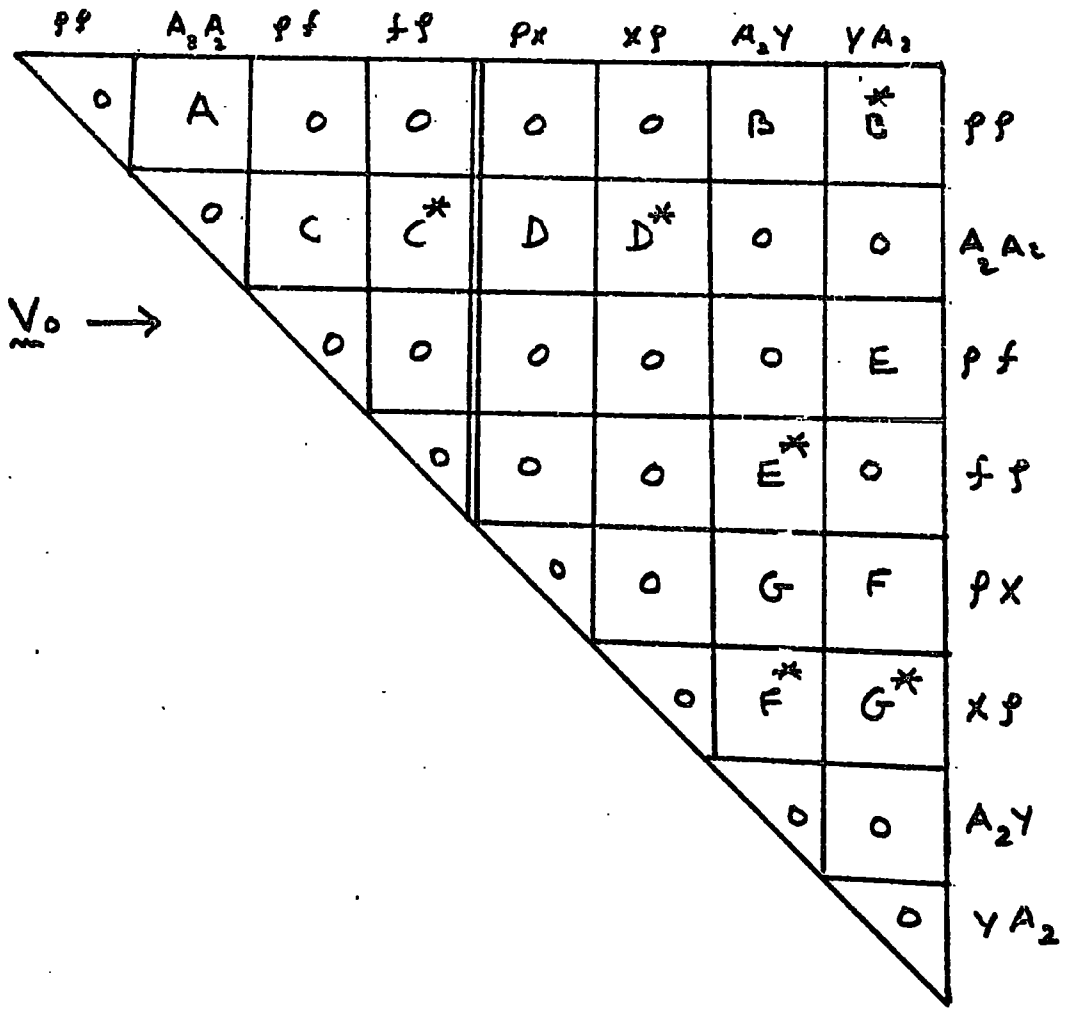

First we calculate the highest root of the equation

$$\det\left(\underset{\sim}{1}-\underset{\sim}{V}_0\right)=0 \tag{B.15}$$

$$\Rightarrow \quad 1-c^2-c^{*2}-A^2=0 \tag{B.16}$$

$$\Rightarrow 1-2G_1^2G_2^2b^2\left(\mathfrak{z}_1^2+\mathfrak{z}_1^{*2}\right)-G_1^4a^2b^2=0 \tag{B.17}$$

(See $\underset{\sim}{V}(s)$ matrix in the text.)

where
$$a^2=\frac{f_\rho^* f_\rho}{s-\beta_{\rho\rho}}\,,\quad b^2=\frac{f_{A_2}^* f_{A_2}}{s-\beta_{A_2A_2}}\,,\quad \mathfrak{z}_1^2=\frac{f_\rho^* f_f}{s-\beta_{\rho f}} \tag{B.18}$$

With the values of G_1, G_2 and α_ρ, α_{A_2}, α_f given in the text (Ch. III, eqs. 10-13) equation (B.17) becomes;

$$s^3+0.5\,s^2-0.36\,s-0.021=0 \tag{B.19}$$

$$\Rightarrow \quad s_0=0.44 \tag{B.20}$$

Now we proceed to calculate the effect of exotic exchange, i.e. $s_2^{(\rho)}$

If we take

$$|\lambda_0\rangle = \begin{pmatrix} \lambda_0^1 \\ \lambda_0^2 \\ \vdots \\ \lambda_0^8 \end{pmatrix} \tag{B.21}$$

the eq.

$$(\underline{1} - \underline{V}_0)|\lambda_0\rangle = 0 \Rightarrow$$

$$\begin{aligned} &\lambda_0^1 - A\lambda_0^2 = 0 \\ &-A\lambda_0^1 + \lambda_0^2 - C\lambda_0^3 - C^*\lambda_0^4 = 0 \\ &-C\lambda_0^2 + \lambda_0^3 = 0 \\ &-C^*\lambda_0^2 + \lambda_0^4 = 0 \end{aligned} \tag{B.22}$$

$$\lambda_0^5 = \lambda_0^6 = \lambda_0^7 = \lambda_0^8 = 0$$

which gives

$$|\lambda_0\rangle = \begin{pmatrix} A \\ 1 \\ C \\ C^* \\ 0 \\ 0 \\ 0 \\ 0 \end{pmatrix} \tag{B.23}$$

hence

$$\underset{\sim}{V}_1 |\lambda_0\rangle = \begin{pmatrix} 0 \\ 0 \\ 0 \\ 0 \\ D \\ D^* \\ BA + E^* C^* \\ B^* A + EC \end{pmatrix} \tag{B.24}$$

which is perpendicular to $|\lambda_0\rangle$ as we mentioned in eqs. (B.10;1

Next we take $(\underset{\sim}{1} - \underset{\sim}{V}_0)|\lambda_1\rangle = \underset{\sim}{V}_1 |\lambda_0\rangle \Rightarrow$

$$\begin{aligned}
&\lambda_1^1 - A\lambda_1^2 = 0 \\
&-A\lambda_1^1 - \lambda_1^2 - C\lambda_1^3 - C^*\lambda_1^4 = 0 \\
&-C\lambda_1^2 + \lambda_1^3 = 0 \\
&-C^*\lambda_1^2 + \lambda_1^4 = 0 \\
&\lambda_1^5 = D \quad , \quad \lambda_1^6 = D^* \\
&\lambda_1^7 = BA + E^* C^* \\
&\lambda_1^8 = B^* A + EC
\end{aligned} \tag{B.25}$$

$$\Rightarrow \quad |\lambda_1\rangle = \begin{pmatrix} A \\ 1 \\ C \\ C^* \\ D \\ D^* \\ BA + E^* C^* \\ B^* A + EC \end{pmatrix} \tag{B.26}$$

From (B.24) we get

$$\langle \lambda_0 | V_1 = \underbrace{\begin{matrix} 0 & 0 & 0 & 0 & D & D^* & AB + E^* C & B^* A + EC^* \end{matrix}} \tag{B.27}$$

Eqs. (B.26) and (B.27) gives the right hand side of eq. (B.13).

$$\langle \lambda_0 | V_1 | \lambda_1 \rangle = D^2 + D^{*2} + A^2 (B^2 + B^{*2}) + CC^* (E^2 + E^{*2})$$

$$+ [BA\, E^* C^* + C.C.] + [BA E^* C + C.C.] \tag{B.28}$$

Now we turn to calculate the denominator of eq. (B.14)

$$V_0(J_0) = \begin{pmatrix} 0 & A' & 0 & 0 & & \\ A' & 0 & C' & C'^* & & \\ 0 & C' & 0 & 0 & & 0 \\ 0 & C'^* & 0 & 0 & & \\ & & & & 0 & \end{pmatrix}$$

, where A' means the derivative of A; $A' = \frac{\partial A}{\partial J}$, and so C', C

then

$$\overset{\circ}{V}_0 |\lambda_0\rangle = \begin{bmatrix} A' \\ AA' + cc' + c^{*}c^{*\prime} \\ c' \\ c^{*} \\ 0 \\ \vdots \end{bmatrix} \tag{B.29}$$

hence

$$\langle \lambda_0 | \overset{\circ}{V}_0 | \lambda_0 \rangle = AA' + AA' + cc' + c^{*}c^{*\prime} + c'c^{*} + cc'^{*} \tag{B.30}$$

Finally J_2^{g} is given by

$$-J_2 = \frac{\langle \lambda_0 | V | \lambda \rangle}{\langle \lambda_0 | \overset{\circ}{V}_0 | \lambda_0 \rangle} = \frac{(B.28)}{(B.30)} \tag{B.31}$$

The calculation of (B.28) and (B.30) is quite lengthy one, and we will not write it here. It is enough to note that with J_0 given by (B.20) and G_1, G_2 and α_{in} given by eqs. (III, 10-13), J_2 can be calculated in terms of g^2, and the result in our example is

$$J_2^{g} = -\frac{1.01\, g^2}{5.04} = -0.2\, g^2 \tag{B.22}$$

REFERENCES

(1). G.F. Chew and A. Pignotti, Phys. Review 176 (1968) 2112.

(2). G.F. Chew and A. Pignotti, Phys. Review Letters 20 (1968) 1078.

(3). H. Lee, Phys. Review Letters, 30 (1972) 719.

(4). Chan Hong-Mo, Ken-ichi Konishi, J. Kwiecinski, and R.G. Roberts, "The breaking of exchange degeneracy in dual unitarisation", Rutherford Laboratory report RL-76-056 T.161 (1976).

(5). D. Horn, Physic Reports, 4C (1972) 1.

(6). E.J. Squires and D.M. Webber Nucl. Phys. B99 (1975) 499.

(7). M. Fukugita, T. Inami, N, Sakai and S. Yazaki, UT-265 preprint (1976), and Nucl. Phys. B121 (1977) 93.

(8). M. Baker, and K.A. Ter-martirosyan, Phys. Reports 28C (1976) 1.

(9). D. Amati, A. Stanghellini, and S. Fubini, Nuovo Cimento 26 (1962) 896.

(10). C.E. Detar, Phys. Review D3 (1971) 128.

(11). E.M. Friedländer, Phys. Review Letters 5 (1960) 212.

(12). F. Salzman & G. Salzman, Phys. Review Letters S (1960) 377.

(13). C. Schmid and C. Sorensen, Nucl. Phys. B96 (1975) 209.

(14). Claudio Rebbi and Richard Slansky, Reviews of Modern Physics 42 (1970) 68.

(15). M.E. Rose, Elementary theory of angular momentum, 1957, (Wiley; London & New York).

(16). J.W. Lamsa, et al., Phys. Rev. Letters 37 (1976) 73.

(17). C. Schmid, D.M. Webber and C. Sorensen, "The IOZ Rule and Exotic Exchange: A Connection through Unitarity" ETH Preprint (1976).

(18). G. Veneziano, Nucl. Phys. B74 (1974) 365. Phys. Letters 52B (1974) 220.

(19). C. Rosenzweig and G.F. Chew, Phys. Letters 58B (1975) 93.

(20). G. Zweig, CERN preprint 8182/TH.401, Jan. (1964), unpublished, S. Okubo, Phys. Lett. 5 (1966) 165; J. Iizuka, Prog. Theor. Phys. Suppl. 37-38 (1966) 21.

(21). J. Mandula, J. Weyers and G. Zweig, Ann. Rev. Nucl. Sc. 20 (1970) 289.

(22). K. Zalewski, Proc. of the XVII International Conference (London, 1974).

(23). C. Lovelace, Phys. Letters 32B (1970) 703.
G. Frye and L. Susskind, Phys. Letters 31B (1970) 589.

(24). K. Fialkowski and H. Miettinen, Phys. Letters 43B (1973) 61.

(25). Chan, H.M., J.E. Paton and Tsou, S.T. Nucl. Phys. B86 (1975) 479; Chan, H.M., J.E. Paton, Tsou, T.S. and Ng Sing Wai, Nucl. Phys. B92 (1975) 13.

(26). P.W. Coulter and D,R. Snider, Phys. Rev. D8 (1973) 4055.

(27). A Neveu and J. Scherk, Nucl. Phys. B36 (1972) 317.

(28). G.F. Chew and C. Rosenzweig, Phys. Rev. D. 12 (1975) 3907.

(29). P.W. Coulter and D.R. Snider, Phys. Rev. D8 (1973) 4055.

(30). J.E. Paton and Chan, H.M. Nucl. Phys. B10 (1969) 516.

(31). P. Stevens, G.F. Chew, and C. Rosenzweig. Nucl. Phys. B110, 355 (1975).

(32). Tsou Sheung Tsun, Phys. Lett. 65B, 81 (1976).

(33). Y. Eylon, University of California preprint, (July 1976) Berkeley CA 94720.

(34). C. Schmid, D.M. Webber and C. Sorensen; The IOZ rule and Exotic exchange. A connection through unitarity (Jan. 1976).

(35). D.W. Duke, The Pomeron - f identity and Vector Meson Production, FERMILAB-Pub-77/76-THY, August 1977.

(36). G. Veneziano, Nuc. Phys. B108 (1976) 285.

(37). D.R. O. Morrison "Comments", talk given at VIIth International Colloquium on multiparticle reactions, Munich (1976), CERN/EP/PHYS 76-45.

(38). J.R. Freeman, Y. Zarmie and G. Veneziano, "Constraints on Reggeon Amplitudes from analyticity and planar unitarity" CERN Th.2211 (1976).

(39). A.H. Shehadeh and E.J. Squires, "Unitarity, Pion Production and Exotic trajectories", Durham Preprint, Oct. 1976.

(40). A.H. Shehadeh and E.J. Squires, J. Phys. G : Nucl. Phys., Vol. 3, No. 7, L135 (1977).